THE EFFECT OF PLASMA TREATMENT ON FLAX FIBRES

A Thesis
Submitted to the College of Graduate Studies and Research
in Partial Fulfillment of the Requirements for
the Degree of Master of Science
in the
Department of Agricultural and Bioresource Engineering
University of Saskatchewan
Saskatoon, Saskatchewan

By

Rahim Oraji

PERMISSION TO USE

In presenting this thesis in partial fulfilment of the requirements for a graduate degree from the University of Saskatchewan, I agree that the Libraries of this University may make it freely available for inspection. I further agree that permission for copying of this thesis in any manner, in whole or in part, for scholarly purposes may be granted by the professor who supervised my thesis work or, in his absence, by the Head of the Department or the Dean of the College in which my thesis work was done. It is understood that any copying or publication or use of this thesis or parts thereof for financial gain shall not be allowed without my written permission. It is also understood that due recognition shall be given to me and to the University of Saskatchewan in any scholarly use which may be made of any material in my thesis.

Requests for permission to copy or to make other use of material in this thesis in whole or part should be addressed to:

Head of the Department of Agricultural and Bioresource Engineering

University of Saskatchewan

Saskatoon, Saskatchewan S7N 5A9

ABSTRACT

In recent years, interest in using composites with natural fibres as reinforcement and/or filler has increased because of the advantages of natural fibres, such as low density, low cost, high mechanical properties, and biodegradability. Unmodified-hydrophilic natural fibres show poor compatibility with polymer matrix when they are used as reinforcement in polymer composites. Several methods of modifications of natural fibres, such as chemical and plasma modification of natural fibres have been performed to improve the interfacial compatibility of natural fibre and matrix, and also to decrease water absorption of fibres.

The purpose of this study was to examine the effect of plasma treatment on Saskatchewan-grown oilseed flax fibre that can be used in biocomposites. For comparison, the fibres have also been chemically modified using sodium hydroxide and silane. A comparison has been made between the results from both cases.

In this thesis, both plasma and chemically modified flax fibre are characterized to understand its crystallinity, color changes, mechanical properties, morphological changes, and thermal properties. Techniques such as X-ray diffraction (XRD), color test, tensile test, scanning electron microscopy (SEM), differential scanning calorimetry (DSC), and soft X - ray spectromicroscopy are used to study the structural changes of flax fibre after physical and chemical modifications. A fitting method with four Gaussian functions was used to determine crystallinity of cellulose.

Results showed that the crystallinity of cellulose in modified (physical or chemical) fibres decreased. Chemical treatment did not improve the tensile strength nor the stiffness of the fibres. Morphological studies showed that the fibre surface changes in both treatments were significant, however, the surfaces of flax fibres exposed to the plasma were modified in the near-surface regions. There was no trace of lignin before and after chemical treatment except in the one-hour chemically treated fibres. The color of the fibres became lighter after chemical treatment. Chemical bonding between resin and fibre was observed in the untreated fibres, the one-hour chemically modified fibres and two-hour chemically modified fibres.

Results of this research also showed that plasma treatment can be used as a surface modifying method for flax fibres, however there were some restrictions of utilizing the plasma modification method, e.g. sample size and non-uniformity of plasma gas.

ACKNOWLEDGEMENTS

I would like to express my sincere gratitude to all those who have directly or indirectly contributed to this work. I would like to thank:

1) my supervisor Dr. Satya Panigrahi for his guidance, help, and for his financial support;

2) the members of my advisory committee Dr. Lope Tabil and Dr. Trever Crowe, for their guidance and help;

Department of Agricultural and Bioresource Engineering for financial support;

technical staff in the Department of Agricultural and Bioresource Engineering, Randy Lorenz and Louis Roth for their help in different situations;

Department of Physics and Engineering Physics for providing facilities for doing plasma treatment;

Biolin Research Inc. for providing flax fibres and measuring fibre thickness;

my friends Dr. Kamal Barghout and Barbara Spurr for their unlimited assistance on different occasions; and

all my colleagues at Department of Agricultural and Bioresource Engineering.

My appreciation also goes to Thomas Bonli for his help in XRD and SEM. I in particular thank Dr. Chithra Karunakaran for assisting and helping me at the Canadian Light Source Inc.

I am truly grateful to my dearest friend, Majid Damircheli and his family for their support and encouragement during this research work.

DEDICATION

I dedicate this thesis to my dear friend Nasrin Sagai who tragically passed away on June 7, 2007. Nasrin was encouraging and supporting me to continue my education.

TABLE OF CONTENTS

LIST OF TABLES

LIST OF FIGURES

NOMENCLATURE

A = Flax fibre cross section area (μm^2)

A_o= Flax fibre cross section area (m^2)

C 1s = Atomic subshell of carbon (quantum numbers: n=1, l=0)

d = Interplanar spacing (Å)

DSC = Differential scanning calorimetry

DP = Degree of polymerization

D = Fibre thickness (μm)

$E/\Delta E$ = Spectral resolving power

f_i = Relative frequency

F1 = Untreated flax fibre with a purity of 78.4%

F2 = Untreated flax fibre with a purity of 92.5%

F_{max} = Maximum load (N)

I_t = Transmitted intensity (the number of transmitted soft X-ray photons or counts)

I_o = Incident intensity (the number of incident soft X-ray photons or counts)

I = X-ray intensity (the number of scattered hard X-ray photons or counts)

L, a, b = Color coordinates of the samples

MC = Moisture content (%)

n_α = Plasma density for each type of particles in plasma gas (cm^{-3}), α = e (electrons), i (ions) or n (neutral particles)

N = The number of counted fibres

N_i = The number of fibres with the thickness of D_i (μm)

NEXAFS = Near-edge X-ray absorption of fine structure

OD = Optical density

P1 = Five- minute plasma treated flax fibres

P2 = Ten- minute plasma treated flax fibres

P3 = Fifteen- minute plasma treated flax fibres

R^2 = Coefficient of determination

STXM = Scanning transmission X-ray microscopy

SEM = Scanning electron microscopy

SCCM = Standard cubic centimetres per minute

T1 = One-hour chemically treated flax fibres

T2 = Two- hour chemically treated flax fibres

T3 = Three- hour chemically treated flax fibres

T4 = Tour- hour chemically treated flax fibres

T_e = Temperature of negative particles or electrons (eV or K)

T_i = Temperature of positive particles or ions (eV or K)

T_n = Temperature of neutral particles (eV or K)

TEM = Transmission electron microscopy

W = Crystallite thickness (Å)

XRD = X-ray diffraction

X_C = Degree of crystallinity (%)

X_1, X_2, X_3, and X_4= The angular position of Bragg's peaks (in degree or radians)

$\beta_{\frac{1}{2}}$ = The full width at half maximum of Bragg's peak from crystalline lattice (in radians)

λ = 1.54 Å (the wave length of hard X -ray beam)

μ = Mass absorption coefficient (cm^2/g)

θ_B = The angular position of Bragg's peaks (in degree or radians)

ρ = Density of material (g/cm^3)

σ_{max} = Maximum tensile strength (Pa)

1. INTRODUCTION AND OBJECTIVES

Biocomposite materials consist of natural fibres as reinforcement and biodegradable or non-biodegradable polymers as matrix. Recently, increasing interest in biodegradable plastics has been revived due to new technologies. Natural fibres such as flax, hemp, jute, and wood fibres, which originate from renewable resources, are used as reinforcement in polymer-based engineering composites. They show adequate mechanical properties, good resistance to breakage during processing, low density, and low cost. High level of moisture adsorption, poor wettability and adhesion between polymers and untreated fibres favour the chemical or plasma treatment for fibres.

Plasma is an ionized gas containing negative, positive, and neutral particles. When a sample is exposed to a plasma gas, energetic charged-particles inside the plasma are able to interact chemically with the surface of the sample. Such interactions can affect material properties. The effect of plasma treatment on materials might be categorized in two types of surface and structure changes (bulk modification). Plasma surface modification involves the use of energetic charge particles generated by an ionized gas to modify the surface properties without affecting the desirable bulk properties of materials e.g. plasma surface modification may affect the wettability, dyeability, and adhesion of materials (Xu and co-researchers 2006). In general, plasma surface treatment does not change or break the bulk materials; it does not remove or

deposit more than a few layers to the surface of materials; and it does not remove bulk materials (Roth 2001).

In the biocomposite manufacturing process, the surface properties of natural fibres play an important role. The conventional method of treatment (or chemical treatment) produces large amounts of waste materials; therefore, a need for environmentally friendly treatment of materials with less pollution and various applications is growing fast.

Some studies have been done in order to understand the structure and properties of natural fibres (Bledzki and Gassan 1999; Bledzki et al. 1996) and on the other hand, by ignoring what really happens to the fibre structure, a macroscopic approach has been developed. In the latter choice, properties such as heat conductivity, elastic modulus, elongation, and hardness of composites made of flax fibres, have been at the center of studies by Hornsby and co-workers (1997), Baiardo and co-workers (2004), and Olaru and co-workers (2005).

Using plasma treatment in different areas has been studied by many researchers and the treatment sometimes has shown promising results, e.g. an improvement in the dyeability and wettability of bamboo fibres after argon plasma treatment has been reported by Xu and co-researchers (2006). Marais and co-workers (2005) have studied the mechanical properties of unsaturated polyester composites reinforced with helium plasma treated flax fibres. They have reported an improvement in fibre/matrix adhesion after exposing the flax fibres to helium plasma treatment. The effect of oxygen plasma treatment on bombyx mori silk fibres has been studied by Chen and co-workers (2004). Their results showed that the crystallinity of the fibres was decreased.

No studies involving modification of natural fibre have been done at the University of Saskatchewan using plasma as a modification method. This research was aimed at using plasma as a treatment method for natural fibres, particularly flax fibre. The main goal of this study was to investigate the capability and the limitations of utilizing the plasma treatment technique for modifying flax fibres. To approach this goal, it was necessary to study about both the chemical and plasma modifications of natural fibres done by other researchers.

This project is divided into two parts.

1. Plasma treatment, which is a treatment with an electric gas discharge, can change the surface characteristics of fibres. Plasma treatment changes structural and surface properties of the fibres. Mechanical bonding between fibres and polymer such as thermoplastic and thermoset resins can be influenced by the time of exposure and the nature of the gas used (argon, nitrogen, and oxygen). A variety of plasma treatments can be achieved by changing the processing time and gas flow rate.
2. Chemical treatment which is based on the following rule: a third component as a coupling agent is used in improving the compatibility of two materials which originally are incompatible.

In this project, both treatment methods (chemical and plasma) have been used and the results have been compared by using the following test methods: 1) X-ray diffraction (XRD) for measuring the percentages of crystallinity of flax fibres; 2) scanning electron microscopy (SEM) for investigating morphological changes of flax-fibre surface before and after treatment; 3) soft X-ray spectromicroscopy for compositional analysis of flax fibres; 4) color test; 5) density test; and 6) mechanical properties test including tensile strength measurements.

1.1 Objectives

The main goal of this project was to study the effect of plasma and chemical treatments on the structure of flax fibre, including mechanical properties, crystallinity, color change, and surface alteration. In particular, the specific objectives of this study were:

1. to evaluate the effect of plasma treatment on the microscopic structure of flax fibre;
2. to investigate also the effect of chemical treatment on the microscopic structure of flax fibre;
3. to compare the results obtained from part 1 and 2; and
4. to study the advantages and disadvantages of using plasma/chemical modification of flax fibres.

The objectives of this study are discussed in Chapter 1. A literature review about flax fibre and fibre modification is given in Chapter 2. Chapter 3 is devoted to the materials and methods used in this project, including testing methods and how the related properties were measured. Results and discussion are provided in Chapter 4. Conclusion, a list of suggestions for future research, and references are in Chapter 5, Chapter 6, and Chapter 7, respectively. Supporting data are located in the Appendices.

2. LITERATURE REVIEW

To use natural fibres as reinforcement, a good basic understanding of its structure and properties would be of assistance, because any changes in its structure may significantly affect its properties. This chapter summarizes previous works done concerning the composition of flax fibre and the effect of both plasma and chemical treatments on the structure of flax fibre.

2.1 The Characteristic of Flax Fibres

In this chapter, flax fibre history, flax-fibre bundles, composition and structure of flax fibre, chemical structure of cellulose, and mechanical properties of flax fibres are discussed.

2.1.1 Flax-fibre history

The oldest agricultural plant known to man is perhaps flax. Flaxseeds and fishing nets made of flax have been found dating back to 7000 B.C. (Sharma and van Sumere 1992). There are two different groups of varieties of *Linum usitatissimum*, called flax and linseed (or seed flax). Flax or, in other words, flax fibre is grown for production of short and long fibres. The process of retting and environmental conditions can affect the quality of the fibres. Both the seeds and the stem of the flax plant can be used for industrial and non-industrial applications. Long fibres are used for linens, rugs, and strong threads. Linseed oil is extracted from crushed linseeds and this oil can be

used in oil paints, varnishes, and linoleum. Today, Canada is one of the major flaxseed producer and exporter to other countries. Tow (short fibre) can be produced from linseed straw.

2.1.2 Flax-fibre bundles

A bundle of flax fibre usually is made of 10-40 fibres, and bound as one by pectin and lignin (Baley 2002) as shown in Figure 2.1. Each fibre has a polygon-shaped cross section with 5-7 sides (Figure 2.2) and the transverse (thickness) and the longitudinal dimensions of fibre, reported by Baley (2002), lie in the range of 5-76 μm and 4-77 mm, respectively. The presence of fibre nodes (Figure 2.3) in the longitudinal direction influence fibre properties. One hundred to 500 fibre nodes in a single fibre, 2-5 cm long were reported by Khalili and co-workers (2002).

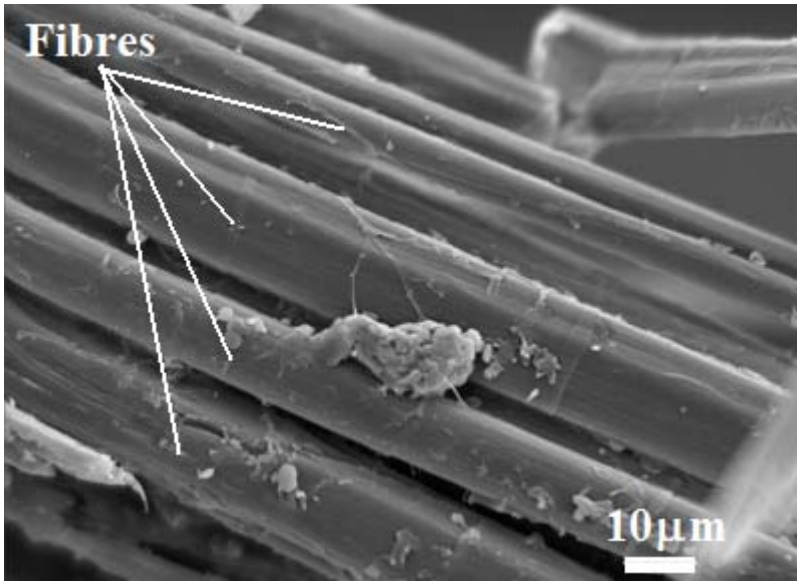

Figure 2.1 A bundle of flax fibres.

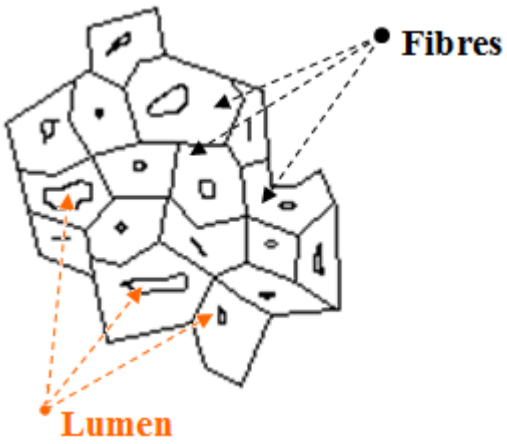

Figure 2.2 Cross section of a fibre bundle (reproduced from Baley 2002).

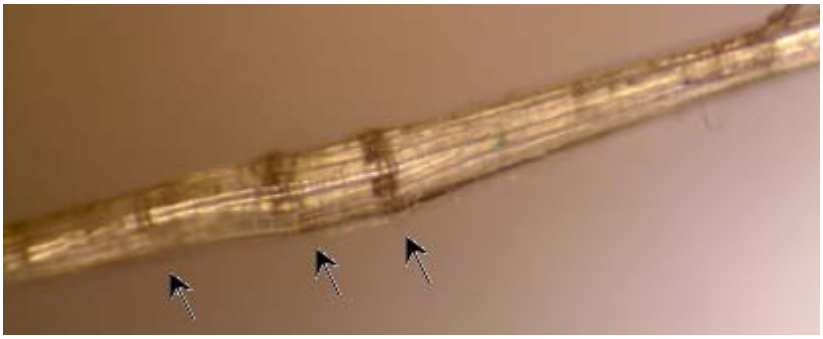

Figure 2.3 Location of nodes in a flax fibre (arrows show the locations of fibre nodes).

2.1.3 Composition and structure of flax fibre

The chemical components of flax fibre can be categorized into two separate groups: cellulosic (cellulose) and non-cellulosic substances (hemicellulose, lignin, waxes, water soluble substances, pectin, and water). In other words, flax fibre is a composite material in which pectin, lignin, and hemicellulose hold the individual cells together and act as bonding agents.

The yellow color of flax fibres is attributed to the presence of lignin and other non-cellulosic materials which in turn decrease the crystallinity of flax fibre (Reddy and Yang 2005), and also they can not be studied by X-ray diffraction (reminding that the effect of non-cellulosic materials on X-ray diffraction curves is reflected on the amorphous regions). Table 2.1 shows the percentages of these materials in typical flax fibre reported by many authors.

Table 2.1 Chemical composition (%) of flax straw.

Cellulose	Hemi-cellulose	Pectin	Lignin	Water soluble	Wax	Water	Source
64.1	16.7	1.8	2.0	3.9	1.5	10.0	Bledzki and Gassan (1999)
71.0	18.6	2.3	2.2	-	1.7	10.0	Bledzki et al. (1996)
65-87	-	-	small	-	-	12	Wiener et al. (2003)
66.14	16.24	2.14	2.0	3.49	1.09	8.9	Bhattacharya and Shah (2004)

The structure and chemical composition of flax fibre depend on climate, age, soil quality, the level of plant maturity, and retting process (Pallesen 1996). This can explain the variability of the values mentioned on Table 2.1.

The flax fibre cell, with a small hole in the middle, the lumen, consists of two concentric cell walls, the primary wall and secondary wall, and the secondary wall in turn consists of three layers called S_1, S_2, and S_3 (Figure 2.4). S_2 mainly forms the bulk of the fibre cell (Stamboulis et al. 2001). The angle of cellulose orientation (fibrils) inside the flax fibre is about 10^o and the cellulose is surrounded by hemicellulose and lignin, therefore, the flax fibre cell can be imagined as a composite material (Figures 2.4 and 2.5) (Bledzki and Gassan 1999; Hearle 1963).

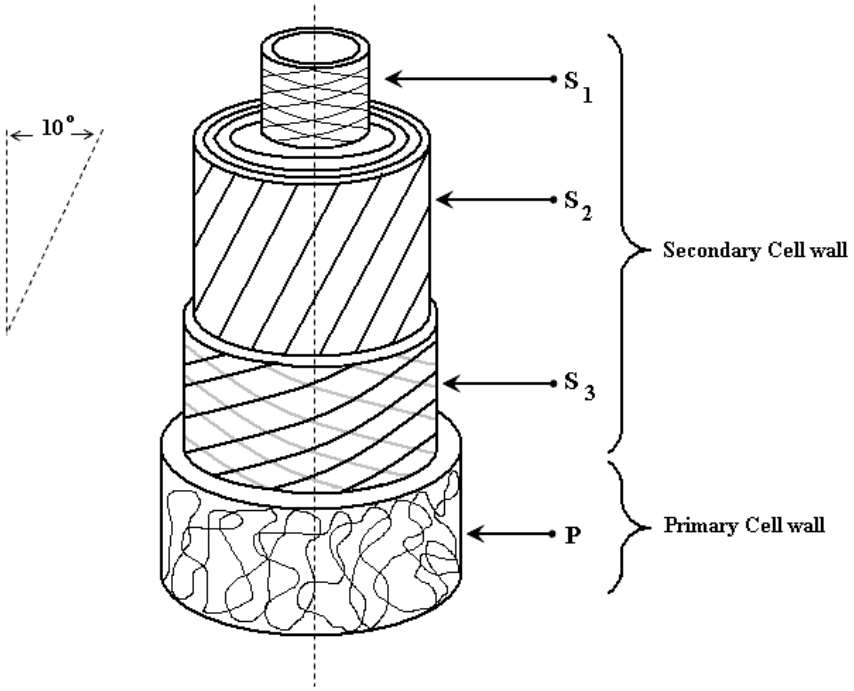

Figure 2.4 Schematic of flax fibre cell with primary and secondary walls (reproduced from Baley 2002).

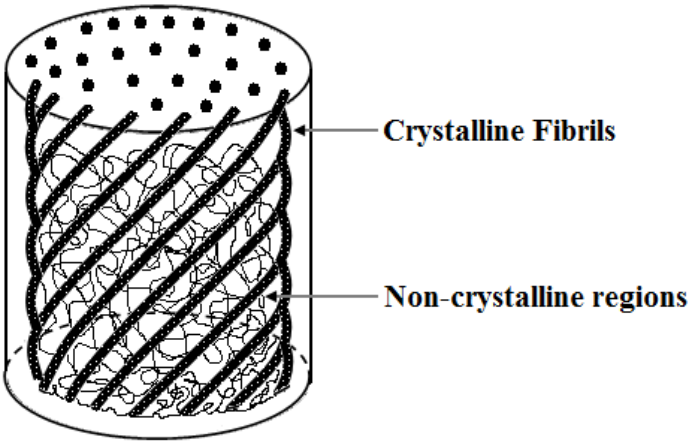

Figure 2.5 Fibril arrangement in natural cellulose fibre (reproduced from Hearle 1963).

2.1.4 Chemical structure of cellulose

Cellulose is the main component of vegetable fibres. The repeating unit (monomer) is called anhydro-d-glucose (Figure 2.6). Three alcohol hydroxyls (**-OH**), which are attached to the monomer unit, play an important role in chemical interaction (hydrogen bonds) between the cellulose molecules and other molecules (Bledzki et al. 1996).

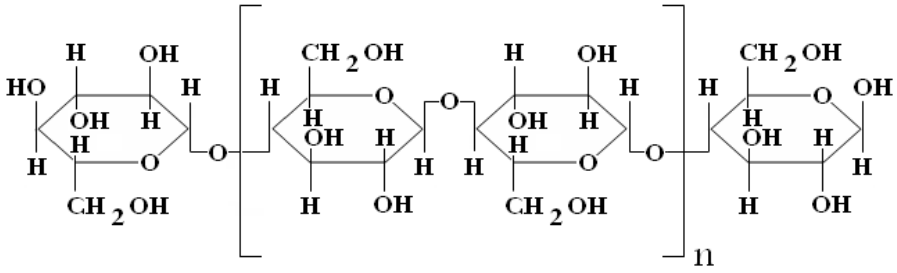

Figure 2.6 Cellulose macro molecule (reproduced from Bledzki et al. 1996).

The four different forms of cellulose, having different molecular structures are: cellulose I, II, III, and IV. The native form of cellulose is cellulose I. Cellulose II can be obtained by mercerization of cellulose I. Cellulose III and IV are derived from cellulose I and II (called cellulose III_I, IV_I, III_{II}, and IV_{II}) (Ishikawa et al. 1997). The X-ray diffraction curve for each cellulose form is different from each other (Figure 2.7). Converting cellulose I to cellulose II in pine wood has been studied by Borysiak and Doczekalska (2005). They used a sodium hydroxide (NaOH) treatment with different concentrations and different treatment times. Their results showed that the amount of cellulose II increased when both the concentration of the sodium hydroxide (NaOH) solution and treatment time increased. They also reported an overall decrease in crystallinity of the pine wood after it was subjected to the mercerization process. The diffraction curves

from flax fibre cellulose, in its native form (cellulose I), before and after surface treatment show three well-defined sharp peaks in different angles which are related to different Bragg's planes. The directions of these planes and the angular positions of the peaks for water-retted flax reported by Ansari and co-workers (2001) are shown in Figure 2.8.

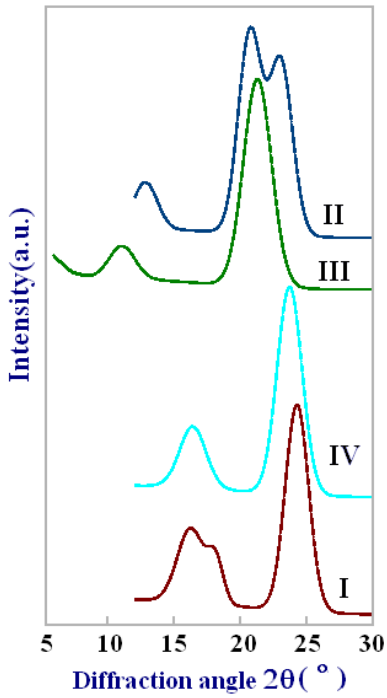

Figure 2.7 X-ray diffraction pattern for ramie cellulose I, II, III, and IV (reproduced from Ishikawa et al. 1997).

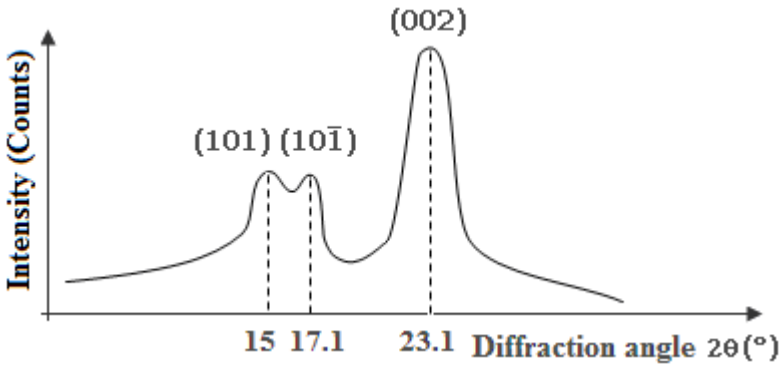

Figure 2.8 X-ray diffraction pattern for water- retted flax fibre. The directions of Bragg's planes are given by $(101), (10\,\bar{1})$, and (002) (Ansari et al. 2001).

Table 2.2 and Figure 2.9 show the unit-cell dimensions and the positions of atoms in cellulose I derived from flax and cotton fibres reported by Ansari and co-workers (2001) and Bledzki and Gassan (1999).

Table 2.2 Unit-cell dimensions of cellulose I (natural cellulose) derived from flax fibre (Ansari et al. 2001).

a(nm)	b(nm)	c(nm)	β(°)	Space Group	Crystalline Density
0.823	1.037	0.788	83.5	$P2_1$	1.609

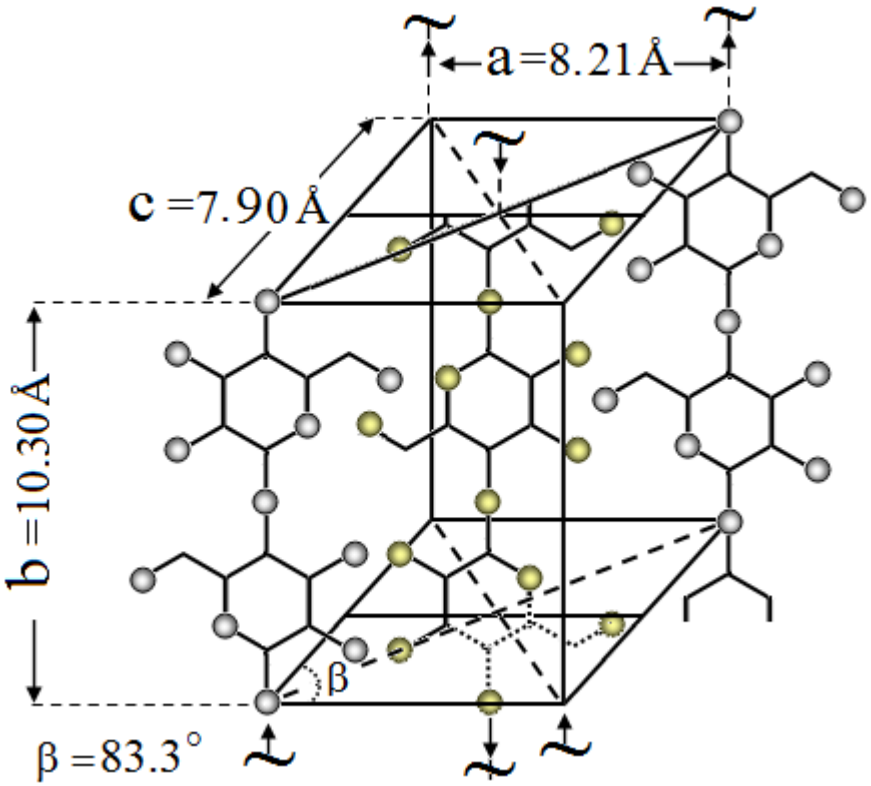

Figure 2.9 Unit-cell dimensions and space group of cellulose I derived from cotton fibre (reproduced from Bledzki and Gassan 1999).

The degree of polymerization, molecular orientation, and crystallinity are the concepts, used to explain some properties of the cellulose macro molecule inside the natural fibre.

In this work, the last concept has been used. In general, both molecular orientation and crystallinity play an important role in the mechanical properties of macro molecules. It is well known that cellulose macro molecules in flax fibres exist in both amorphous and crystalline forms, and it is important to know the orientation of crystallites and the percentage of cellulose in the fibre in achieving high stiffness and strength (Ward 1962; Hearle 1963).

2.1.5 Mechanical properties of flax fibres

The density of flax and man-made fibres quoted by different researchers is listed in Table 2.3. The density of flax fibre is about 1.5 g/cm^3 (the density for carbon and aramide is 1.4 g/cm^3) and, as a result, shows a comparable specific strength in comparison to the synthetic fibres (Table 2.3).

Table 2.3 Mechanical properties of flax and synthetic fibres.

Fibre	Tensile Strength (MPa)	Elastic modulus (GPa)	Density (g/cm^3)	Source
Flax				
Flax	345-1035	27.6	1.5	Bledzki and Gassan (1999)
Flax	-	-	1.53	Baley (2002)
Flax	344	27	1.5	Saheb and Jog (1999)
Flax	780	27.6	-	George et al. (2001)
Flax	1100	100	1.50	Bledzki et al. (1996)
E-glass	2000-3500	70.0	2.5	Bledzki and Gassan (1999)
S-glass	4570	86.0	2.5	Bledzki and Gassan (1999)
Aramide (normal)	3000-3150	63.0-67.0	1.4	Bledzki and Gassan (1999)
Carbon (Standard)	4000	230.0-240.0	1.4	Bledzki and Gassan (1999)

As previously stated, the structure of flax fibres depends on climate and therefore, the mechanical properties of flax fibres are mainly determined by their structure. In general, the mechanical properties of flax fibres are dependent on the following factors:

1. Environmental conditions - The fibre structure is affected by environmental conditions and in turn a change in the structure causes a change in mechanical properties.
2. Hydrophilic nature of flax fibre - The ability of flax fibre to absorb water mainly hinges on the content of the non-cellulosic part (mainly hemicelluloses) and the porous content of the fibre (Bledzki and Gassan 1999) which is related to the fibre structure and composition.
3. The initial size of flax fibre - Shorter fibres are more uniform than longer ones e.g. the number of fibre nodes in long fibres is more than short ones.
4. Temperature - Temperature can change both the degree of polymerization (DP) and crystallinity of cellulose in flax fibre. Gassan and Bledzki (2001) reported an insignificant decrease in both tenacity and DP of untreated flax fibre at a temperature less than 170°C. They also mentioned that when the temperature increased above 170°C, the DP and tenacity dropped off quickly. The fibres in both cases were thermally treated for 120 min.

Other factors such as defects, fibre nodes, moisture content, and non-uniform chemical composition in flax fibres also determine the characteristic values of the fibres.

2.2 Surface Treatment of Flax Fibres

The reasons for offering a surface treatment of flax fibres are as follows:

a) Hydrophilic nature of flax fibres - High water absorbability of natural fibre causes the swelling of fibres and, therefore, results in the production of micro cracks in composites and degradation of mechanical properties. A proper method of treatment might help decrease the ability of fibres to absorb moisture, e.g. chemical treatment decreases the amount of pectic substances and hemicelluloses (having a relatively high water absorption) in fibre, and it also can change the structure of the cellulosic component.

b) Poor adhesion between matrix and fibres - High-performance light-weight thermoplastics like polyethylene and polypropylene are inert materials, and composites made of these materials and natural fibres do not show sufficient strength. Surface modification of natural fibres may enhance their adhesion to polymer matrices.

Chemical treatment which consumes a large amount of energy leaves large amounts of unwanted and waste material behind; therefore, the need for environmentally friendly treatment of materials is necessary. Plasma surface treatment might be a good candidate for environmentally friendly treatment of material for the following reasons:

1. The capability of plasma to create free radicals and active groups for improving the interfacial adhesion (Lieberman and Lichtenberg 2005);
2. Plasma treatment produces less environmental contaminants than chemical ones; and
3. Plasma treatment might be used in order to remove organic surface contamination from fibre.

2.2.1 Plasma treatment of flax fibre

The word plasma comes from the Greek language and it means something molded. In physics, plasma or the fourth state of matter is a partially hot ionized gas containing positive and negative charges which shows collective behaviour (Figure 2.10). The motion of each particle inside the plasma gas is controlled by electromagnetic fields produced by other particles and external sources (Lieberman and Lichtenberg 2005).

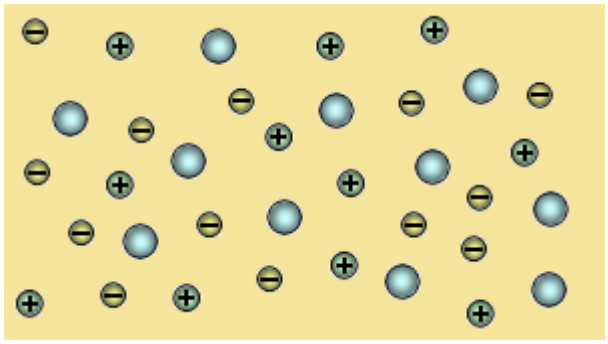

Figure 2.10 Schematic of plasma gas containing neutral, positive, and negative particles.

Two characteristics of a plasma gas are:

1. Temperature - Plasma temperature is measured in electron volts (eV) or Kelvin (K) and a specific temperature is devoted to each type of particles e.g. the temperature of neutral particles (T_n), the temperature of negative particles or electrons (T_e), and the temperature of positive particles or ions (T_i).
2. Density - Plasma density for each type of particles is defined as the ratio of the number of species to its volume (Figure 2.11), expressed in units of particles per cubic centimetre and given by

$$\text{Plasma density} = n_\alpha = \frac{(\text{Particle number})_\alpha}{\text{Volume}} = \frac{(\text{Particle number})_\alpha}{\Delta V}, \qquad (2.1)$$

where: α = n (neutral particles), e (negative particles or electrons) or i (positive particles or ions), and

ΔV = the volume of particles (cm^3).

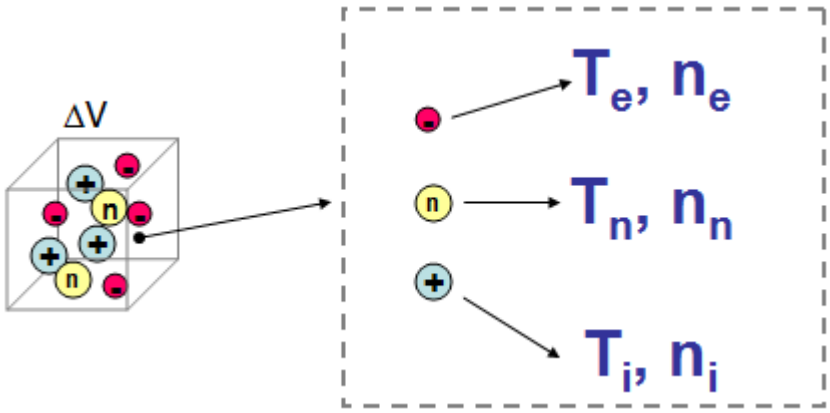

Figure 2.11 For each type of particles inside a small volume of ΔV, density and temperature are different e.g. the temperature (density) of electrons, neutral particles, and ions are shown with $T_e(n_e)$, $T_n(n_n)$, and $T_i(n_i)$, respectively.

2.2.1.1 Degree of ionization

The degree of ionization in plasma is defined by

$$\text{Degree of ionization} = \frac{n_i}{n_i + n_n}, \tag{2.2}$$

where: n_i = the density of positive particles or ions (particles per cubic centimetre), and

n_n = the density of neutral particles (particles per cubic centimetre).

2.2.1.2 Hot and cold plasma

In hot plasma, the degree of ionization is high or almost 100%, while this value in cold plasma is less than 3%. In hot plasma, the temperature of electrons is really high (e.g. 10^6 K), whereas this value in cold plasma is low (e.g. 10^3 K).

2.2.1.3 Direct current (DC) glow discharge plasma

In a DC glow discharge plasma reactor, the plasma is formed by applying a DC potential between two electrodes. The electrodes are located inside a glass container under vacuum. Plasma-forming gas is employed after vacuum has been applied. The interaction of a cosmic ray or a photon with a molecule or an atom of plasma gas releases an electron and creates an ion. Collision between the electron and other molecules or atoms of plasma gas occurs while accelerating the electron toward the positive electrode. This collision produces more ions and free electrons inside the gas and results in the production of plasma. In the same way, a high energy ion can help generate more ions and electrons in plasma gas.

Electric discharge (cold plasma) is one of the methods used for changing the chemical structure as well as the topography of the surface of a material. When a sample is exposed to plasma, ionized atoms and molecules are able to react chemically with exposed surfaces. Different effects are often observed including etching, modification of the material surface, and surface oxidation (Lieberman and Lichtenberg 2005).

Depending on type, nature of the gases used, treatment time, gas flow rate, and applied voltage between two plates, a variety of surface modification could be achieved. The effect of plasma treatment on natural fibre might be categorized in two types of surface and structure changes (bulk modification), however, cold plasma does not affect the bulk properties of materials.

Wong and co-workers (2000) used radio frequency plasma (RF) with a radio frequency of 13.56 MHz for treating flax fibres. In this experiment, the samples were exposed to argon and oxygen gases with different treatment times. They reported formation of cracks and voids on the surface of flax fibres due to the plasma erosion.

They also noticed that as the treatment time increased, the depth of voids (micropores) etched by the plasma increased with pore width.

Xu and co-researchers (2006) observed the appearance of some cracks on the surface of bamboo fibres after 1 min of argon plasma treatment, and they also remarked upon an improvement in its dyeability and wettability after plasma treatment. They realized that as the treatment time was increased, the change on the fibre surface became more obvious and the fibre surface became rougher. In comparison to bamboo fibres, it seems that helium plasma treatment does not affect water sorption of flax fibres after treatment, because Gouanve and co-workers (2006) reported no change in the surface modification of flax fibres after treatment.

The effect of plasma treatment on the mechanical properties of natural fibre-based composites has been studied by many researchers. Olaru and co-researchers (2005) used cold high-frequency methane plasma for treating wood fibres. It was observed that the values of elastic modulus and strength of the composites (polyethylene as a matrix) were promoted or the plasma treatment of the wood fibres improved the compatibility between fibre and polymer matrix (Figure 2.12).

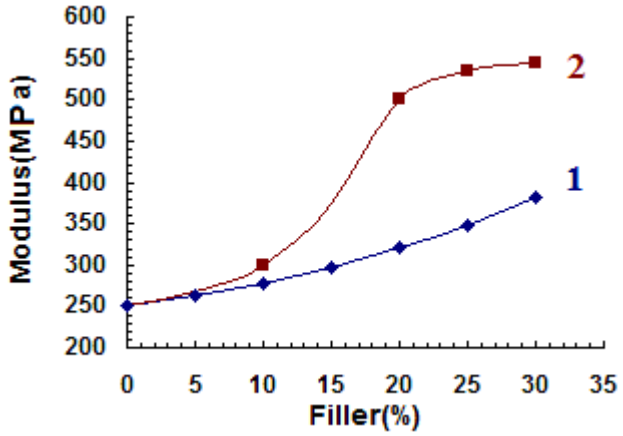

Figure 2.12 Elastic modulus versus percentage of filler for untreated (1) and plasma treated (2) wood fibres (reproduced from Olaru et al. 2005).

High-frequency capacitive discharge plasma (HFC) with air as a plasma-forming gas has been used by Khammatova (2005) to determine the effect of plasma treatment on the strength (breaking load) of textile thread made of flax fibres. The results showed an increase in strength by 64%.

It is well known that cellulose, one of the flax fibre components, can be in both crystalline and amorphous states. The effect of plasma treatment on flax fibre structure is reflected on the peaks obtained from X-ray diffraction (XRD) curves. By analysing these peaks, the crystallinity of flax fibre before and after treatment, and the size of the coherent scattering regions can easily be determined. Khammatova (2005) reported a significant increase in both crystallinity and the regions of coherent scattering of flax fibres (peak number 3) treated by HFC discharge plasma.

2.2.2 Chemical treatment of flax fibre

As cited earlier, there are many reasons that make flax fibres incompatible with polymers in composites. In order to improve the mechanical properties of

biocomposites, chemical treatment (surface modification) of flax fibre will be necessary. For instance, chemical treatment may help to obtain a strong adhesion between the reinforcing fibres and the matrix for the purpose of having an efficient transfer of stress and load distribution throughout the interface. Chemical treatment is based on the following rule:

It is often possible to improve compatibility between two incompatible materials (in this case polymers and natural fibres) by bringing in a third material (coupling agents).

In silane treatment of natural fibre, silane as a coupling agent acts as a link between the matrix (polymer) and the cellulose by creating a chemical bond with both the cellulose and the polymer (George et al. 2001). The linkage between cellulose and silane occurs through a siloxane bridge whereas, the organofunctional group of silane attaches to the polymer (George et al. 2001) (Figure 2.13).

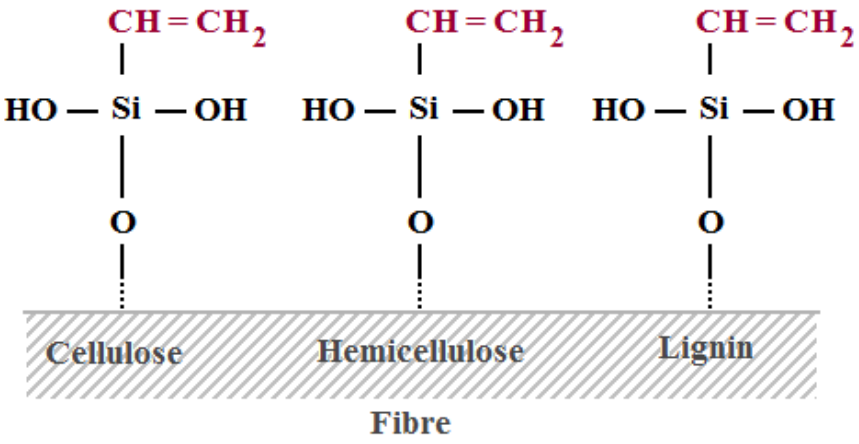

Figure 2.13 Schematic of interaction between natural fibre and silane (Sreekala et al. 2000).

A variety of fibre surface modifications, such as mercerization, peroxide treatment, silane treatment, isocyanate treatment, and graft copolymerization can be

applied in the reduction of hydrophilicity and enhancing interfacial adhesion between the matrix and fibre (George et al. 2001).

Sharma and van Sumere (1992) reported a decrease of moisture regain in boiled flax fibres (2% NaOH). In their report, this reduction was attributed to the removal of non-cellulosic material such as hemicellulose and pectic substances from fibres.

Wang (2004) applied three different treatments: silane, benzoylation, and peroxide on flax fibres and observed a reduction in water absorption. She also reported a higher tensile strength in the silane- and peroxide-treated fibres than that of the untreated fibres. In her report, lower tensile strength was observed in benzoylation treated fibres.

Chemical treatments on natural fibres affect structural characteristics of untreated fibres. Gassan and Bledzki (2001) reported a reduction in the degree of polymerization (DP) of both jute and flax fibres after alkali treatment, and their results also showed a reduction in the crystallinity of flax and jute fibres after modification. The flax fibres were treated for 20 min at a temperature of 20°C with a solution of sodium hydroxide.

2.3 Summary

This chapter was devoted to a review about flax fibre history, composition, mechanical properties, chemical structure, and surface modification. Only few studies in literature were related to the effect of plasma treatment on the microscopic structure of flax fibres and also some properties of flax fibres such as crystallinity, tenacity, and the size of coherent scattering region were calculated. The results of these studies were limited by testing conditions, e.g. treatment time, gas, and pressure. In fact, plasma surface modification of flax fibres is affected by many factors for instance, plasma gas,

gas flow rate, pressure, and plasma reactor type; therefore, more studies need to be done in order to find the best plasma treatment conditions for flax fibres.

One part of this chapter was also dedicated to previous studies related to the effect of chemical treatment on the microscopic structure of flax fibres and flax fibre properties for example; crystallinity, water absorption, and tensile strength in this section were discussed.

This study was aimed to develop and study the plasma/chemical treatment of flax fibres by using different treatment times and soft X-ray spectromicroscopy was introduced as a new method to analyse the flax fibre structure and fibre-matrix interfacial properties. Thermal properties of untreated/treated flax fibres were measured using the differential scanning calorimetry.

3. MATERIALS AND METHODS

In this chapter, the materials, devices, and experimental procedures used to accomplish this study are introduced, and also a theoretical background about measuring the crystallinity of flax fibre, as a method for comparing modified and unmodified flax fibres, is presented.

3.1. Materials

The main material used in this project was flaxseed fibre grown in Saskatchewan. Many steps such as retting, decortication, scutching, hackling, etc., are involved in order to separate fibres from flax straw. The amount of shives (woody parts of the fibre) inside the fibre defines its purity of flax fibre, e.g. fibre with 85% purity contains 15% shives. In this study, two varieties of flax fibre with purities of: 1) 78.4% designated as F1 and used for chemical treatment; and 2) 92.5% designated as F2 and used for plasma treatment were employed. Both fibres were provided by Biolin Research Inc., Saskatoon, SK.

Chemical treatment of flax fibre consisted of two steps: 1) sodium hydroxide; and 2) silane treatments. The main materials used for chemical treatment in this study were: 1) sodium hydroxide (PPG Industries, Inc., PA); 2) vinyltrimethoxysilane (Sigma-Aldrich, MO, USA); and 3) isopropyl alcohol ACS grade (EMD Chemicals Inc., NJ).

The general steps in sample preparation of soft X-ray spectromicroscopy are: fixation, dehydration, infiltration, embedding, and sectioning. Flax fibres are flexible and soft materials, and need to be embedded in a polymer resin named trimethylolpropane triglycidyl ether (TTE) amine resin, in order to be easily sectioned. TTE amine resin with a molecular formula of $C_{30}H_{56}O_6N_2$ (Sigma-Aldrich, Inc., MO) is a 1:1 ratio of TTE to 4,4'– methylenebis (MMHA). Information about TTE and MMHA is given in Table 3.1.

Table 3.1 Information about trimethylolpropane triglycidyl ether (TTE) and 4,4' – methylenebis (MMHA) resins used in soft X- ray spectromicroscopy.

Polymer	Density (g/ml) at 25 ºC	Molecular Formula
TTE*	1.157	$C_{15}H_{26}O_6$
MMHA**	0.94	CH_2 $[C_6H_9$ (CH_3) $NH_2]_2$

* Trimethylolpropane triglycidyl ether

** 4,4' – Methylenebis (2- methylcyclohexylamine)

3.2 Flax Fibre Thickness

The thickness of untreated fibres (F1) was measured in Biolin Research Inc., Saskatoon, SK, Canada. The fibres were first spread on the glassy part (surface) of a scanner (Epson Photo Smart, Epson, Tokyo, Japan) and then were scanned (Figure 3.1). Data analysis was done using a special software called Fibreshape version 4.3 (IST-Innovative Sintering Technologies Ltd, Vilters, Switzerland). The thickness of 10 different samples was measured. The author was not involved in using the software for measuring the fibre thickness and therefore, more information about the method used for fibre thickness measurement can be found in software users manual.

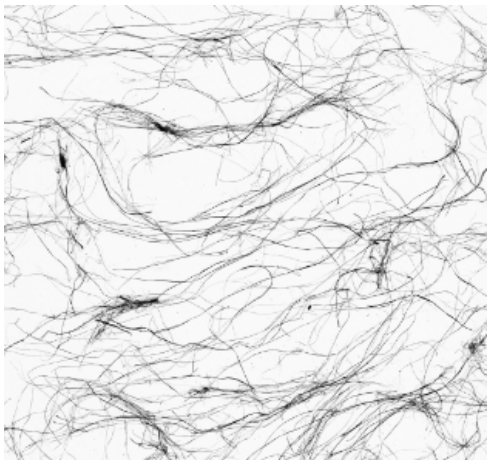

Figure 3.1 Photograph of scanned fibres.

3.3 Flax Fibre Density

The density of a body is defined as the ratio of its mass to its volume. The mass of samples (untreated flax fibres) was measured using a Galaxy 160D weighing scale (OHAUS Scale Corporation, Florham Park, NJ) and the volume of the samples was measured using a gas-operated pycnometer (Quantachrome Corporation, Boynton Beach, FL) at room temperature (about 23°C). Pressure was 101.6 kPa. In order to calculate the density, three samples (with average mass of 4.61 g) were chosen and then the density of each was measured. At the end, the average of these three measurements was calculated and reported as actual density of flax fibre expressed in g/cm^3.

3.4 Color Test

The color of chemically treated and untreated flax fibres (F1) was determined using the HunterLab Color Analyzer – LabScan System (Hunter Associates Laboratory,

Inc., Reston, VA) (the setting is given in Table 3.2). The values of a (-a=green to +a=red), b (-b=blue to +b=yellow) and L (0=black to 100=white) were measured and converted to RGB system (red, green and blue, using OpenRGB software version 2.01.80406 (Logicol Company, Trieste, Italy) with the aim of visualizing color changes. A further examination of color changes in flax fibre was done by calculating the index ΔE as given by:

$$\Delta E = \sqrt{(L - L_{base})^2 + (a - a_{base})^2 + (b - b_{base})^2} \quad , \tag{3.1}$$

where: L, a, b = color coordinates of the treated fibre samples, and

L_{base}, a_{base}, b_{base} = color coordinates of untreated fibre samples (F1).

Table 3.2 Settings used in HunterLab color analyzer.

Area view	Port size	Illuminant	Observer
12.7 mm(0.50 in)	25.4 mm(1 in)	D65	10°

Three specimens of treated/untreated fibres, with average weight of 4.40 g each, were taken and put inside a plastic petri dish. Sufficient amounts of fibres were used to prevent the transmission of light through the fibres inside the petri dish (the incident light was reflected from the sample surface without passing through the sample). The color measurement was done for each sample which produced 4 times reading and at the end, the average of L, a, and b values was calculated.

3.5 Tensile Test

Flax fibres were extracted by hand from untreated/chemically treated fibres (F1) and then mounted on a rectangular paper and glued with epoxy (Henkel Canada

Corporation, Brampton, ON). Afterwards, the mounted fibre was put on a texture analyser TA.XT2 (Texture Technologies Corp., Scarsdale, NY), controlled by a PC (operated by the software package Texture Expert Exceed version 2.64, Stable Micro System Ltd., Surrey, England), and the paper was carefully cut with a pair of scissors (Figure 3.2).

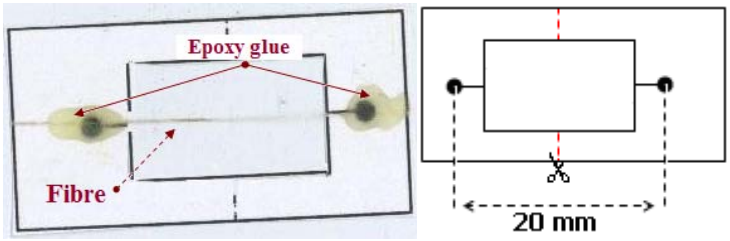

Figure 3.2 Schematic of the rectangular paper, used for tensile test. The initial length of the fibres was 20 mm.

The test was performed at a crosshead speed of 5 mm/min, and approximately 10 fibres were tested for each sample (10 replications for each chemical treatment and 10 replications for untreated fibres), and at one gauge length (20 mm). Before the test, the diameter of the fibres was measured in at least 3 different locations (Figure 3.3) with a light optical microscope (Nikon Optiphot with a magnification of 100 (Nikon Inc., Tokyo, Japan), interfaced with a PC (operated by the software package Pax-it version 6, MIS Inc., Villa Park, IL). The average of these three measurements was calculated and reported as the diameter of fibre. The tests were conducted at the standard laboratory temperature of 23°C.

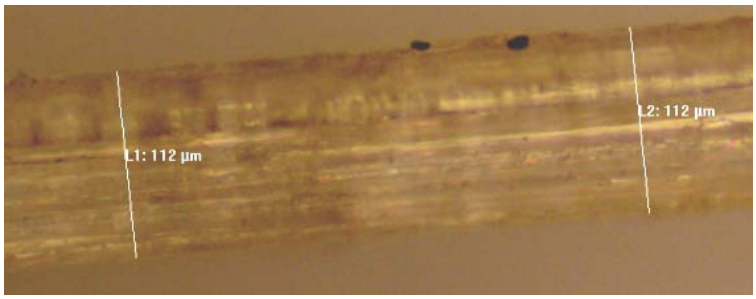

Figure 3.3 Fibre diameter was measured in at least 3 different locations (2 locations are shown).

The texture analyser was set up to display the force-displacement curve. For reasons of simplicity, the fibres were assumed to be round. The maximum strength (tensile strength) as defined by:

$$\sigma_{max} = \frac{F_{max}}{A_o} \quad , \tag{3.2}$$

where: F_{max} = maximum load (N), and

A_o = fibre cross section area (m^2),

and elastic modulus of the fibres were calculated from the tensile test results using a linear fitting method.

3.6 Surface Modification of Flax Fibres

In this study, both chemical and plasma treatments were used in order to modify the surface of flax fibres. The treatment methods are explained below.

3.6.1 Chemical modification of flax fibres

Untreated flax fibres (F1) were dried in an oven (Despatch LDB-1-67, Despatch Industries, Minneapolis, MN) for about 48 h at 70ºC and then were weighed using a

balance (Adventurer Pro AV812, OHAUS Scale Corporation, Pine Brook, NJ). The flax fibres were treated in four different durations: 1, 2, 3, and 4 h, designated as T1, T2, T3, and T4, respectively. In order to provide similar conditions for the fibres (temperature, pressure, and sodium hydroxide concentration), an empty bucket was used, and then the bucket was partitioned into four equal parts using two plastic blades (Figure 3.4). The fibres were soaked in a 5% sodium hydroxide (NaOH) solution in distilled water for different times.

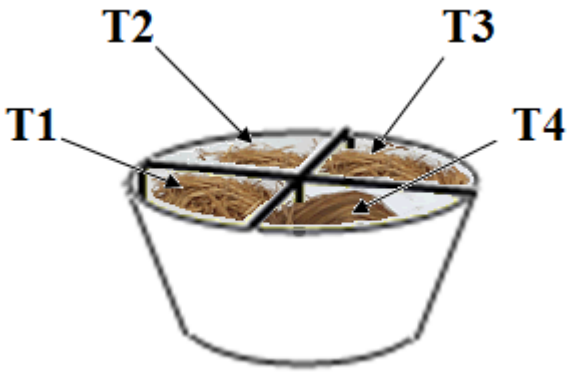

Figure 3.4 Schematic of the partitioned bucket used for chemical treatment of flax fibres. The fibres inside the bucket were treated four different durations: 1, 2, 3, and 4 h designated as T1, T2, T3, and T4, respectively.

The pre-treated fibres were dipped in an alcohol water mixture (60:40) containing vinyltrimethoxysilane (1%) and the pH of the solution was maintained between 3.5 and 4.0 using pH indicator strips. When the chemical treatment was done, all fibres were washed and rinsed in distilled water at least 5 times and were dried again in the oven for 24 h at 70 ±1ºC. The fibres were weighed again after drying in order to measure the weight loss after the chemical treatment.

3.6.2 Plasma modification of flax fibres

The experimental system, used to study the flax fibres (F2) is a plasma reactor, called DC Glow Discharge Plasma (Figure 3.5) in the Department of Physics and Engineering Physics at the University of Saskatchewan. In order to produce uniform plasma, two plane–parallel metal plates were used. The plates (electrodes) are separated by a uniform gap of about 20 mm, through which two different gas flows can be passed simultaneously.

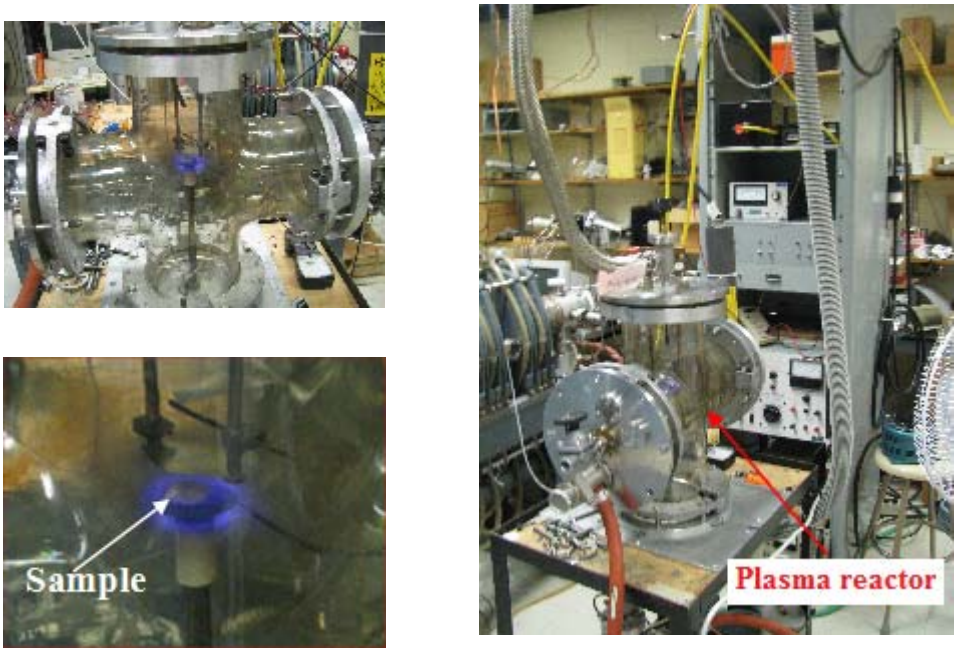

Figure 3.5 Different perspectives of the plasma reactor used in this work.

The electrodes were connected to a variable DC power supply (Figure 3.6), and to measure the temperature, a thermocouple was joined to the lower-metal electrode. Two vacuum pumps were used to pump out the air inside the reactor after the specimen was placed inside. The dimensions of the upper electrode are given in Figure 3.7 and

more details about the surface of the electrode were discovered after using the optical microscope mentioned in the previous section (3.5). Surface roughness of the electrodes causes the production of non uniform plasma (shown in Figure 3.8).

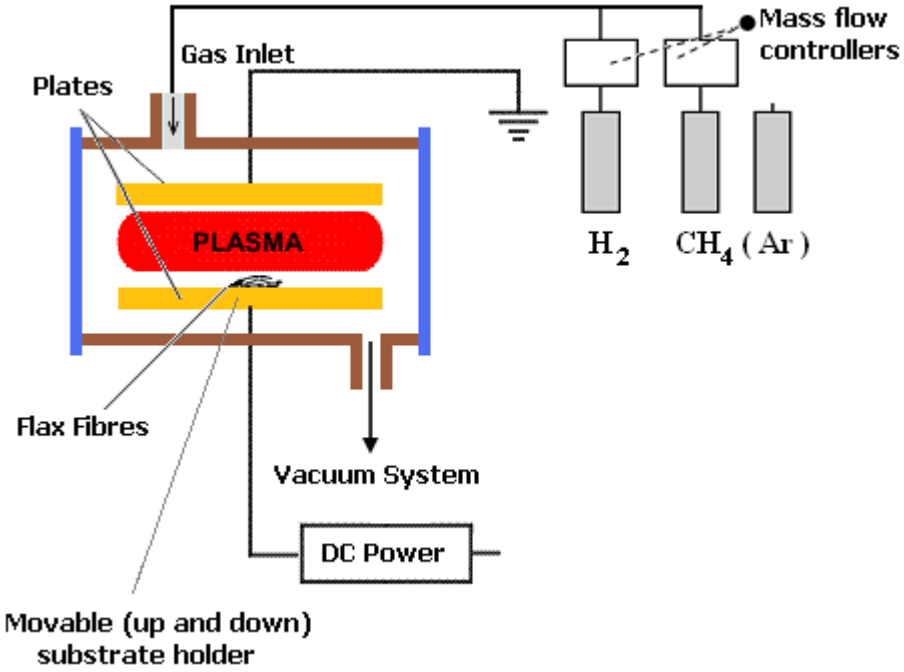

Figure 3.6 Experimental setup for the DC glow discharge plasma reactor.

Figure 3.7 Dimensions of the upper electrode.

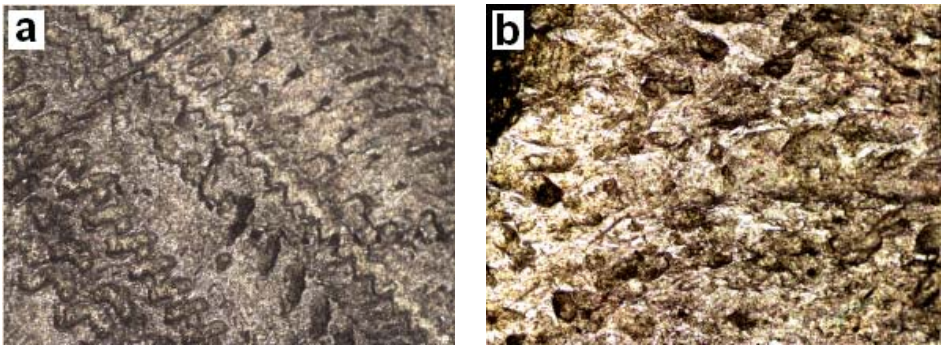

Figure 3.8 Photographs of the upper electrode showing: a) center part and b) near edge of the electrode surface.

The average sample mass used in this experiment was about 64.39 mg, and in order to treat the flax fibres uniformly and prevent the fibres from being sucked into the vacuum pump, the flax fibre was squeezed first (for this the reason, the finer fibres (F2) were used) and put inside the reactor at the center of the lower plate. Then the reactor was evacuated to a final pressure of 0.013 Pa (10^{-4} torr) and argon gas was introduced in a controlled flow around 2 SCCM (standard cubic centimetres per minute, referring to cubic centimetres per minute at 0°C and 1 atmospheric pressure). The minimum required voltage range when the argon gas started to glow (at this stage, the plasma was produced) was between 380 and 400 V. The fibres were treated for three different treatment times: 5, 10, and 15 min, designated as P1, P2, and P3, respectively. Plasma treatment conditions are listed in Table 3.3.

Table 3.3 Plasma treatment conditions for flax fibres.

	T (min)	Temp (ºC)	Gas	Pressure (Pa)	Gas rate (SCCM*)	Voltage (V)
P1	5	39	Ar	119.99-133.32	2.0	380
P2	10	51	Ar	26.66	1.9	400
P3	15	51	Ar	133.32-399.97	1.9	400

Note:SCCM=standard cubic centimetres per minute; P1, P2, and P3= 5, 10 and 15-minute argon plasma treated flax fibres, respectively.

3.7 X–Ray Diffraction (XRD)

X-ray diffraction was used in order to calculate the crystalline interplanar distances, the crystallinity, and crystallite size of flax fibre. The degree of crystallinity can be determined via XRD using X-ray diffraction intensity curves (Vonk 1973; Hindeleh and Johnson 1972 and 1974). Crystallinity measurement calculations require the separation of peaks from crystalline structure and the amorphous part; therefore, using a fitting method is required.

In the case of flax fibre, 4 peaks and a linear function (with two parameters) were considered; the three peaks (1, 2, and 3) were reserved for the cellulose and the fourth peak was devoted to the amorphous phase of the flax fibre (Figure 3.9). The functional form of the fitting equation is given by:

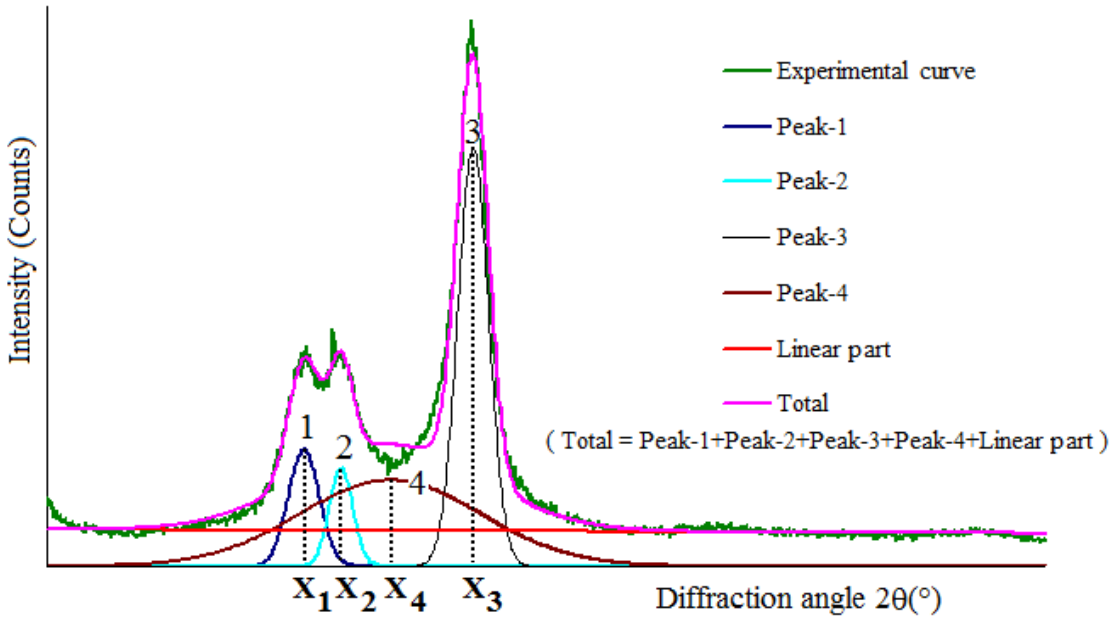

Figure 3.9 Peak resolution for flax fibre. Peak-1, Peak-2, and Peak-3 were considered for the cellulose and Peak-4 was assigned for the amorphous phase. A linear equation with two fitting parameters was added to the four peaks to complete the fitting function.

$$I(X) = \underbrace{Ae^{-\left(\frac{X-X_1}{B}\right)^2}}_{Peak-1} + \underbrace{Ce^{-\left(\frac{X-X_2}{D}\right)^2}}_{Peak-2} + \underbrace{Ee^{-\left(\frac{X-X_3}{F}\right)^2}}_{Peak-3} + \underbrace{Ge^{-\left(\frac{X-X_4}{H}\right)^2}}_{Peak-4} + \underbrace{\alpha X + \beta}_{Linear\ part}, \quad (3.3)$$

$$I(X) = \underbrace{I_1}_{Peak-1} + \underbrace{I_2}_{Peak-2} + \underbrace{I_3}_{Peak-3} + \underbrace{I_4}_{Peak-4} + \underbrace{\alpha X + \beta}_{Linear\ part}, \quad (3.4)$$

where: *I(X)* = intensity (the number of scattered X-ray photons or counts),

A, B, C, D, E, F, G, H, α, and β = fitting parameters, and

X_1, X_2, X_3, and X_4 = the location of the four peaks, respectively (°).

The crystalline and amorphous regions can be formed by an arrangement of polymer chains (shown in Figure 3.10). A crystalline region is part of macromolecules arranged in regular order. In amorphous regions (found between the crystalline regions), the arrangement of these macromolecules are in random and disorganized states.

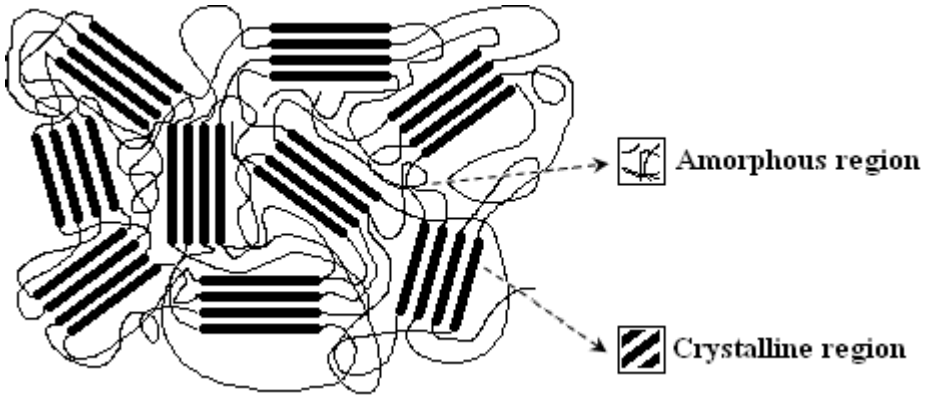

Figure 3.10 A solid semicrystalline polymer is made of two phases, crystalline and amorphous regions.

The degree of crystallinity (X_C) or the degree of structural order in a solid was defined by Kasai and Kakudo (2005):

$$Xc = \frac{The\ \ mass\ \ of\ \ crystallin\, e\ \ regions}{Total\ mass} \times 100 \ = \frac{S_{Crystallin\ e\ parts}}{S_{Total}} \times 100\ , \qquad (3.5)$$

where: $S_{Crystalline\ parts} = S_1 + S_2 + S_3$,

$$S_{Total} = S_{Crystallin\, e\ parts} + S_4(\ Amorphous\ \ parts\ )\ ,$$

$$S_i = \int_{S_0}^{S_p} s^2 I_i(s)\, ds\ ,\ s = \frac{2\sin(\theta)}{\lambda}\ ,$$

$$S_i = \int_{S_0}^{S_p} s^2 I_i(s)\, ds = \int_{\alpha_0=3}^{\alpha_p=50} \underbrace{\frac{1}{\lambda}\cos(\tfrac{\alpha}{2})\sin^2(\tfrac{\alpha}{2}) I_i(\alpha)}_{I_i^*}\, d\alpha\ ,\ \alpha = 2\theta,$$

$$S_i = \int_{\alpha_0=3}^{\alpha_p=50} I_i^*(\alpha)\, d\alpha\ ,i = 1,2,3,4\ ,\ \text{and}$$

λ = 1.54 Å (the wave length of X -ray beam).

More detail about the S_i is given in Figure 3.11.

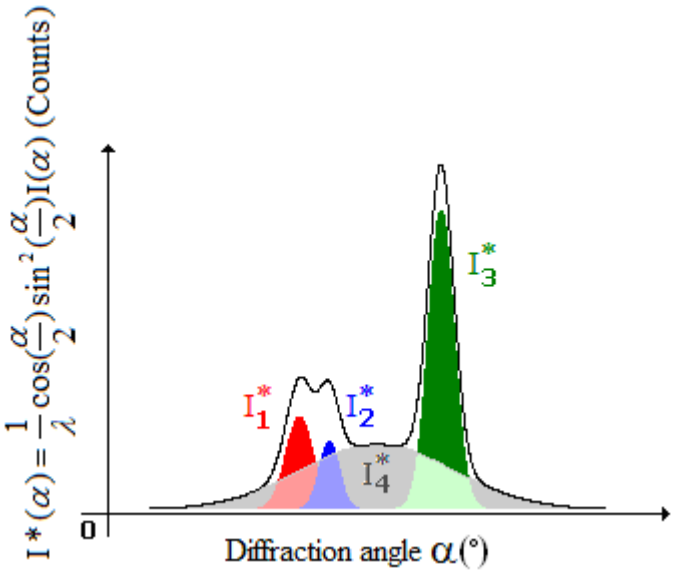

Figure 3.11 S_i (i =1, 2, 3, 4) is equal to the area under the curve (I_i^*) and the horizontal axis (α).

An estimate of crystallite thickness can be obtained from Scherrer's equation as given by Kasai and Kakudo (2005):

$$W = \frac{\lambda}{\beta_{\frac{1}{2}} \cos(\theta_B)}, \tag{3.6}$$

where: λ = 1.54 Å (the wave length of X -ray beam),

$\beta_{\frac{1}{2}}$ = the full width at half maximum of Bragg's peak from crystalline lattice (in radians) (Figure 3.12), and

θ_B = the angular position of Bragg's peaks (in radians or degree).

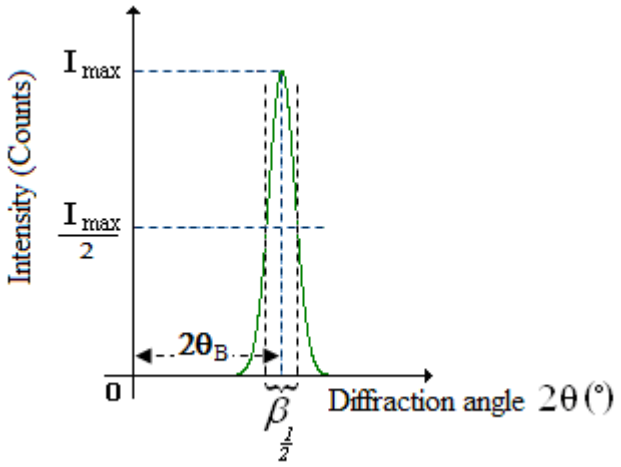

Figure 3.12 A schematic of $\beta_{½}$. By calculating $\beta_{½}$ from the XRD curve or from the fitted peak after fitting the crystallite size can easily be estimated.

In this work, the crystallite size of Peak 1, Peak 2, and Peak 3 has been calculated and shown as W1, W2, and W3, respectively.

Bragg's law (Figure 3.13) which relates the X-ray diffraction angle with interplanar spacing is defined by:

$$d = \frac{n\lambda}{2\sin(\theta_B)} \quad , \quad n = 1,2,3.... \quad , \tag{3.7}$$

where: λ (Å) = 1.54 (the wavelength of X - ray beam),

d = the interplanar spacing of the crystal (Å), and

θ_B = the angular position of Bragg's peaks (in radians or degree).

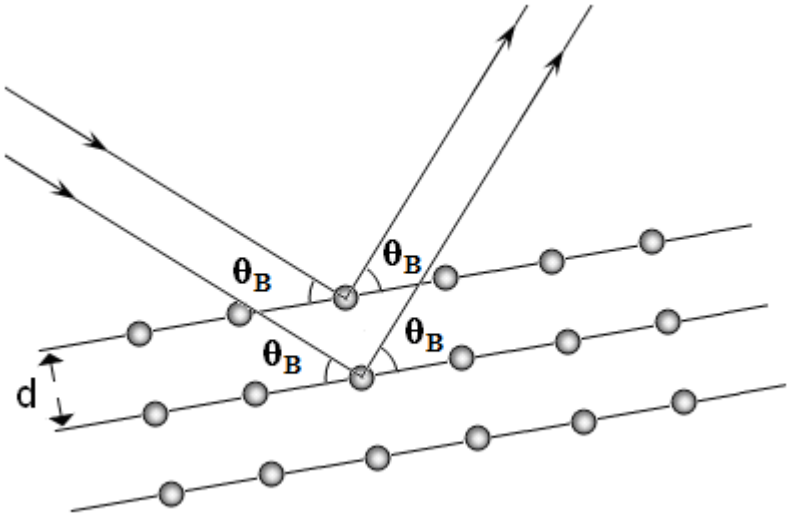

Figure 3.13 Schematic of the interplanar spacing and X-ray diffraction angle.

The spacing was calculated for the three peaks 1, 2, and 3 (designated as called d1, d2, and d3, respectively). The calculation was carried out for the first order (n=1).

The untreated and chemically/plasma treated fibres were analyzed with an X-ray diffractometer RICAKU 200R rotating copper anode with graphite monochromator, (RICAKU Co., Tokyo, Japan) and the wavelength was 1.54 Å (K_α). In this experiment, the samples were scanned from 2θ =3° to 2θ =50°. TableCurve version 5.01 (Systat Software Inc., Chicago, IL) was used for the purpose of fitting the experimental XRD curves, and the integration limits for calculating crystallinity(Xc) were S_0=0.03Å^{-1} (2θ =3°) and S_P= 0.55Å^{-1} (2θ =50°). The samples were exposed to X-ray radiation at

room temperature (~22°C) and the sample mass in this experiment ranged from 14.9 to 22.2 mg (Figure 3.14).

Figure 3.14 Photograph of the samples used for XRD test.

3.8 Morphological Characterization

In order to evaluate changes in the fibre surface morphology, the untreated and plasma/chemically treated fibres were analyzed by using a scanning electron microscope (JEOL 840A, JEOL Ltd, Tokyo, Japan) at an accelerating voltage of 15 kV. To achieve good electrical conductivity all fibres first were vacuum coated with a thin layer of gold on the surface.

3.9 Soft X-Ray Spectromicroscopy

A theoretical background and practical methods of soft X-ray spectromicroscopy are discussed in this chapter.

3.9.1 X–ray absorption

X-ray beams can interact with any matter in such a way that they may be reflected back, transmitted, or absorbed. If the intensities of the incident and the transmitted X-ray beam are I_o and I_t, respectively, then the functional relationship between I_t and I_o is given by (Jenkins and Snyder 1996, Figure 3.15):

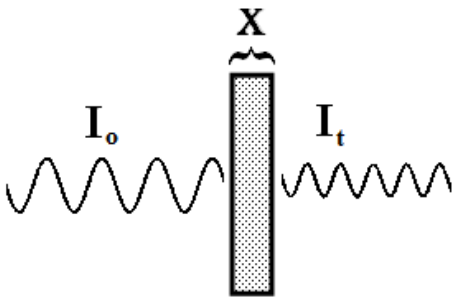

Figure 3.15 Schematic showing the relationship between incident and transmitted X-ray beam intensities, through a thin slab.

$$I_t(E) = I_o\, e^{-\mu(E)\rho x} \quad , \tag{3.8}$$

where: $I_t(E)$ = transmitted X-ray intensity (the number of transmitted soft X-ray photons or counts),

I_o = incident intensity at the other side of the slab (the number of incident soft X-ray photons or counts),

$\mu(E)$ = mass absorption coefficient (cm^2/g),

ρ = density of material (g/cm^3), and

x = the thickness of the slab exposed to the X-ray (cm).

For a sample containing many non-interacting components equation 3.8 can be written as:

$$I_t(E) = I_o\, e^{-\sum_{j=1}^{j=n} \mu_j(E)\rho_j x_j} \tag{3.9}$$

For quantitative image analysis in soft X - ray spectromicroscopy it is common to use optical density (OD) defined by $\ln(I_o/I_t)$ (equation 3.10). OD and μ are defined as a function of the energy of the X-ray beam E, in electron volts (eV).

$$OD(E) = ln(\frac{I_0}{I_t}) = \sum_{j=1}^{j=n} \mu_j(E) \rho_j x_j \quad (3.10)$$

When X-ray radiation is incident on a material, the absorbed photons can cause excitation of the inner shell electrons of the atoms in the material (or sometimes can ionize the atoms). Experimental work has shown that as the wavelength of the incident X-ray increases, the value of μ also increases.

At a certain value of incident wavelength, μ reaches its maximum value (Jenkins and Snyder 1996). This discontinuity is called an absorption edge (Figure 3.16).

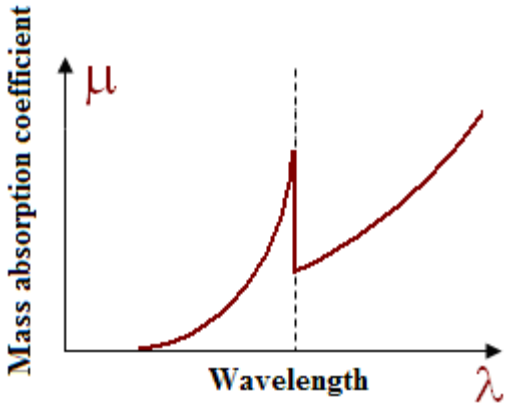

Figure 3.16 Variation of mass absorption coefficient with wavelength.

The absorption edge is related with each inner shell energy of an atom, and for unlike shells (different principal quantum numbers), absorption edges are different, e.g. K-edge and L-edge (Figure 3.17). When elements are exposed to X-ray beams, they show an X-ray absorption edge in the soft X-ray energy range of 100-1200 eV (Koprinarov and Hitchcock 2000).

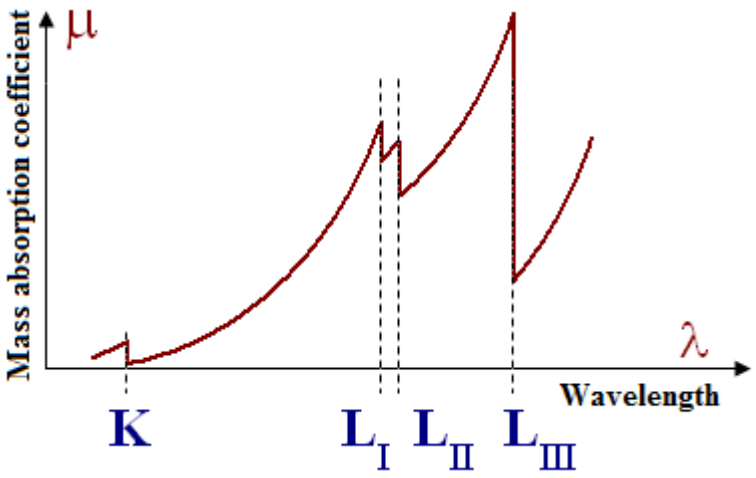

Figure 3.17 Variation of mass absorption coefficient with K and L (inner shell energy).

Based on X-ray absorption, a modern and powerful technique has been developed and practiced at synchrotron facilities. This method is known as near-edge X-ray absorption of fine structure or NEXAFS (Stöhr 1992). Each element in a sample has a characteristic NEXAFS structure at the absorption edge. The theory and application of NEXAFS are expounded by Fu (2006), Karunakaran and co-workers (2008), and Stöhr (1992). In this study, NEXAFS using scanning transmission X-ray microscope (STXM) was used to investigate the compositional (lignin and cellulose) changes of flax fibre before and after chemical treatment of the fibre (F1).

3.9.2 Sample preparation

The sample preparation method for scanning transmission X-ray microscopy (STXM) is similar to the sample preparation method for the transmission electron microscopy (TEM). The dry flax fibres were fixed using TTE amine resin (Sigma-Aldrich, Inc., St. Louis, MO), and the embedded samples were sectioned (longitudinal sections) about 90 nm (Figure 3.18) using an ultramicrotome. The cut sections were

mounted on foamvar-coated copper grids commonly used for TEM, shown in Figure 3.19 (the optimal thickness of samples for C 1s (atomic subshell of carbon) measurements in the transmission mode is about 100 nm). In this study, the samples were prepared at the Microscopy Centre of McMaster University (Hamilton, ON).

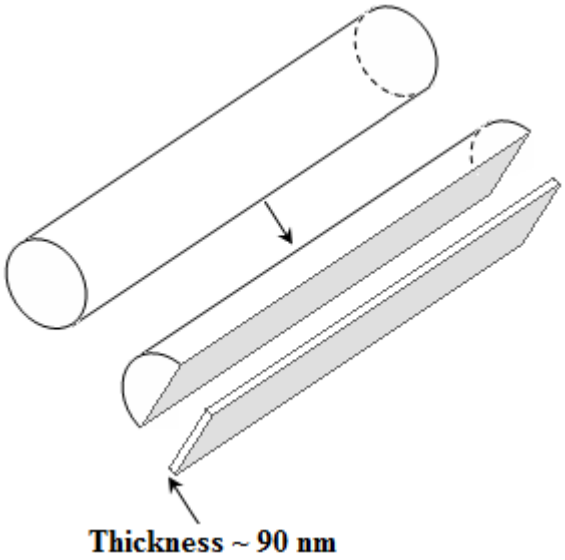

Figure 3.18 Schematic showing the cross sections of samples cut (embedded in a polymer resin, the resin is not shown here) using ultramicrotome (longitudinal sections, thickness about 90 nm).

Figure 3.19 Ultrathin sections of samples on foamvar-coated copper grids.

In this work, the main goal was to trace the changes of both cellulose and lignin on untreated and chemically treated flax fibres. To minimize absorption of X-rays by air and to reduce radiation damage of the sample, the chamber containing the sample was filled with dry helium during data collection (Karunakaran et al. 2008). One section from each type of sample was selected for data collection in STXM.

3.9.3 Data collection and analysis

The data were collected using the STXM at the Canadian Light Source (CLS, beamline 10ID-1) and Advanced Light Source (ALS, beamline 5.3.2) soft X-ray spectromicroscopy beamlines. Transmitted X-ray photon was measured by single photon counting, and counting periods (dwell times) for a point scan or a line scan were about 800 ms and 8 to 10 ms, respectively. The spectral resolving power was 3000 (E/ΔE) in the C 1s region by controlling beamline slit sizes (Karunakaran et al. 2008).

3.10 Differential Scanning Calorimetry (DSC)

DSC measurements were completed using a differential scanning calorimeter (DSC Q 2000, TA Instruments, New Castle, DE). The DSC system was operated in dynamic mode with a heating temperature of 10 to 400ºC at a heating rate of 10ºC/min. Three samples from each fibre (untreated, chemically treated, and plasma treated fibres) were chosen, prepared, and tested (the total number of tested samples were 27). The sample weight ranged from 5 to 10 mg and during testing, heat flow was measured as a function of temperature or time. The moisture of the samples was measured before testing, using a moisture determination balance (OHAUS MB200, OHAUS Scale Corp.,

Florham Park, NJ). The fibres were previously dried for 25 min at 85±1°C. Three replications from each fibre were chosen and then the moisture of each was measured. At the end, the average of these three measurements was calculated and reported as the moisture content of the sample. The degradation temperature of each fibre sample was obtained from second endothermic peak in the DSC thermogram. Since three measurements were done for each sample, the degradation temperature read from the DSC thermogram was averaged. Degradation temperatures were analyzed using analysis of variance (ANOVA) with Duncan's multiple range test (DMRT) to find out if the difference between the degradation temperatures of different flax fibre samples were statistically significant at $p=0.05$.

4. RESULTS AND DISCUSSION

This chapter discusses the effect of plasma and chemical treatments on flax fibres. The results of tests conducted to characterize structural changes in flax fibres before and after plasma/chemical treatment are discussed in this chapter.

4.1 Untreated Flax Fibre

Morphological characterization, fibre crystallinity and crystallite size, fibre thickness, and fibre density for untreated flax fibres are discussed in this section.

4.1.1 Morphological characterization

SEM images of untreated fibres (F1, F2) are shown in Figure 4.1. From this figure, it can be observed that the surface of F1 and F2 is contaminated after they have been extracted from the plant (Shamolina et al. 2003). Single fibres in both cases are joined with glue-like materials which hold these fibres together, and generating a fibre bundle. The presence of these materials might increase the strength of the fibre bundle.

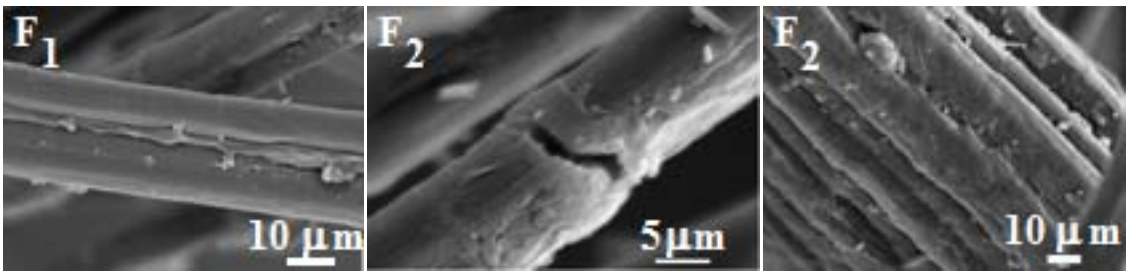

Figure 4.1 SEM micrographs of untreated fibres of 78.4% purity (F1) and 92.5% purity (F2).

4.1.2 Flax fibre crystallinity and crystallite size

As stated in part 4.1.1 two different flax fibres with different purities (F1, F2) were used. The X-ray diffraction curves (XRD) are shown in Figure 4.2. The figure shows both XRD curves are similar, and it does not depend on the purity of the fibres. One may assume that high purity results in high crystallinity; however, this assumption is not true in general. Referring to Figure 4.2, it can be observed that F1 has less intensity than the F2 at about 19.6° (amorphous region), and therefore resulting in high crystallinity (Table 4.2). This shows that purification of the fibre (using physical methods) has probably increased the size of the amorphous phase, keeping in mind that stress, compression, bending and point defects in materials change the position or the shape of the peaks in the XRD curve (Appendix D).

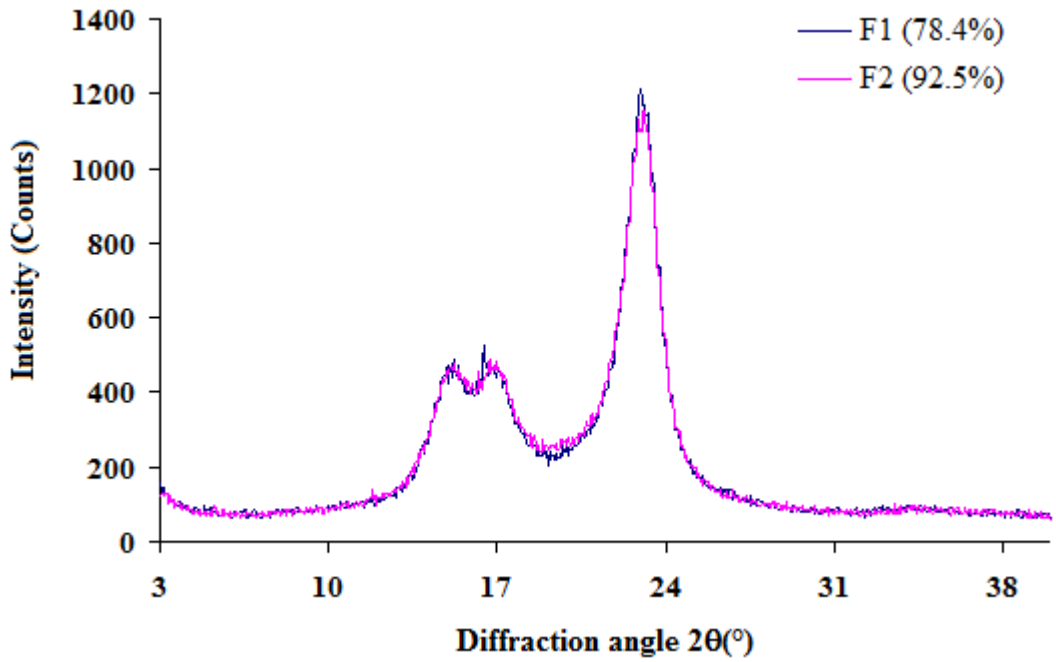

Figure 4.2 XRD curves of untreated flax fibres (F1, F2).

XRD results showed that the cellulose present in all untreated flax fibres is of the cellulose I structure (Figure 4.2).

The following discussions are made from Table 4.1 and 4.2:

1. The purification process of flax fibres did not change the interplanar spacing (d) of cellulose (d_1, d_2, and d_3 have similar values for both F1 and F2). In other words, the structure of cellulose present in flax fibres before and after the purification process has not been altered.

2. The purification process of flax fibres might affect slightly the mechanical properties of flax fibres. By referring to Table 4.2, it can be observed that the crystallinity of F2 (with a high purity value in comparison to F1) is less than F1, indicating that the stiffness of natural fibre depends on the content of the crystalline parts (cellulose) in the fibre (Bledzki and Gassan 1999).

Table 4.1 Peak resolution (fitting parameters) for untreated flax fibres (F1, F2).

	A	B	X_1(°)	C	D	X_2(°)	E	F	X_3(°)	G	H	X_4(°)	β	α	R^2
F1	258.63	1.03	15.10	217.54	0.79	16.85	929.76	1.03	23.05	190.50	6.03	19.15	82.39	-0.19	0.99
F2	246.72	0.96	15.10	199.25	0.79	16.85	889.18	1.06	23.05	210.76	5.93	18.85	78.74	-0.09	0.99

Note: F1= untreated flax fibres with a purity of 78.4%; F2= untreated flax fibres with a purity of 92.5%; R^2= coefficient of determination; A, B, C, D, E, F, G, H, α, and β = fitting parameters; X_1, X_2, and X_3= the angular position of Bragg's peaks; X_4= the angular position of amorphous peak.

Table 4.2 Crystallite size (W), interplanar spacing (d), and crystallinity (Xc) of untreated flax fibres (F1, F2).

	W_1(Å)	W_2(Å)	W_3(Å)	d_1(Å)	d_2(Å)	d_3(Å)	X_C (%)
F1	51.90	67.81	52.51	5.86	5.26	3.85	58.27
F2	55.68	67.81	51.02	5.86	5.26	3.85	56.21

Note: F1= untreated flax fibre with a purity of 78.4%; F2= untreated flax fibre with a purity of 92.5%.

4.1.3 Flax fibre thickness

Results showed that the average thickness of 10 samples ($\bar{d}$) ranged from 30.94 to 33.16 μm and was concentrated around 32.15 μm. The functional form of the thickness distribution for each sample was almost bell shaped (Figure 4.3) (Appendix B). The minimum thickness (d_{min}) for each sample was between 10 to 11 μm, whereas the maximum thickness (d_{max}) for each thickness measurement showed more variation starting from 89.8 to 126.2 μm. More details about these measurements are provided in Table 4.3. Flax fibre thickness has been reported to be 5 to 76 μm by Baley (2002).

Table 4.3 Thickness measurements of untreated flax fibre.

Sample	1	2	3	4	5	6	7	8	9	10
$\bar{d}$ (μm)	32.32	30.94	31.25	32.7	32.81	32.75	32.09	31.99	31.53	33.16
Std (μm)	11.89	10.84	10.79	12.1	11.59	12.58	11.45	11.27	10.61	12.29
d_{max} (μm)	104.2	89.8	105.5	104.8	124.8	126.2	97.4	90.4	113.6	101.7
d_{min} (μm)	10.5	11.0	10.7	10.5	10.7	10.4	11.2	10.6	10.8	10.8
NCF	7329	8547	10032	8478	11487	8289	6418	7665	9627	8433

Note: NCF= number of counted fibres; $\bar{d}$ = average thickness, d_{min}= minimum thickness; d_{max}= maximum thickness; Std= standard deviation.

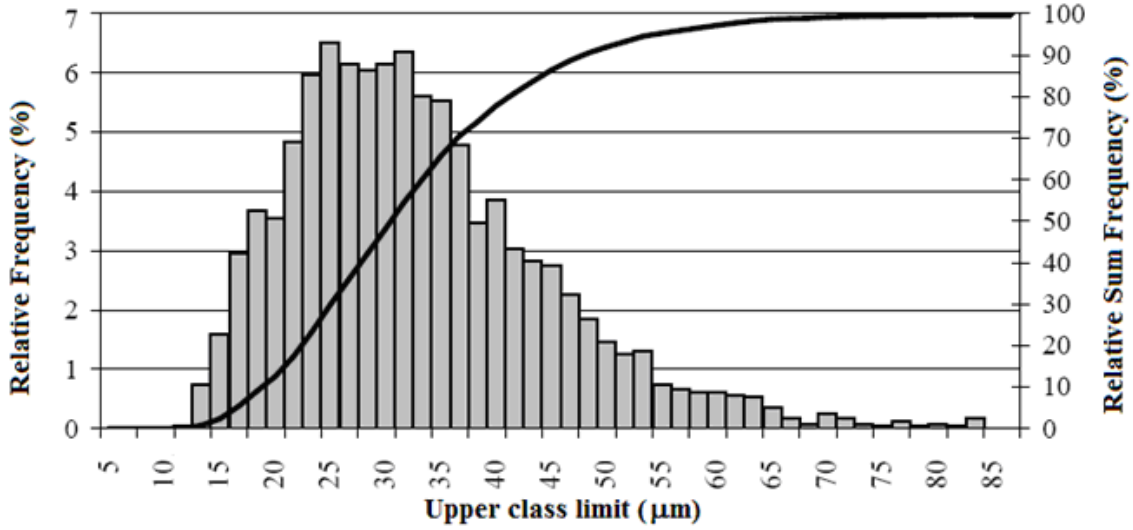

Figure 4.3 Schematic of flax fibre thickness distribution.

The cross sectional area of the fibre can easily be calculated using Figure 4.3. A value to fibre cross sectional area(A) can be assigned by:

$$A = \frac{\pi < D^2 >}{4}, \quad < D^2 > = \frac{\sum_i D_i^2 N_i}{N} = \sum_i D_i^2 \frac{N_i}{N} = \sum_i D_i^2 f_i \quad , \qquad (4.3)$$

where: N = number of counted fibres,

N_i = the number of fibres with the thickness of D_i (μm), and

f_i = relative frequency.

This number might be helpful in predicting the mechanical behaviour of composites with flax fibres (Homayonifar and Zebarjad 2007).

4.1.4 Flax fibre density

There are many problems involved in attaining a reliable value for fibre density, for instance, the porous nature and the purity of the fibres, moisture content, and non-uniform chemical composition in flax fibres. The actual density of flax fibres has been measured by many researchers. Baley (2002) has used a volumetric method to measure the density for flax fibres. He has reported 1.53 (g/cm^3) for fibre density. Siaotong (2006) has reported 1.618 (g/cm^3) for the actual density of ground flax fibre. In this work, 1.39 (g/cm^3) was obtained for the actual density of fibre using a gas-operated pycnometer (Table 4.4)

Table 4.4 The actual density of flax fibre.

Actual density (g/cm^3)+	Std*
1.39	0.06

***** standard deviation
+ average of 3 measurements

4.2 Chemical Modification of Flax Fibre

Chemical treatment caused many changes in the untreated flax fibres with a purity of 78.4% (F1). These changes were:

1. removal of non-cellulosic materials resulting in weight loss (Table 4.5);
2. improvement of the fineness of the fibres so that they could easily be separated resulting in a decrease of fibre bundle tensile strength;
3. change in structure, e.g. crystallinity; and
4. change in color.

The weight loss values of the fibres after chemical treatment is shown in Table 4.5. From Table 4.5, it can be concluded that there were no significant changes in weight loss after 1, 2, 3, and 4 h of chemical treatment.

Table 4.5 Weight loss of the flax fibres after chemical treatment at different times.

Sample	T1	T2	T3	T4
Weight loss (%db)	10.70	9.03	10.79	11.35

Note: T1, T2, T3, and T4 = 1, 2, 3, and 4-hour chemically treated flax fibres, respectively.

4.2.1 Morphological characterization

Figure 4.4 shows three images of untreated flax fibres with a purity of 78.4% (F1). It can be seen that some other materials (glue-like) adhered to the fibres. These materials may cause weak interfacing with polymer in the case of biocomposites.

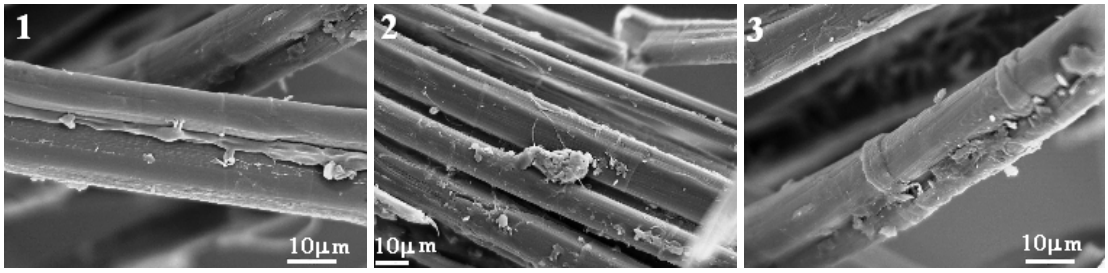

Figure 4.4 Longitudinal SEM photographs of untreated flax fibres of 78.4% purity (F1). Non-cellulosic materials can be seen on the surface of untreated flax fibres.

Figure 4.5 shows images of chemically treated fibres at different treatment times. The surface of all fibres are cleaned; glue-like materials or non-cellulosic materials are removed from the cracks present on the fibre surface and between fibres (Figure 4.5 (T1) and 4.4 (1)). Cleaning cracks causes good mechanical bonding between fibre and the matrix in biocomposites Morphological and structural changes of flax fibres have been studied by a number of researchers, e.g. a fibre bundle splitting and fibre surface cleaning in flax fibres after exposing to both alcohol and chemical treatments have been reported by Shamolina and co-workers (2003). Referring to Figure 4.5, it can be observed that fibrillar units have appeared clearly on the surface of fibres after chemical treatment.

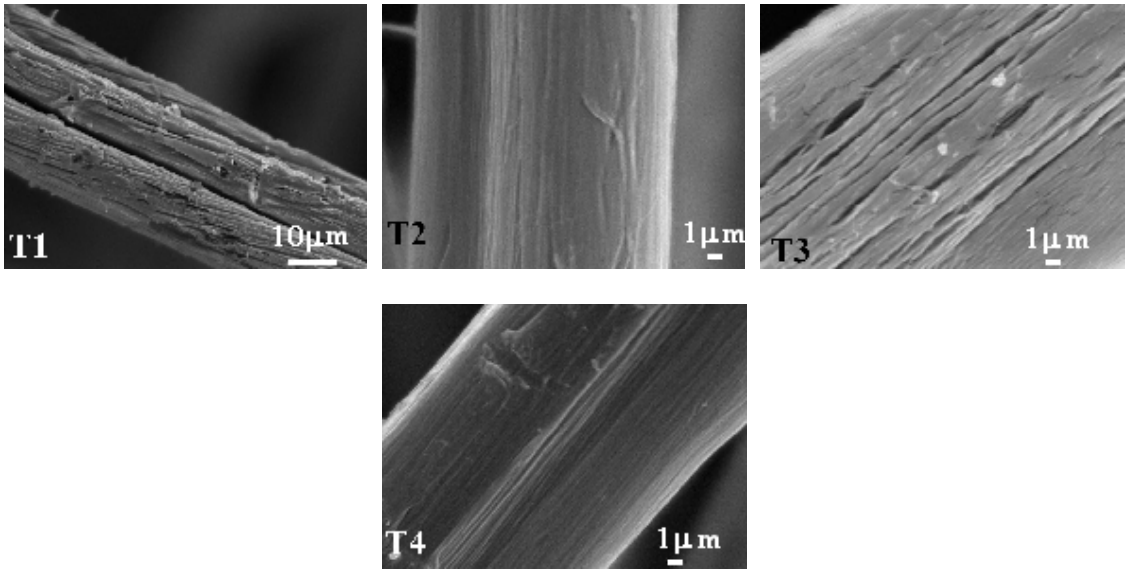

Figure 4.5 Longitudinal SEM photographs of chemically treated flax fibres at different durations: 1, 2, 3, and 4 h shown as T1, T2, T3, and T4, respectively. After chemical treatments the surface of the fibres were cleaned and fibrillar units were appeared.

4.2.2 Crystallinity

The diffraction curves of untreated/chemically treated fibres are shown in Figure 4.6; peak resolution, crystallite size, interplanar spacing, and crystallinity are reported in Table 4.6, Table 4.7, and Appendix A. As can be observed from Figure 4.6, slight changes in intensity have occurred to the fibres after treatment are reflected mostly on peak 3. From this figure, it can be concluded that the cellulose present in treated flax fibres is of the cellulose I structure, and it means that chemical treatment has not changed the structure of the cellulose. Mercerization can change the structure of cellulose from cellulose I to cellulose II, e.g. a gradual change from cellulose I to cellulose II in the structure of chemically treated flax fibres after increasing the concentration of sodium hydroxide have been reported by Sharma and van Sumere (1992).

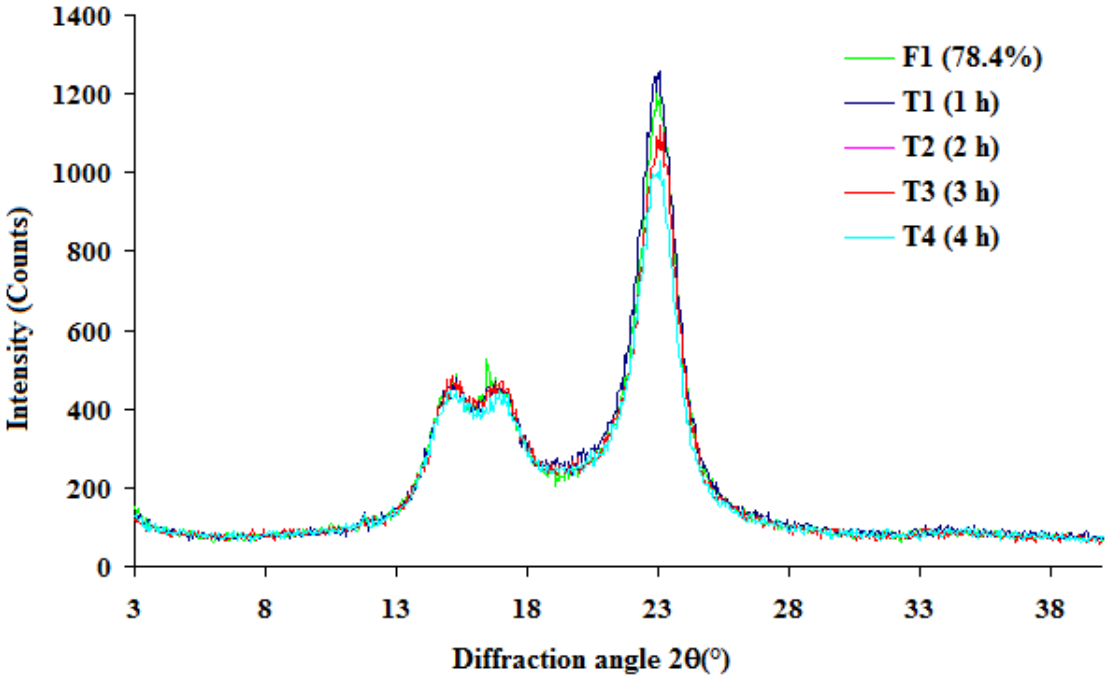

Figure 4.6 Diffraction curves of untreated (F1) and chemically treated (T1, T2, T3, and T4) flax fibres. Slight changes occurred in intensity to the fibres after treatment reflected mostly on peak 3.

As can be seen from (Table 4.7) that when the treatment time was increased, the crystallinity of the treated fibres decreased or the treatment has increased the amorphous phase in each sample. It seems that exposing flax fibre to chemical treatment for long time affects the cellulose structure. Decreasing crystallinity after treatment might open the bonds in the cellulose for interaction with the matrix in composites.

Table 4.6 Peak resolution (fitting parameters) for untreated and chemically treated flax fibres.

	A	B	X_1(°)	C	D	X_2(°)	E	F	X_3(°)	G	X4(°)	H	β	α	R^2
F1	258.63	1.03	15.10	217.54	0.79	16.85	929.76	1.03	23.05	190.50	19.15	6.03	82.39	-0.19	0.99
T1	246.26	1.11	15.20	180.30	0.73	16.85	961.44	1.03	23.05	217.41	19.40	5.8	81.78	-0.12	0.99
T2	258.70	1.05	15.2	197.98	0.79	16.85	842.80	1.02	23.05	201.04	19.40	5.95	82.47	-0.29	0.99
T3	258.22	1.08	15.15	193.02	0.81	16.85	900.76	1.03	23.15	212.75	19.55	5.55	75.86	-0.09	0.99
T4	248.25	1.11	15.15	166.71	0.78	16.85	739.19	1.04	23.15	205.7	19.55	5.27	89.13	-0.40	0.98

Note: R^2= coefficient of determination; F1= untreated flax fibres with a purity of 78.4%; T1, T2, T3, and T4 = 1, 2, 3, and 4-hour chemically treated flax fibres, respectively; A, B, C, D, E, F, G, H, α, and β = fitting parameters; X_1, X_2, and X_3= the angular position of Bragg's peaks; X_4= the angular position of amorphous peak.

Table 4.7 Crystallite size (W), interplanar spacing (d), and crystallinity (Xc) of untreated and chemically treated flax fibres. The crystallinity of chemically treated flax fibres decreased when the treatment time increased.

	W_1(Å)	W_2(Å)	W_3(Å)	d_1(Å)	d_2(Å)	d_3(Å)	X_C (%)
F1	51.90	67.81	52.51	5.86	5.26	3.85	58.27
T1	48.16	73.38	52.51	5.82	5.26	3.85	55.81
T2	50.91	67.81	53.02	5.82	5.26	3.85	54.47
T3	49.50	66.13	52.52	5.84	5.26	3.84	56.31
T4	48.16	68.68	52.01	5.84	5.26	3.84	54.38

Note: F1= untreated flax fibres with a purity of 78.4%; T1, T2, T3, and T4 = 1, 2, 3, and 4-hour chemically treated flax fibres, respectively.

4.2.3 Color analysis

Experimental results for the response variable ΔE (color index) at different treatment times and for untreated flax fibres with a purity of 78.4% (F1) are presented in Table 4.7. HunterLab values L, a, and b are averages of twelve values (three replications with four readings for each replication). The last three columns in Table 4.8 are devoted to RGB values, obtained from HunterLab values L, a, and b. The color test results (Table 4.8 and Table 4.9) showed that after treatment, the fibres became lighter, and the lightest color belonged to fibres which were chemically treated for two hours (ΔE=9). In other words, when the treatment time increased, the color of the fibres became darker again (ΔE↓). The real color of each fibre detected by the spectrocolorimeter is shown in Figure 4.7, keeping in mind that any RGB value corresponds to a color, and again by looking carefully at these colors, one can observe that T2 has the lightest color. The yellow color of flax fibres is attributed to the presence of non-cellulosic materials in flax fibres and therefore, the fibres become lighter when the chemical treatment of fibres removes these materials (Reddy and Yang 2005).

Table 4.8 Color coordinates (L, a, and b) and RGB values of untreated and chemically treated flax fibres.

Sample	L		a		b		R	G	B
	Mean	Std	Mean	Std	Mean	Std			
F1	54.65	1.29	2.49	0.23	10.81	0.36	167	144	130
T1	62.15	1.28	1.09	0.13	8.41	0.28	181	164	156
T2	63.69	0.89	1.15	0.12	8.78	0.23	185	167	159
T3	61.35	1.45	1.15	0.14	8.41	0.18	179	162	154
T4	61.31	2.25	1.22	0.20	8.42	0.40	179	161	154

Note: Std= standard deviation; F1= untreated flax fibre of 78.4% purity; T1, T2, T3, and T4 = 1, 2, 3, and 4-hour chemically treated flax fibres, respectively; R= red; G= green; B= blue.

Table 4.9 Color index (ΔE) of chemically treated flax fibres.

Sample	ΔE
T1	7.99
T2	9.36
T3	7.24
T4	7.19

Note: T1, T2, T3, and T4 = 1, 2, 3, and 4-hour chemically treated flax fibres, respectively.

Figure 4.7 Color of untreated and chemically treated flax fibres acquired from RGB values.

4.2.4 Tensile strength

Three different stress-strain curves for flax fibres (observed in this experiment for untreated and chemically treated fibres with different diameters) loaded to the point of breaking are given in Figure 4.8. Figure 4.8 (1) shows a stress-strain curve of flax fibre with almost elastic behaviour (Hookean behaviour). Stress-strain curves for many samples showed a positive and increasing slope (Figure 4.8(2)). One possible explanation for this behaviour is that in the unstrained fibre, microfibrils present in the cell walls are not aligned in the axial direction and after applying the load, they progressively become realigned in the axis of tension and resulted in increased fibre stiffening (Hornsby et al. 1997). In Figure 4.8(3), the fibre gave four failure peaks before total failure (E1>E2>E3>E4). Two suggestions for this phenomenon are: 1) the sample is not a single fibre because it is actually a fibre bundle made of many tiny fibres; and 2) this shows the structure of flax fibre is a layered wall; in fact, the fibre is assumed to be a composite material (Hornsby et al. 1997).

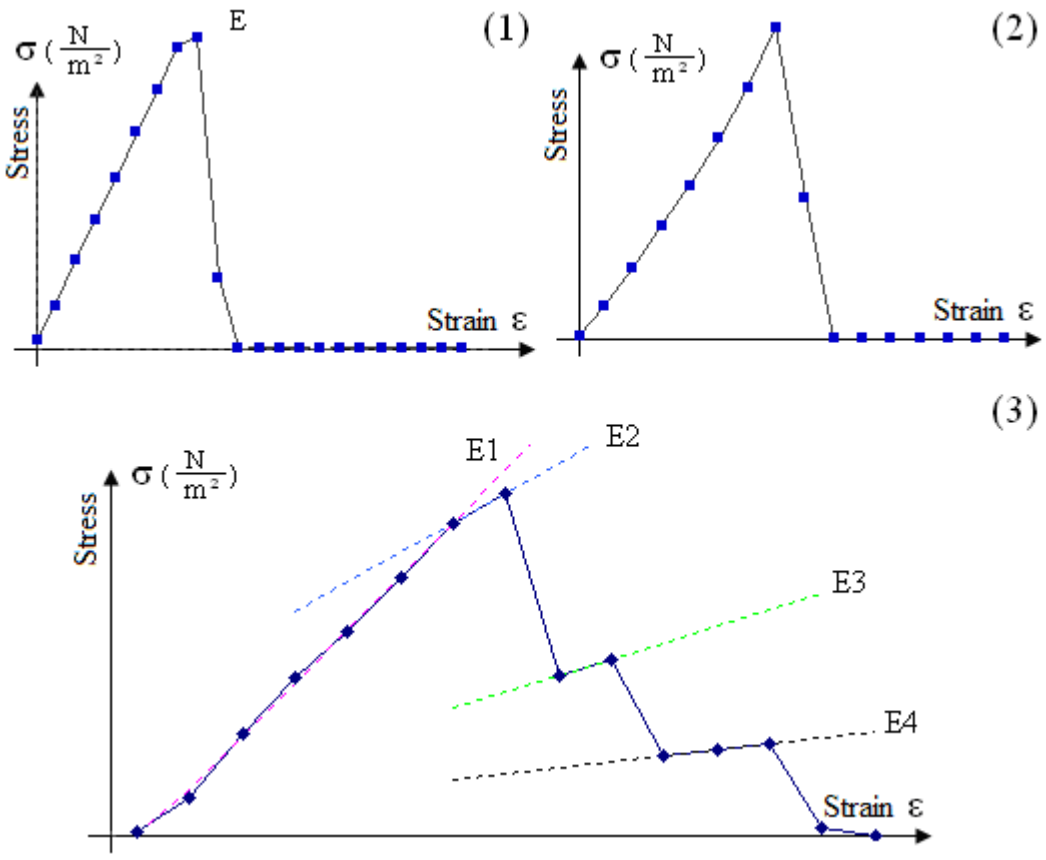

Figure 4.8 Typical stress-strain curves for untreated and chemically treated flax fibres showing: 1) elastic behaviour; 2) strain-hardening behaviour; and 3) composite behaviour.

Experimental results for the tensile strength at different treatment times are presented in Table 4.10 and Table 4.11. From these tables, it can be observed that :1) the high stiffness of fibres (high in elastic modulus) were almost observed among fibres with smaller diameters (Appendix C); 2) there was no obvious trend in stiffness (E) among the treated fibres (Appendix C); 3) there was no obvious trend in tensile strength among the treated fibres (Appendix C); and 4) tensile strength ranged from 62.97 to 374.8 (MPa) and elastic modulus ranged from 6.34 to 34.44 (GPa) of untreated flax fibres were approximately in agreement with the work done previously by Saheb and

Jog (1999), e.g. 344 (MPa) and 27 (GPa), for tensile strength and elastic modulus, respectively.

Fibre fineness of chemically treated flax fibres increased (they could easily be separated). In general, a bundle of single fibres is made of short and long fibres which are stuck to each other with glue-like materials especially pectin and lignin, and removing these materials from a bundle might decrease its strength.

Table 4.10 Mechanical properties of untreated and chemically treated flax fibres.

Sample	Fibre diameter (μm)				Elastic modulus(GPa)			
	Min	Max	Mean	Std	Min	Max	Mean	Std
F1	67	211.11	122.96	38.85	6.34	34.44	16.55	8.85
T1	57.11	212.56	121.03	44.56	4.15	20.18	11.88	5.33
T2	109.33	225.78	154.26	31.71	7.55	16.48	11.30	3.18
T3	86.67	161.17	124.98	27.70	4.84	29.88	13.08	7.91
T4	96	186.33	133.07	30.12	8.08	18.05	12.69	3.02

Note: Std = standard deviation; F1= untreated flax fibre with a purity of 78.4%; T1, T2, T3, and T4 = 1, 2, 3, and 4-hour chemically treated flax fibres, respectively; E = elastic modulus; D = the diameter of fibre.

Table 4.11 Tensile strength (TS) of untreated/chemically treated flax fibres.

Sample	Tensile strength (MPa)			
	Min	Max	Mean	Std
F1	62.97	374.8	161.57	87.43
T1	23.75	340.94	105.16	88.39
T2	70.55	179.13	113.61	31.71
T3	53.97	453.08	142.79	125.41
T4	55.33	182.69	126.88	39.48

Note: Std= standard deviation; F1= untreated flax fibre with a purity of 78.4%;
T1, T2, T3, and T4 = 1, 2, 3, and 4-hour chemically treated flax fibres, respectively.

4.2.5 Soft x - ray spectromicroscopy

Soft x-ray spectromicroscopy was used to investigate the chemical components and structure of untreated/chemically treated flax fibres. This method was also applied in studying the interfacial compatibility of untreated/chemically treated flax fibres (F1, T1, T2, T3, and T4) and resin.

The resin spectra extracted from the samples (shown with a small circle and the letter R, e.g. in Figure 4.10b the circle has a red color) are given in Figure 4.9. Three different images for each fibre (F1 (untreated), T1, T2, T3, and T4) are obtained from X-ray absorption near edge structure (NEXAFS) data. The first figure (a) (e.g. Figure 4.10a) shows the spectra extracted from each sample (optical density versus photon energy) and any spectrum is presented with a color relating to the concentration of cellulose inside the sample (keeping in mind that higher cellulose concentration causes higher optical density). The spectrum of the resin is included in this figure as well (e.g. the yellow spectrum in Figure 4.10a). The second figure (b) (e.g. Figure 4.10b) shows a picture of the scanned sample. The distribution of cellulose inside the scanned sample is exhibited with different colors in the third figure (c) (e.g. Figure 4.10c). When comparing the spectra of resin and cellulose, it can be observed that the resin spectra show a small shoulder before the first peak e.g. in Figure 4.9 the shoulder is located between 285 and 290 eV (the dashed circle). The appearance of a small peak around 285 eV in the cellulose spectrum can be attributed to the existence of aromatic compounds such as lignin and β-glucan (lignin and β-glucan show a strong absorption peak at 285.2 eV). The only trace of lignin was observed in the sample chemically treated for one hour

(T1). Referring to Figure 4.11, it can be concluded that the concentration of the aromatic compounds is much lower than the cellulose concentration.

The presence of a shoulder in the cellulose spectra (similar to the resin spectra) can be attributed to the bond created between resin and fibre. The existence of chemical bonding between the resin and the fibre was observed in the untreated fibre (F1) in the outer layer, the one-hour treated fibre (T1) and the two-hour treated fibre (T2). This bonding has appeared at the interface between F1 and the resin (the brown and green spectra) (Figure 4.10). The yellow areas in Figure 4.11 show the penetration of resin inside the treated fibre (T1) during sample preparation, and the chemical bonding in this case is created in two different regions: 1) at the interface between the fibre and resin (the violet curve); and 2) inside the fibre (the green curve). The interfacial bonding between resin and fibre in T2 (Figure 4.12) is similar to F1. Figure 4.12 contains some red spots probably resulting from sample preparation (while cutting the sample some resin residues were moved from the corner to the center part of the fibre). No trace of lignin and the interfacial bonding between resin and fibre were observed in T3 and T4 (Figures 4.13 and 4.14).

The spectra from different regions (these regions are called R1 and R2) have been taken (shown in Figure 4.15) in order to compare the distribution of cellulose in different samples. This figure shows that the concentration of cellulose varies in different samples.

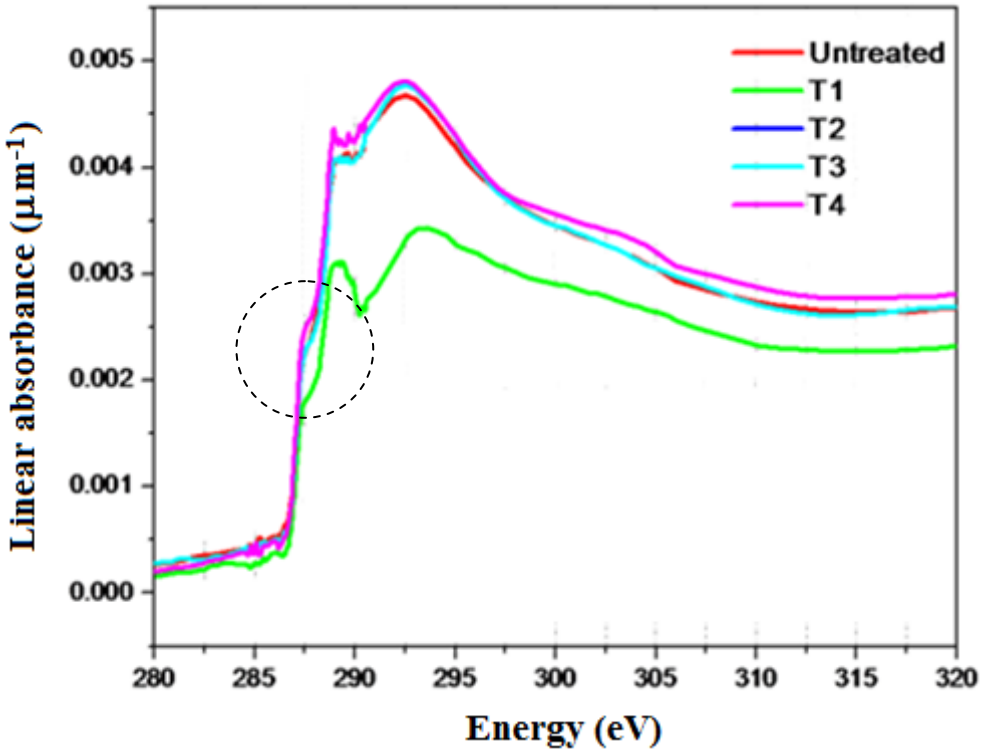

Figure 4.9 Spectra extracted from the resin region in different treatments. The dashed circle shows the presence of a shoulder in resin spectra extracted from different samples.

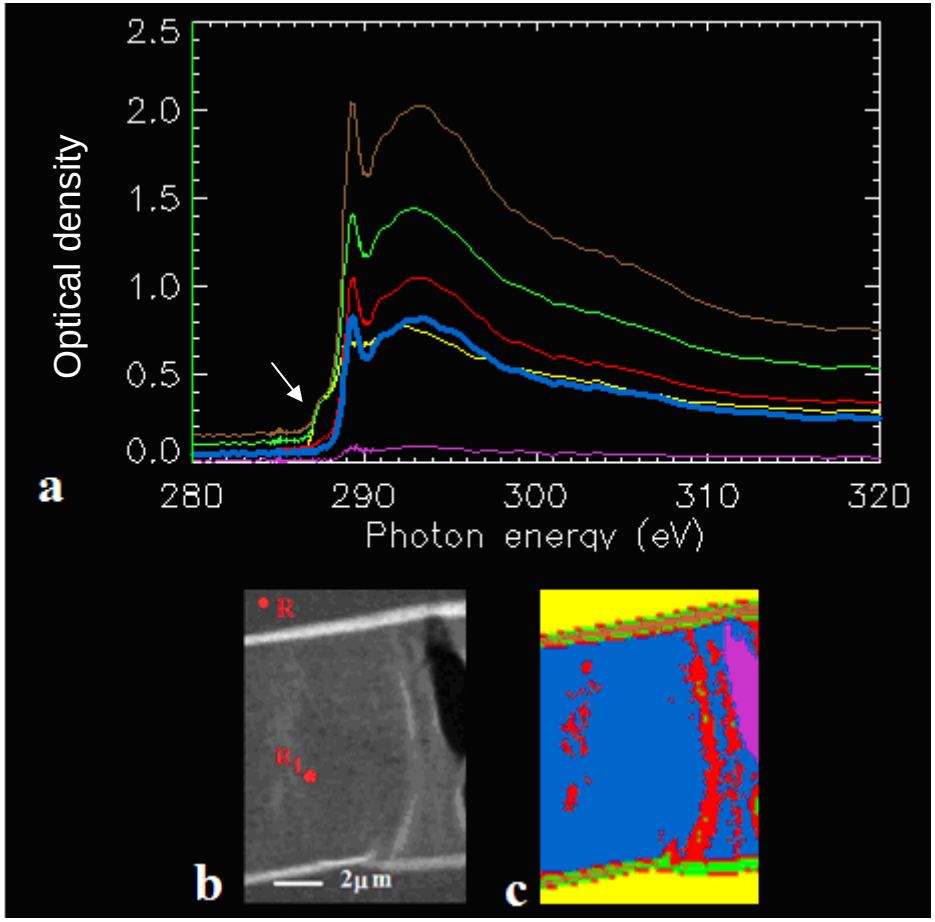

Figure 4.10 NEXAFS data for untreated fibre (F1): a) optical density versus photon energy, b) scanned fibre, and c) cellulose distributions shown with different colors. The green and brown spectra (a) show the creation of a chemical bonding between resin and fibre (the small arrow). The spectrum of resin was extracted from the region shown with the letter R, and in order to compare the distribution of cellulose in different fibres, R1 region was selected from F1.

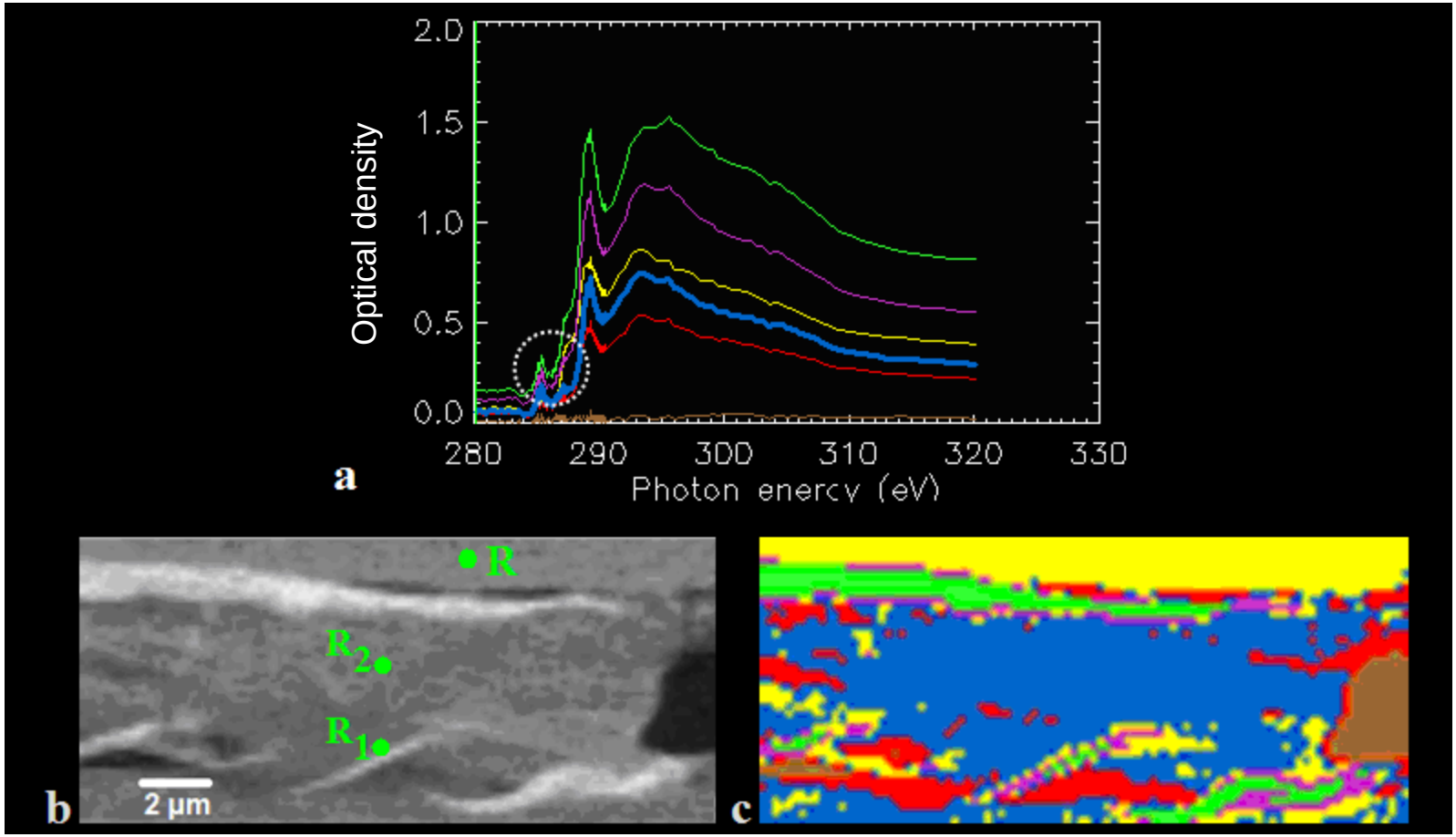

Figure 4.11 NEXAFS data for one-hour chemical treated fibre (T1): a) optical density versus photon energy, b) scanned fibre, and c) cellulose distributions shown with different colors. The only trace of resin was observed in this sample (the dashed circle). The interaction between fibre and resin were appeared in two different regions (the green and violet spectra). The yellow areas show the penetration of resin inside the treated fibre. The spectrum of resin was extracted from the region shown with the letter R, and in order to compare the distribution of cellulose in different fibres, R1 and R2 regions were selected from T1.

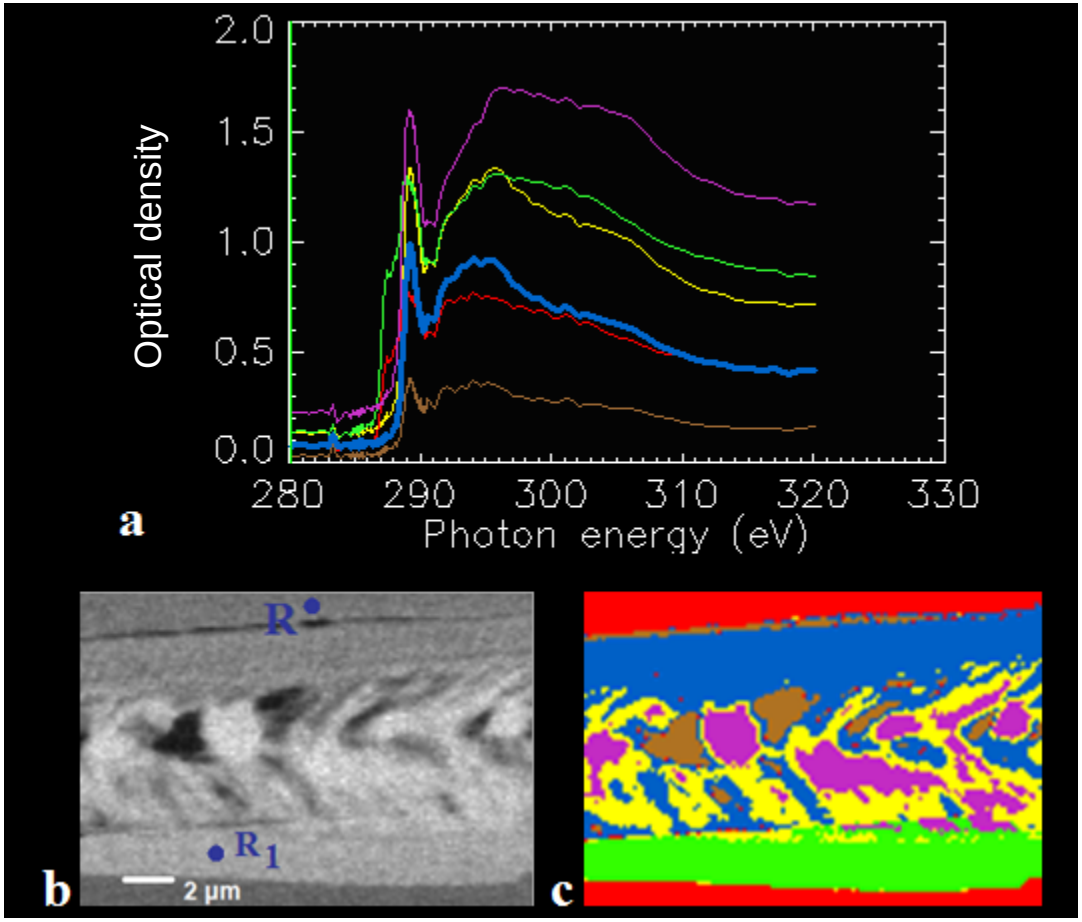

Figure 4.12 NEXAFS data for two-hour chemical treated fibre (T2): a) optical density versus photon energy, b) scanned fibre, and c) cellulose distributions shown with different colors. The green spectrum (a) shows the existence of interfacial boding between resin and fibre. The spectrum of resin was extracted from the region shown with the letter R, and in order to compare the distribution of cellulose in different fibres, R1 region was selected from T2.

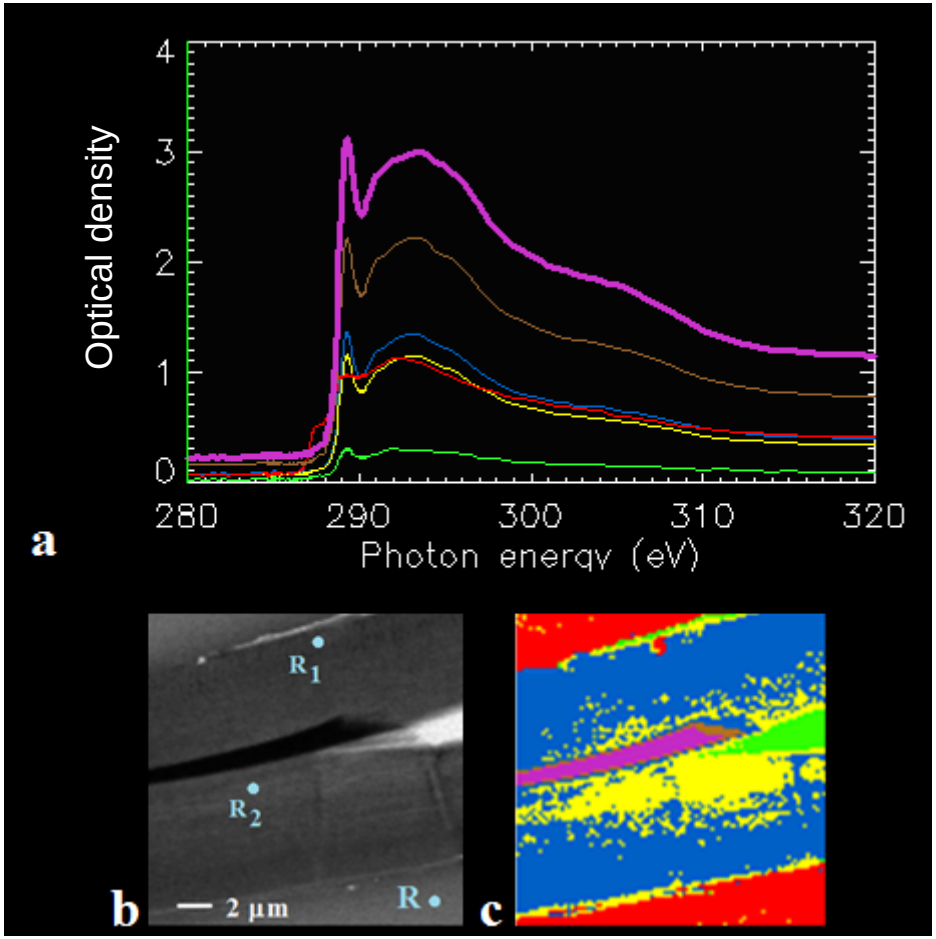

Figure 4.13 NEXAFS data for three- hour chemical treated fibre (T3): a) optical density versus photon energy, b) scanned fibre, and c) cellulose distributions shown with different colors. The spectrum of resin was extracted from the region shown with the letter R, and in order to compare the distribution of cellulose in different fibres, R1 and R2 regions were selected from T3.

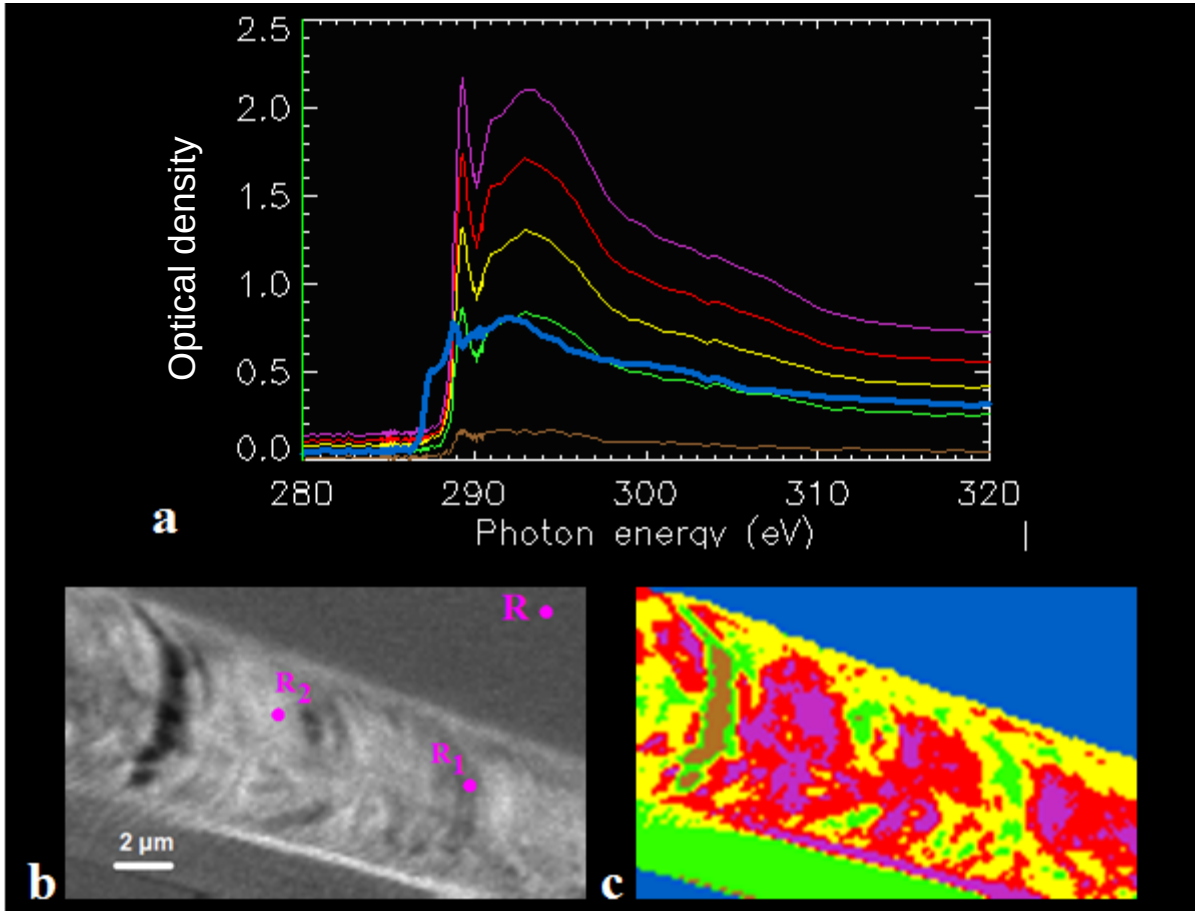

Figure 4.14 NEXAFS data for four-hour chemical treated fibre (T4) a) optical density versus photon energy, b) scanned fibre, and c) cellulose distributions shown with different colors. The spectrum of resin was extracted from the region shown with the letter R and in order to compare the distribution of cellulose in different fibres, R1 and R2 regions were selected from T4.

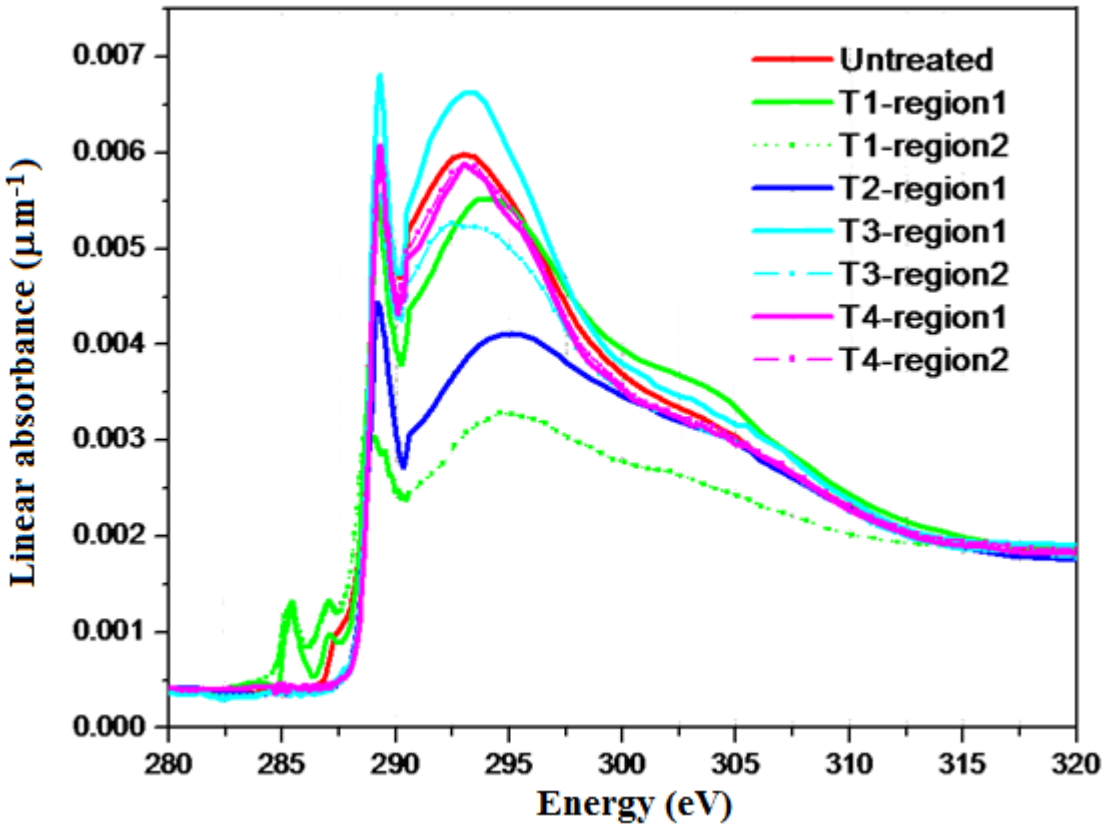

Figure 4.15 A comparison between the distribution of cellulose in different samples. Spectra extracted from different regions (R1, R2) in the untreated and chemically treated fibres. Some treatments only one spectrum and for others two spectra were extracted.

4.3 Plasma Treatment of Flax Fibre

In this chapter, the structural changes of flax fibres after exposure to argon plasma treatment are studied using scanning electron microscopy (SEM) and X-ray diffraction methods.

4.3.1 Morphological characterization

SEM images of argon plasma treated flax fibres (Figure 4.16) illustrate a progressive change of the surface morphology as a function of time. For a 5-min

treatment, the change is not distinguishable from the untreated sample (Figure 4.16, P1 and F2) but some changes (etching patterns) begin to appear on the surface after plasma treatment for 10 or more than 10 min (Figure 4.16, P2 and P3), and after 15 min of treatment, almost one layer of the fibre has separated.

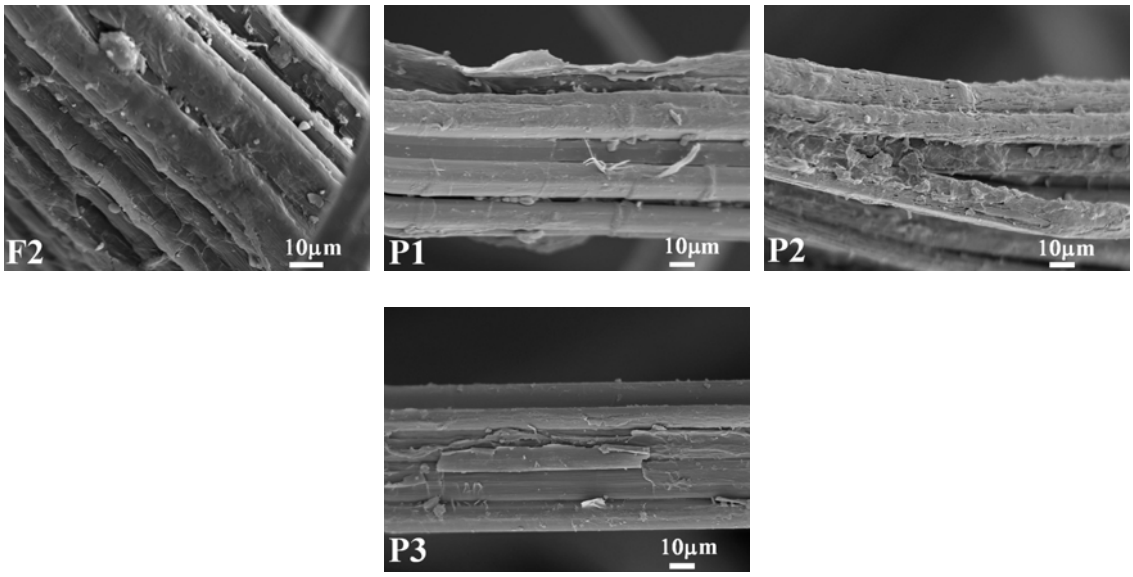

Figure 4.16 Longitudinal SEM photographs of 1) untreated flax fibre (F2, 92.5% purity) and 2) 5, 10, and 15-minute plasma treated flax fibres shown as P1, P2, and P3, respectively. Etching patterns appeared after 10 min treatment (P2) and one layer of the fibre was separated after 15 min treatment (P3).

Changes in the morphology of the flax fibres after being exposed to oxygen and argon plasma treatment have been studied by Wong and co-workers (2000). They reported the formation of cracks and voids on the surface of flax fibre due to the plasma erosion. They also reported that as the treatment time increased, the depth of voids etched by the plasma increased with pore width.

4.3.2 **Crystallinity**

The diffraction pictures of untreated/plasma treated fibres and other information such as peak resolution, crystallite size, interplanar spacing, and crystallinity are reported in Figure 4.17, Table 4.12, and Table 4.13, respectively. The effect of plasma treatment on fibres can clearly be observed from the diffraction pictures, and especially the changes on the amorphous region are very significant. The angular position of the peaks at different treatment times was encountered with little variation. The crystallinity of the fibres decreased, but the structure of the cellulose was untouched (cellulose I structure).

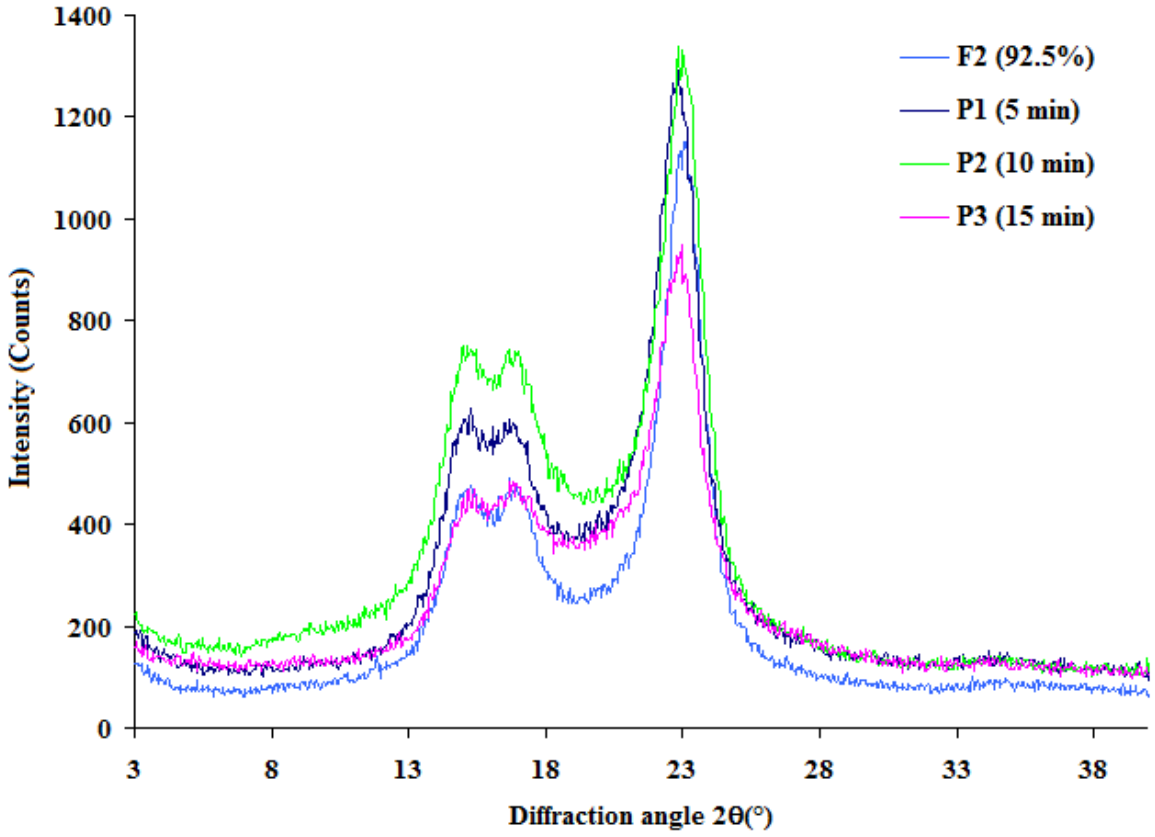

Figure 4.17 XRD curves of untreated (F2) and plasma treated fibres (P1, P2, and P3).

Studies of plasma treatment effects on the crystallinity of natural fibre have been reported by various researchers. Khammatova (2005) reported a significant increase in both crystallinity and the regions of coherent scattering of flax fibres treated by high-frequency capacitive discharge plasma (HFC) with air as a plasma-forming gas. The fibres were treated for around 180 to 720 s. The effect of oxygen plasma treatment on bombyx mori silk fibres has been studied by Chen and co-workers (2004). The fibres were treated at times of 10 and 30 min. Their result showed that the crystallinity of the fibres decreased in both cases.

Table 4.12 Peak resolution (fitting parameters) for plasma treated flax fibres.

	A	B	X_1(°)	C	D	X_2(°)	E	F	X_3(°)	G	X4(°)	H	β	α	R^2
F2	246.72	0.96	15.10	199.25	0.79	16.85	889.18	1.06	23.05	210.76	18.85	5.93	78.70	-0.09	0.99
P1	304.06	1.18	15.20	179.13	0.66	16.85	901.22	1.14	22.95	301.23	19.1	5.24	122.30	0.14	0.98
P2	363.17	1.22	15.20	230.08	0.74	16.95	909.85	1.06	23.1	355.42	19.1	5.61	180.31	-1.67	0.99
P3	161.45	1.03	15.20	109.67	0.69	16.95	587.01	1.17	23	268.95	19.1	5.42	123.77	0.04	0.98

Note: R^2= coefficient of determination; F2= untreated flax fibres with a purity of 92.5%; P1, P2, and P3= 5, 10 and 15-minute argon plasma treated flax fibres, respectively; A, B, C, D, E, F, G, H, α, and β = fitting parameters; X_1, X_2, and X_3= the angular position of Bragg's peaks; X_4= the angular position of amorphous peak.

Table 4.13 Crystallite size (W), interplanar spacing (d) and crystallinity (Xc) of untreated and plasma treated flax fibres. The crystallinity of argon plasma treated fibres decreased when the treatment time increased.

	W_1(Å)	W_2(Å)	W_3(Å)	d_1(Å)	d_2(Å)	d_3(Å)	X_C (%)
F2	55.68	67.81	51.02	5.86	5.26	3.85	56.21
P1	45.31	81.17	47.43	5.82	5.26	3.87	52.35
P2	43.82	72.40	51.02	5.82	5.22	3.85	46.73
P3	51.90	77.65	46.22	5.82	5.22	3.86	43.31

Note: F2= untreated flax fibres with a purity of 92.5%; P1, P2, and P3= 5, 10 and 15-minute argon plasma treated flax fibres, respectively.

4.4 Thermal Analysis

The main objective of doing DSC was to determine water evaporation and degradation temperature of the fibre samples. Table 4.14 shows the moisture content of untreated and chemically treated flax fibres used for the DSC test. The degradation temperature for each fibre is reported in Figure 4.18 and these values are in agreement with the temperature range of decomposition for flax fibre published by Ansari and co-workers (1999) and Hornsby and co-workers (1997). Ansari and co-workers (1999) have reported the decomposition of flax fibre in the region of around 350 to 375^{o}C and the onset temperature for decomposition of flax fibre reported by Hornsby and co-workers (1997) was 330^{o}C. DSC results showed that the degradation temperature of plasma/chemically treated fibres slightly decreased (Figure 4.18), however, the analysis of variance (ANOVA) revealed that these changes were not significant except in four-hour chemically treated fibres (T4).

One probable reason for this is that the removal of non-cellulosic materials in chemically treated flax fibres has affected the degradation temperatures of the fibres (Arbelaiz et al. 2006). In the plasma treatment, the interaction between argon gas and the surface of fibres are complicated and the weight loss of treated flax fibres during argon plasma treatment is mostly attributed to the surface etching of fibres (Wong et al. 2000).

Table 4.14 Moisture content (MC) of different samples.

	F1	F2	T1	T2	T3	T4
MC (wt %)	8.17	7.97	7.4	7.47	8.03	6.7

Note: F1= untreated flax fibres of 78.4% purity; F2= untreated flax fibres of 92.5% purity; T1, T2, T3, and T4 = 1, 2, 3, and 4-hour chemically treated flax fibres.

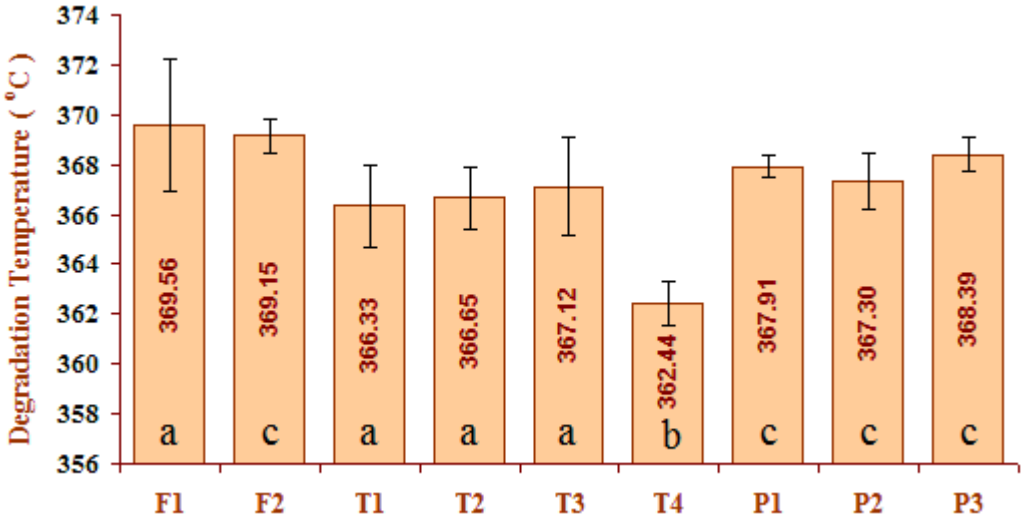

Figure 4.18 Degradation temperatures of untreated, plasma, and chemically treated flax fibres; a, b, and c mean that all samples with the same letter designation are not statistically different by Duncan's multiple range test. In this experiment 1) T1, T2, T3, and T4 were compared with F1 (designated by a and b) and 2) P1, P2, and P3 were compared with F2 (designated by c).

Water evaporation temperature measurements from the DSC thermogram presented conflicting values for each sample (Appendix E). It seems that the first endothermic peak belongs to water evaporation temperature (Ansari et al. 1999) and this temperature for flax fibres reported by Ansari and co-workers (1999) was below 71°C. In Figure 4.19 and 4.20, the aquamarine curves (labelled as a dried fibre) show the DSC thermograms of the dried untreated flax fibres of 92.5% purity (F2) and four-hour chemical treated flax fibres. It can be seen that in both samples (F2 and T4), the first endothermic peak has disappeared after the drying process.

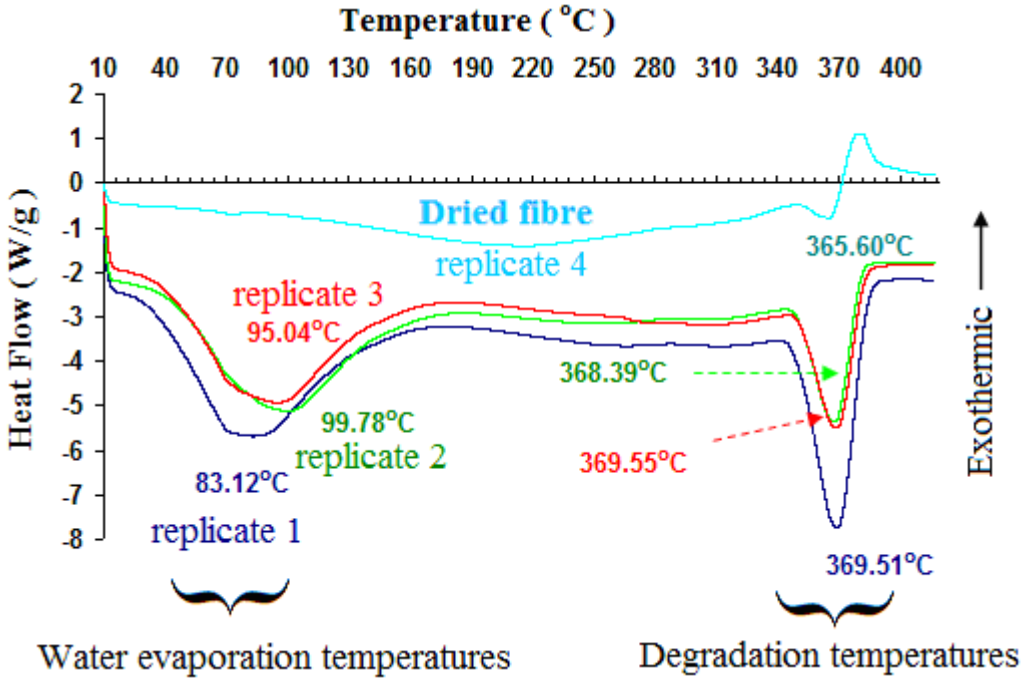

Figure 4.19 First endothermic peak was not present after drying the sample. Four samples (four replications) were chosen from untreated flax fibres with a purity of 92.5% (F2) and one of them was dried.

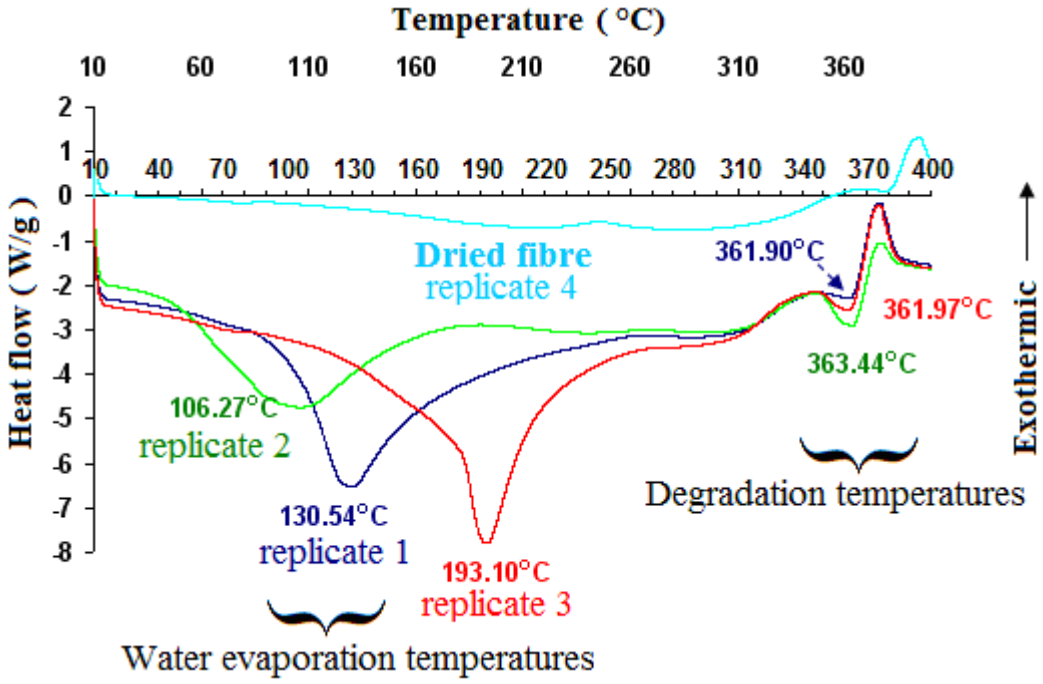

Figure 4.20 First endothermic peak was not present after drying the sample. Four samples (four replications) were chosen from 4-hour chemically treated flax fibres (T4) and one of them was dried.

In this study, sometimes two endothermic peaks below 250°C were observed (Figure 4.21) which belonged to the evaporation of both bound and free water molecules and the decomposition of different compounds in the fibre, e.g. lignin decomposition happens in a wide temperature range from 160 to 900°C (Yang et al. 2007). One explanation for this is that the presence of cracks on the surface of the fibre after physical/chemical modification, which would serve to increase the water absorption of the fibre and the removal of water molecules from these cracks and pits needs more heat. In fact, the water is trapped inside the cracks, absorbing a lot of heat which might cause the superheating of water.

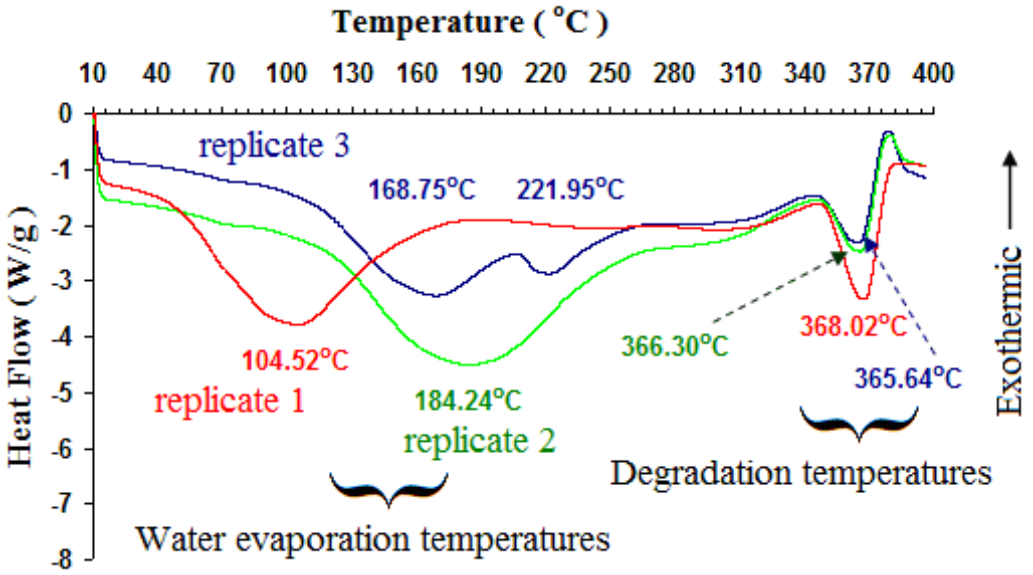

Figure 4.21 Three DSC thermograms (three replications) obtained from two-hour chemical treated fibres (T2) and the blue curve contains two endothermic peaks.

4.5 A Comparison between Plasma and Chemical Treatments

This section is devoted to a comparison between chemical and plasma treatments. A summary of testing method, treatment condition, and testing purpose is given in Table 4.15. Referring to Table 4.15, it can be observed that in comparison to chemically treated flax fibres three testing methods were used to study plasma treated flax fibres. In fact, the sample mass of plasma treated flax fibres was sufficient for DSC, XRD, and SEM tests and the comparison between chemical and plasma treatments is made based on these three common tests.

Table 4.15 A summary of testing method, treatment condition, and testing purpose used in this project.

Testing method	Treatment condition			Testing purpose
	U(1)	C(2)	P(3)	
Density	✓	-	-	To study non-homogeneity of flax fibres (can affect elastic modulus and tensile strength of fibres)
Thickness	✓	-	-	To obtain fibre thickness distribution
Tensile	✓	✓	-	To investigate the effect of chemical modification on mechanical properties
Soft X-ray	✓	✓	-	To study the composition of flax fibre and the interfacial bonding between fibre and matrix
Color	✓	✓	-	To study the color changes of fibres before and after chemical treatment
DSC(4)	✓	✓	✓	To investigate the effect of plasma/chemical modification on thermal properties
XRD(5)	✓	✓	✓	To investigate the effect of plasma/chemical modification on cellulose structure
SEM(6)	✓	✓	✓	To examine the effect of plasma/chemical modification on fibre surface

Note: 1= untreated flax fibres; 2= chemically treated flax fibres; 3= plasma treated flax fibres; 4= differential scanning calorimetry; 5=X-ray diffraction; 6= scanning electron microscopy.

In both plasma and chemically treated flax fibres, the degradation temperatures of samples were slightly decreased and water evaporation temperatures showed a variation among samples.

X-ray diffraction results showed that the crystallinity of chemically/plasma treated flax fibres significantly decreased, but the structure of the cellulose was unchanged (native form or cellulose I structure). It appears that fibres with high crystallinity absorb less water (Ansari et al. 1999), therefore, an increase in the water absorption of plasma and chemically treated flax fibres would be expected from the obtained results in this study. As stated earlier, the mechanical properties of flax fibres depend strongly on their structures. Decreasing or increasing the crystallinity of flax fibre can affect mechanical properties of the fibre (Bledzki and Gassan 1999). Arbelaiz and co-workers (2005) have reported a decrease in mechanical properties of flax fibres, treated in a 20 wt% aqueous solution of sodium hydroxide for 1h. In this project, no improvement was observed in mechanical properties of chemically treated flax fibres and this implies that decreasing crystallinity in chemically treated flax fibres and also probably in plasma treated fibres might cause a reduction in mechanical properties of fibres.

SEM results revealed that the surface of untreated flax fibres was significantly affected by both chemical and plasma treatments in different manners. Chemical modification removed non-cellulosic materials from the cracks and pits present on fibre surface, whereas, the plasma modification affected the fibre surface mostly as plasma etching resulting in separation of thin layers from the fibre surface. Surface modification of flax fibres can influence interfacial properties of fibres and polymer matrix in

biocomposites. Marais and co-workers (2005) have studied the mechanical properties of unsaturated polyester composites reinforced with helium plasma treated flax fibres. An increase in the elastic modulus (improving fibre/matrix adhesion) and a decrease in the breaking strength (weakening fibres by plasma treatments) of biocomposites have been reported in their results. Arbelaiz and co-workers (2005) have found an enhancement in interfacial strength values (using pull out test) for alkali modified single flax fibre. In their studies, a single flax fibre was immersed in a molten polypropylene droplet. Based on attained SEM results in this study, an improvement of fibre/matrix adhesion would be expected in composites reinforced with plasma/chemically treated flax fibres.

As a result, both chemical and plasma modifications exhibited a good potential in modifying flax fibres. Advantages and disadvantages of using plasma/chemical treatment in this study are discussed in the following paragraphs.

The advantages and disadvantages of using chemical treatment in this thesis were:

1. ease of use;
2. no restriction on the amount of fibres for the purpose of treating;
3. a different variety of surface modification could be achieved altering temperature, the concentration of sodium hydroxide (NaOH), and treatment time;
4. many stages such as washing and drying were involved after chemical treatment; and
5. large amounts of chemical residues were produced.

The advantages and disadvantages of using plasma in this thesis were:

1. contained a clean process using an inert- ionized gas;
2. the treatment modified the surface of fibre without touching the bulk properties;

3. a different variety of surface modification could be reached by varying the gas, gas rate, treatment time and pressure;
4. short treatment time (about 15 min);
5. difficult to produce a uniform plasma; and
6. each time a very small amount of fibre (around 64 mg) could be treated.

5. SUMMARY AND CONCLUSIONS

In this chapter, the conclusions based on results extracted from the experiments are discussed. The focus of this thesis was to develop and study the plasma treatment as an alternative to the other surface treatments of flax fibres by using different treatment conditions. In this work, soft X-ray spectromicroscopy was introduced as a new method in analysing the flax fibre structure and fibre-matrix interfacial properties.

The following conclusions are made based on the results extracted from plasma/chemical treatment of flax fibres:

1. Both treatment methods, plasma and chemical treatments, exhibited a significant capability in changing the surface characteristics of flax fibres. The results from scanning electron microscopy showed that plasma treatment modified the fibre surface in less time (15 min) than chemical treatment (4 h). Chemical modification removed non-cellulosic materials from the cracks and pits present on fibre surface, whereas, the plasma modification affected the fibre surface in a different manner mostly as plasma etching and separating thin layers from the fibre surface.
2. X-ray diffraction results showed that the structure of plasma treated fibres in a short time (15 min) was significantly changed (e.g. crystallinity) in comparison to the chemically treated fibres (4 h). In other words, the process of plasma modification seems to be completed in about 15 min while in chemical treatment many stages such as washing and drying are involved after chemical treatment consuming a large

amount of time and energy. In commercial biocomposite production, saving time and energy play an important role in the fibre process.

3. The degradation temperatures of plasma/chemical treated fibres were slightly decreased. In chemically treated flax fibres, decreasing the degradation temperature was attributed to the removal of non-cellulosic materials, whereas this weight loss in plasma treatment is mostly attributed to the surface etching of fibres. Decreasing the degradation temperature of flax fibre after plasma/chemical treatment implies that in biocomposite manufacturing process, the processing temperature should be lower than this temperature to avoid the degradation of flax fibres and their discoloration due to excessive heating.

The results from this study showed that plasma modification can be used as an effective method for surface modification of flax fibres. The advantages of using plasma treatment in this study were: 1) the surface modification of the flax fibres occurred in a short period; 2) surface modification of the flax fibres could easily be controlled by changing applied voltage, gas flow rate, pressure, and gas type; 3) unwanted waste products were not produced after treatment; 4) hazardous materials were not used in treating the fibres (an inert gas was used as plasma-forming gas); and 5) the near-surface region of flax fibres was modified. Thus plasma treatment would be an environmentally wiser choice of treating flax fibre than chemical treatment.

6. RECOMMENDATIONS

The following list of suggestions is introduced for future research.

1. The results from fibre thickness measurement showed that the thickness distribution of flax fibres was almost bell shaped. Additional studies by using a fitting method will give some information about flax fibre thickness which can be useful in predicting the mechanical behaviour of composites based on flax fibre.
2. More work (using soft x-ray absorption) is needed to understand the effectiveness of chemical/plasma treatment on the improvement of the interfacial bonding between fibre and matrix.
3. A study (using soft x-ray absorption) is recommended to estimate the distribution of pectin and hemicellulos in flax fibre after exposure to plasma/chemical treatment.
4. There is a chance of having sodium residues after washing process which may affect the water absorption of flax fibres. Soft x-ray absorption would be useful in identifying the existence of sodium residues on the alkaline treated flax fibres.
5. Supplementary chemical treatment studies are required at different times and on different concentrations of sodium hydroxide (NaOH) e.g. using a high concentration of sodium hydroxide (NaOH) changes the structure of the cellulose.

6. Due to the fact that the uniformity of a plasma gas plays an important role in the plasma treatment process, the plasma reactor must be improved or be replaced by a radio frequency (RF) plasma reactor.
7. In order to study the mechanical properties of composites based on flax fibre as reinforcement, there exists a need to design and build a proper plasma reactor with a large capacity in treating a large amount of flax fibres.
8. Additional plasma treatment studies are required using different gases, treatment times, pressure, and gas flow rate.

7. REFERENCES

Arbelaiz, A., B. Fernandez, J.A. Ramos and I. Mondragon. 2006. Thermal and crystallization studies of short flax fibre reinforced polypropylene matrix composites: Effect of treatments. *Thermochimica Acta* 440: 111-121.

Arbelaiz, A., G. Cantero, B. Fernández, I. Mondragon, P. Gañán and J.M. Kenny. 2005. Flax fiber surface modifications: Effects on fiber physico mechanical and flax/polypropylene interface properties. *Polymer Composites* 26: 324-332.

Ansari, I.A., G.C. East. and D.J. Johnson. 1999. Structure-property relationships in natural cellulosic fibres. Part 1: Characterisation. *Textile Institute* 90(4): 469-480.

Ansari, I.A., G.C. East. and D.J. Johnson. 2001. Structure-property relationships in natural cellulosic fibres. Part 2: Fine structure and tensile strength. *Textile Institute* 92(4): 331-348.

Baley, C. 2002. Analysis of the flax fibres tensile behaviour and analysis of the tensile stiffness increase. *Composites Part A: Applied Science and Manufacturing* 33: 939-948.

Baiardo, M., E. Zini and M. Scandola. 2004. Flax fibre-polyester composites. *Composites Part A*: *Applied Science and Manufacturing* 35 :703-710.

Bledzki, A.K., S. Reihmane. and J. Gassan. 1996. Proerties and modification methods for vegetable fibers for natural fiber composites. *Journal of Applied Polymer Science* 59: 1329-1336.

Bledzki, A.K. and J. Gassan. 1999. Composites reinforced with cellulose based fibres. *Progress in Polymer Science* 24: 221-274.

Bhattacharya, S.D. and J.N. Shah. 2004. Enzymatic treatments of flax fabric. *Textile Research Journal* 74(7):622-628.

Borysiak, S. and B. Doczekalska. 2005. X-ray Diffraction Study of Pine Wood Treated with NaOH. *Fibres & Textiles in Eastern Europe* 13:87-89.

Chen, Y.Y., H. Lin, Y. Ren, H.W. Wang and L.J. Zhu. 2004. Study on bombyx mori silk treated by oxygen plasma. *Journal of Zhejiang University Science* 5(8):918-922.

Fu, J. 2006. Linear dichroism in the NEXAFS spectroscopy of N-Alkane thin films. Unpublished Ph.D. thesis. Saskatoon, Saskatchewan: Department of Chemistry, University of Saskatchewan.

Gassan, J. and A.K. Bledzki. 2001. Thermal degradation of flax and Jute fibers. *Journal of Applied Polymer Science* 82: 1417-1422.

George, J., M.S. Sreekala and S. Thomas. 2001. A review on interface modification and characterization of natural fiber reinforced plastic composites. *Polymer Engineering and Science* 41(9):1471-1485.

Gouanve, F., S. Marais, A. Bessadok, D. Langevin, C. Morvan and M. Metayer, 2006. Study of water sorption in modified flax fibres. *Journal of Applied Polymer Science* 101: 4281-4289.

Hearle, J.W.S. 1963. The fine structure of fibers and crystalline polymers. III. interpretation of the mechanical properties of fibers. *Journal of Applied Polymer Science* 7:1207-1223.

Hindeleh, A.M. and D.J. Johnson. 1972. Crystallinity and crystallite size measurement in cellulose fibres: 1. ramie and fortisan. *Polymer* 13:423-430.

Hindeleh, A.M. and D.J. Johnson. 1974. Crystallinity and crystallite size measurement in cellulose fibres: 2. viscose rayon. *Polymer* 15:697-705.

Homayonifar, M. and S.M. Zebarjad. 2007. Investigation of the effect of matrix volume fraction on fiber stress distribution in polypropylene fiber composite using a simulation method. *Material and Design* 28:1386-1392.

Hornsby, P.R., E. Hinrichsen and K. Tarverdi. 1997. Preparation and properties of polypropylene composites reinforced with wheat and flax straw fibres. Part I fibre characterization. *Journal of Materials Science* 32:443-449.

Ishikawa, A., T. Okano and J. Sugiyama. 1997. Fine structure and tensile properties of ramie fibers in the crystalline form of cellulose I, II, III_I and IV_I. *Polymer* 38(2): 463-468.

IST Ltd. 2003. Users manual. Vilters, Switzerland: IST-Innovative Sintering Technologies Ltd.

Jenkins, R. and R. Snyder. 1996. *Introduction to X-ray Powder Diffractometry.* New York, NY: Wiley.

Karunakaran, C., C.R. Christensen. S.S. Miller, and A.P. Hitchcock. 2008. Soft X-ray Spectromicroscopy – An advanced technique for plant polysaccharides research (Manuscript in preparation). CLS-AUM2008 meeting.

Kasai, N. and M. Kakudo. 2005. *X-ray Diffraction by Macromolecules*. Berlin, Germany: Kodansha Ltd. and Springer-Verlag.

Khalili, S., D.E. Akin, B. Pettersson and G. Henriksson. 2002. Fibernodes in flax and other bast fibers. *Journal of Applied Botany – Agnewandte Botanik* 76: 133-138.

Khammatova, V.V. 2005. Effect of high-frequency capacitive discharge plasma on the structure and properties of flax and lavsan materials. *Fibre Chemistry* 37(4):293-296.

Koprinarov, I. and A.P. Hitchcock.2000. X-ray Spectromicroscopy of Polymers - An introduction for the non-specialist.http://unicorn.mcmaster.ca/stxm-intro/polystxmintro-all.pdf (2008/06/01).

Lagerlöf, P. 2008. EMSE 312 - Diffraction Principles (Lectures). http://dmseg5.mse.cwru.edu/Classes/EMSE312/(2008/01/01).

Logicol. 2008. The color data company. http://www.logicol.com/ (2008/06/01).

Lieberman, M.A. and A.J. Lichtenberg. 2005. *Principles of Plasma Discharges and Materials Processing*. 2nd edition. Hoboken, NJ: John Wiley & Sons.

Marais, S., F. Gouanve, A. Bonnesoeur, J. Grenet, F. Poncin-Epaillard, C. Morvan and M. Metayer. 2005. Unsaturated polyester composites reinforced with flax fibers: effect of cold plasma and autoclave treatments on mechanical and permeation properties. *Composites Part A: Applied Science and Manufacturing*: 36:975-986.

Olaru, N., L. Olaru and GH. Cobiliac. 2005. Plasma-modified wood fibers as fillers in polymeric materials. *Romanian Journal of Physics* 50:1095-1101.

Pallesen, B.E. 1996. The quality of combine-harvested fibre flax for industrials purposes depends on the degree of retting. *Industrial Crops and Products* 5:65-78.

Reddy, N. and Y. Yang. 2005. Long natural cellulosic fibers from cornhusks: structure and properties. *AATCC Review:* 5(7):24-27.

Roth, J.R. 2001. *Industrial Plasma Engineering Volume 2: Application to Nonthermal Plasma Processing.* Bristol, UK: Institute of Physics Publishing.

Saheb, D.N. and J.P. Jog. 1999. Natural fiber polymer composites: a review. *Advances in Polymer Technology*. 18(4): 351–363.

Sharma, H.S.S. and C.F. Van Sumere. 1992. *The biology and Processing of Flax*. Belfast, Northern Ireland: M Publications.

Shamolina, I.I., A.M. Bochek, N.M. Zabivalova, D.A. Medvedeva and S.A. Grishanov. 2003. An Investigation of structural changes in short flax fibres in chemical treatment. *Fibres & Textiles in Eastern Europe* 11:33-36.

Siaotong, B.A. 2006. Effects of fiber content and extrusion parameters on the properties of flax fiber-polyethylene composites. Unpublished M.Sc. thesis. Saskatoon, SK: Department of Agricultural and Bioresource Engineering, University of Saskatchewan.

Sreekala, M.S., M.G. Kumaran, S. Joseph, M. Jacob and S. Thomas. 2000. Oil palm fiber reinforced phenol formaldehyde composites: influence of fiber surface modifications on the mechanical performance. *Applied Composite Materials* 7:295-329.

Stamboulis, A., C. A. Baillie and T. Peijs. 2001. Effects of environmental conditions on mechanical and physical properties of flax fibers. *Composites Part A: Applied Science and Manufacturing* 32:1105-1115.

Stöhr, J.1992. *NEXAFS Spectroscopy.* 1st edition. Berlin, Germany: Springer-Verlag.

Vonk, C.G. 1973. Computerization of Ruland's x-ray method for determination of the crystallinity in polymers. *Journal of Applied Crystallography* 6:148-152.

Wiener, J., V. Kovačič and P. Dejlová. 2003. Differences between flax and hemp. *AUTEX Research Journal* 3(2): 58-63.

Ward, I.M. 1962. Optical and mechanical anisotropy in crystalline polymers. *Proceeding of the Physical Society* 80:1176-1188.

Wang, B. 2004. Pretreatment of flax fibers for use in rotationally molded composites. Unpublished M.Sc. thesis. Saskatoon, SK: Department of Agricultural and Bioresource Engineering, University of Saskatchewan.

Wong, K.K., X.M. Tao, C.W.M. Yuen and K.W. Yeung. 2000. Topographical study of low temperature plasma treated flax fibers. *Textile Research Journal* 70(10):886-893.

Xu, X., Y. Wang, X. Zhang, G. Jing, D. Yu and S. Wang. 2006. Effects on surface properties of natural bamboo fibers treated with atmospheric pressure argon plasma. *Surface and Interface Analysis* 38: 1211-1217.

Yang, H., R. Yan, H. Chen, D.H. lee and C. Zheng. 2007. Characteristics of hemicellulose, cellulose and lignin pyrolysis. *Fuel* 86: 1781-1788.

APPENDIX A- PEAK RESOLUTION

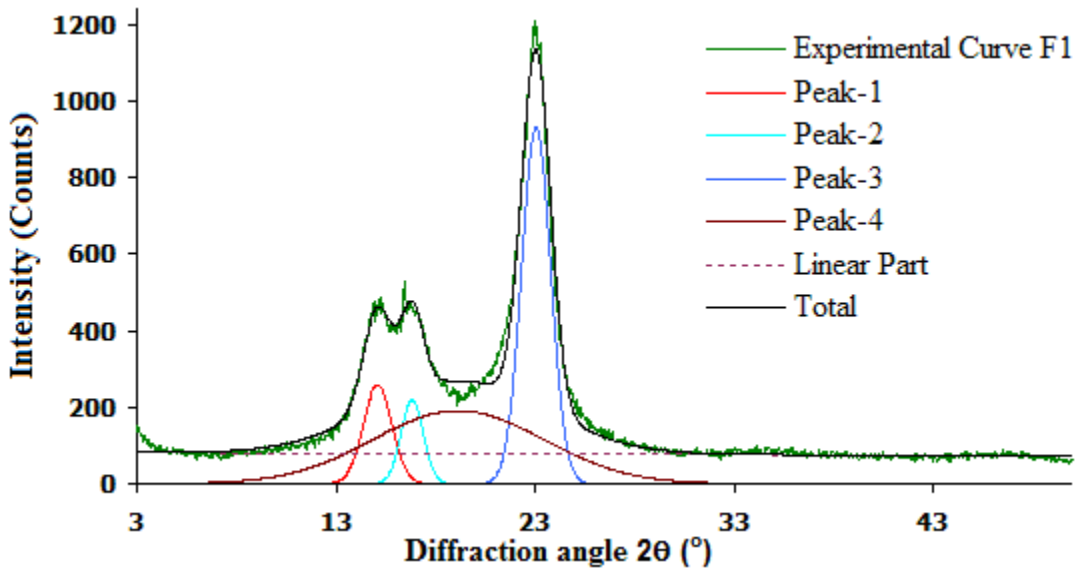

Figure A.1 Peak resolution of untreated fibre (F1).

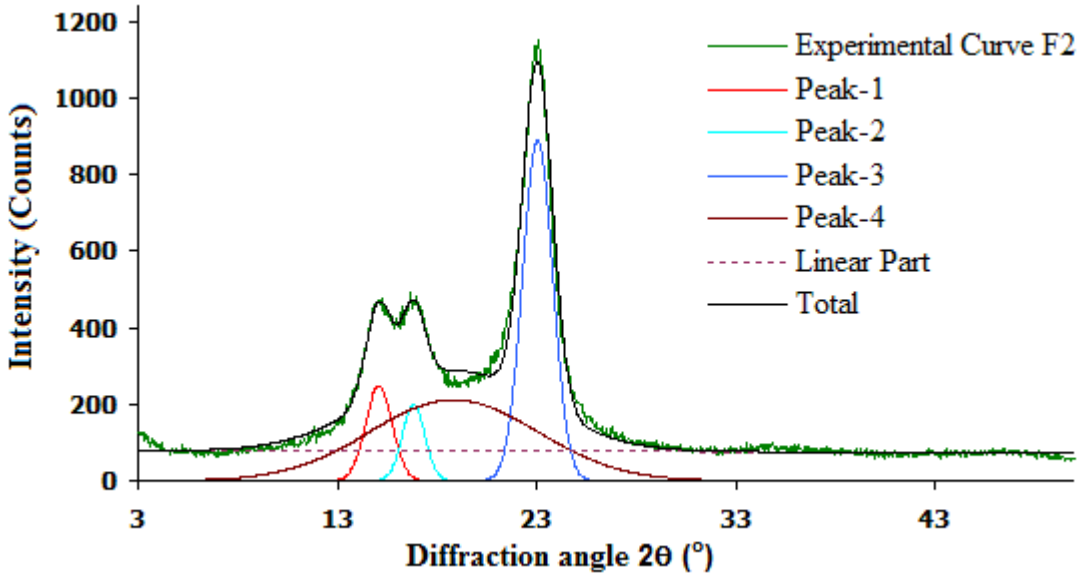

Figure A.2 Peak resolution of untreated fibre (F2).

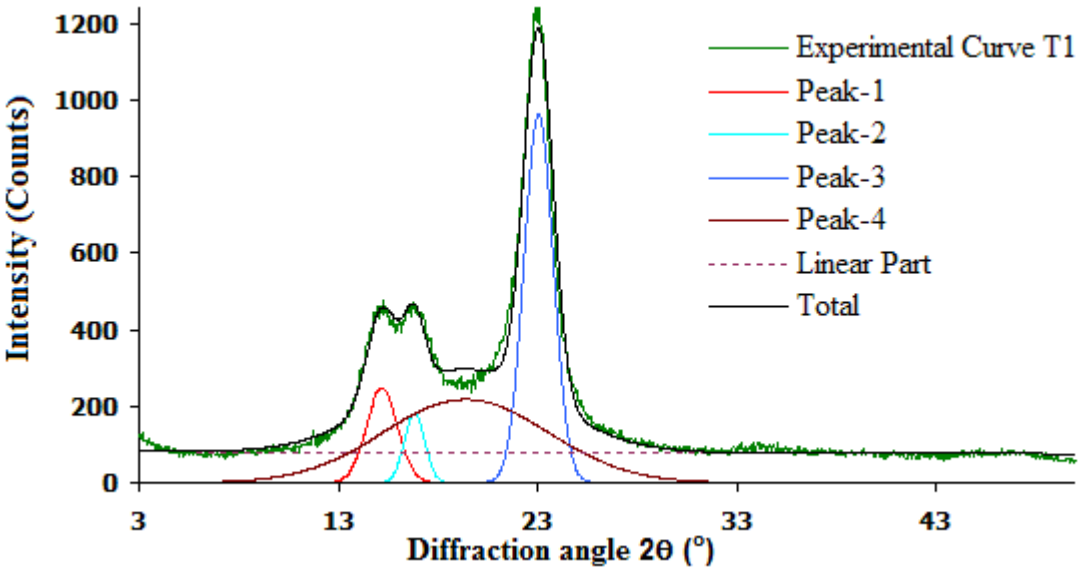

Figure A.3 Peak resolution of chemically treated fibre (T1).

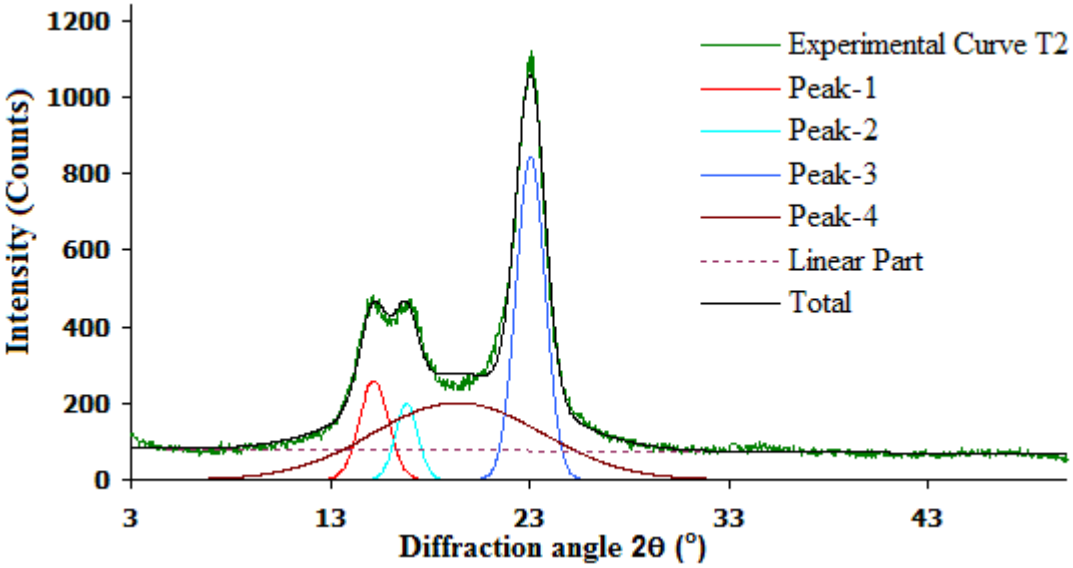

Figure A.4 Peak resolution of chemically treated fibre (T2).

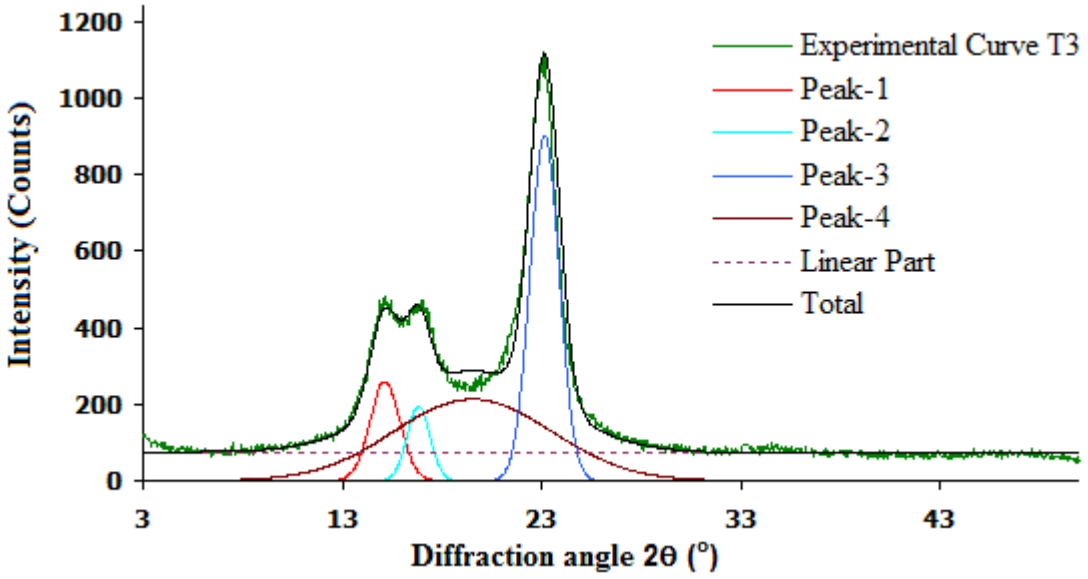

Figure A.5 Peak resolution of chemical treated fibre (T3).

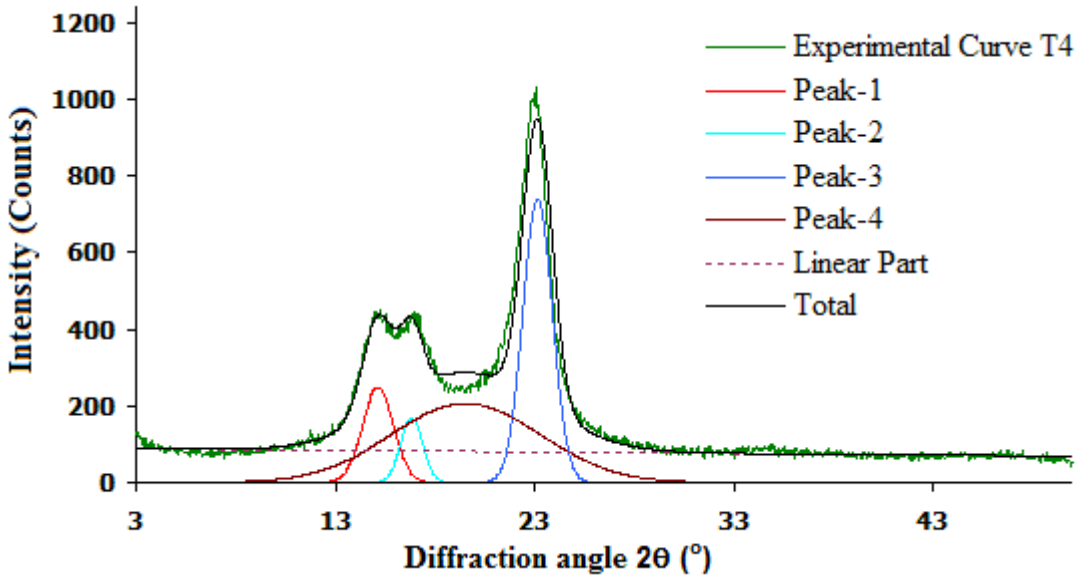

Figure A.6 Peak resolution of chemical treated fibre (T4).

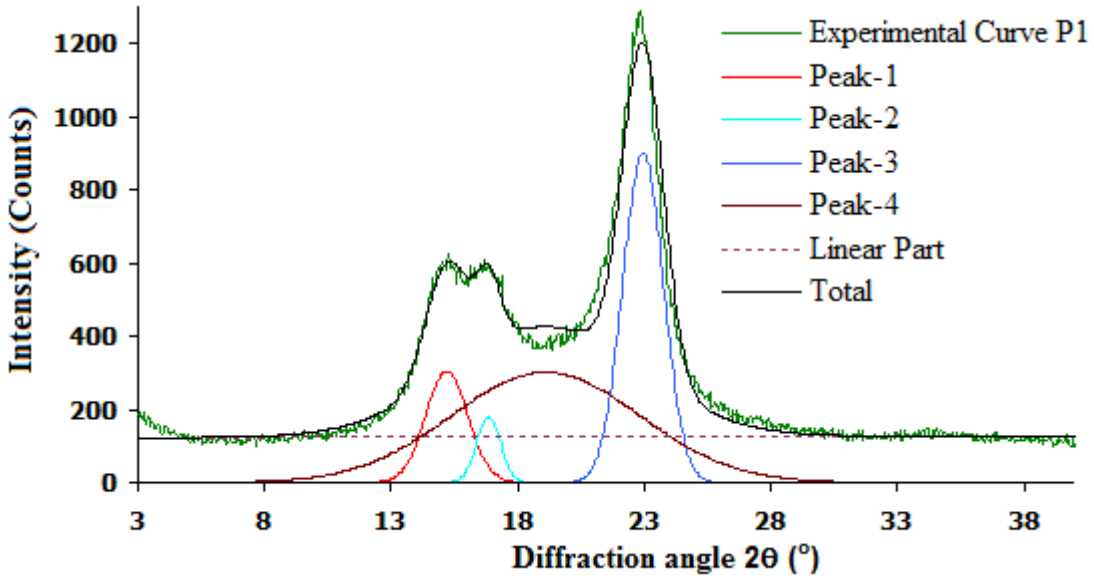

Figure A.7 Peak resolution of plasma treated fibre (P1).

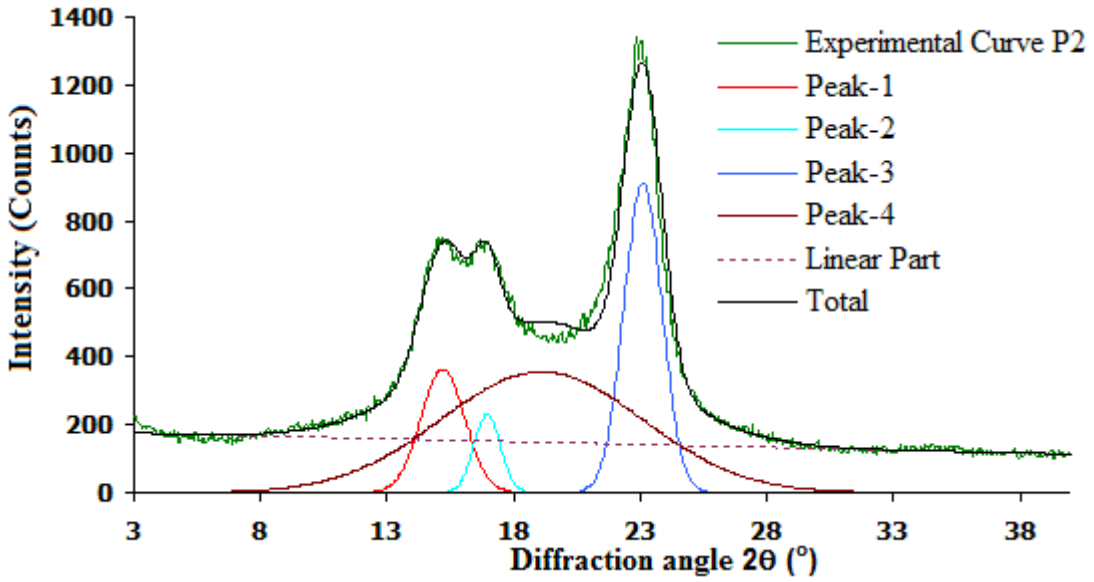

Figure A.8 Peak resolution of plasma treated fibre (P2).

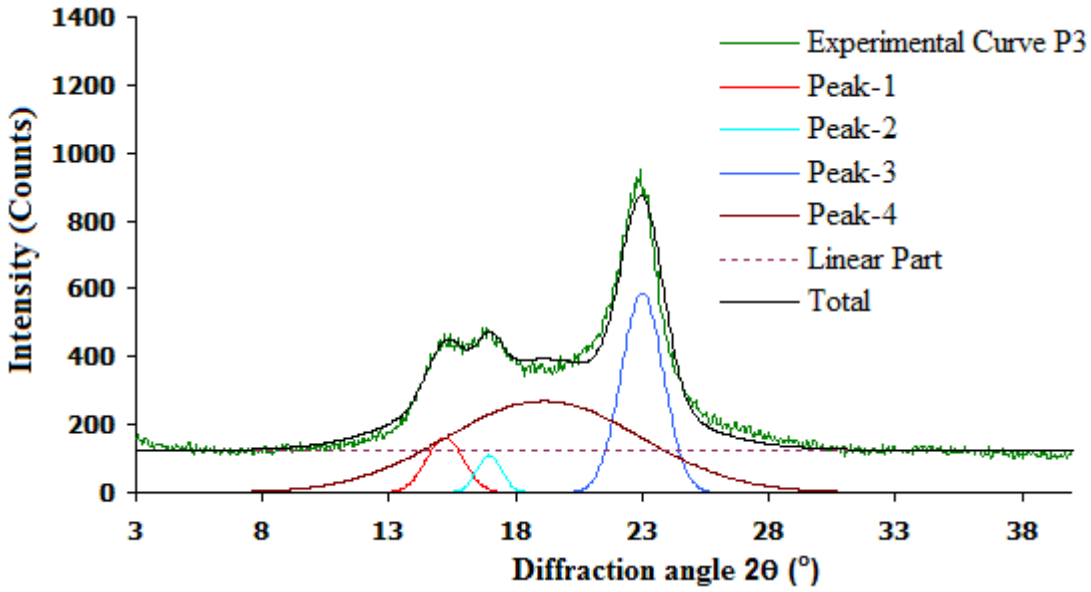

Figure A.9 Peak resolution of plasma treated fibre (P3).

APPENDIX B- FIBRE THICKNESS PROFILES

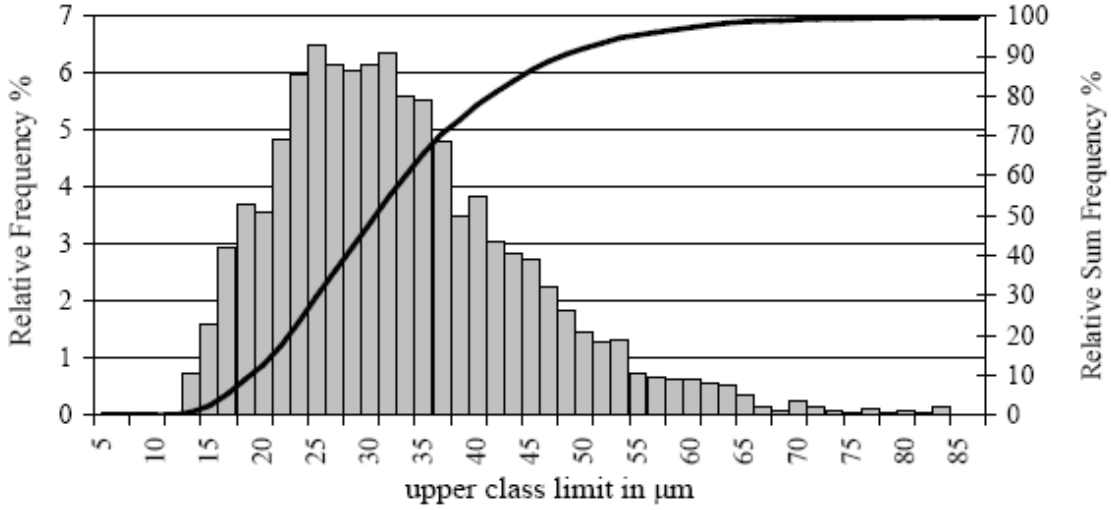

Figure B.1 Schematic of flax fibre thickness distribution (sample 1).

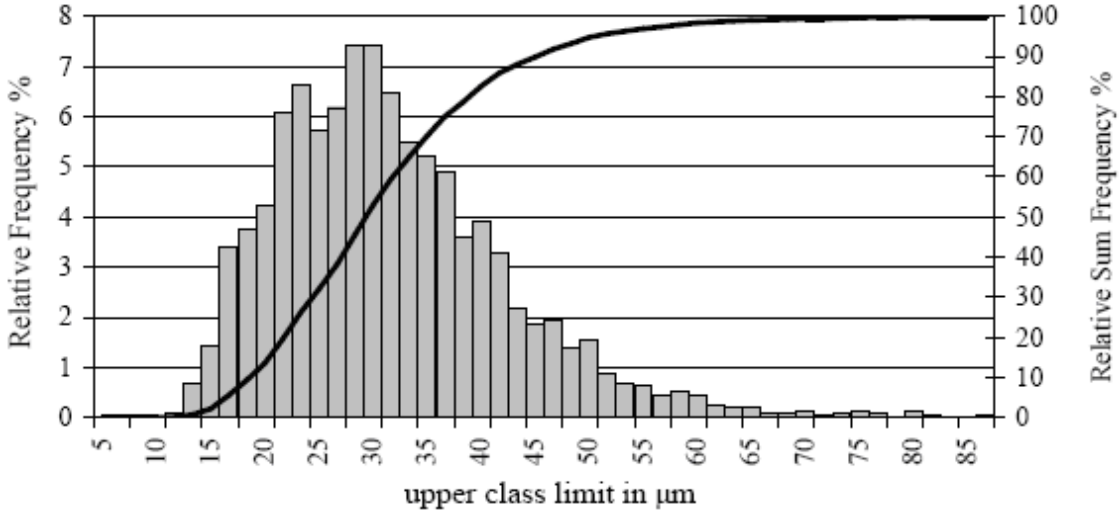

Figure B.2 Schematic of flax fibre thickness distribution (sample 2).

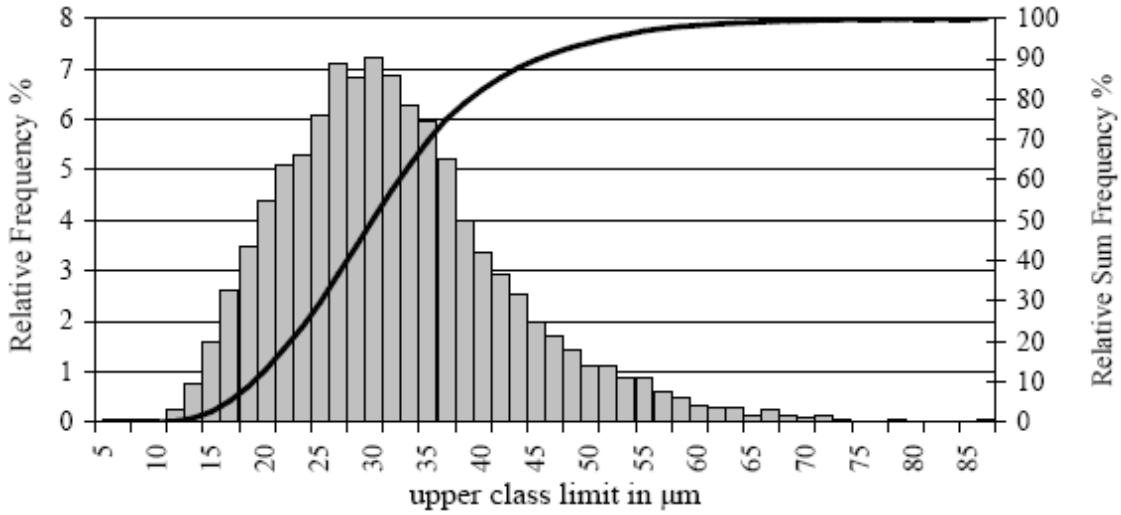

Figure B.3 Fibre thickness distributions profile of sample 3.

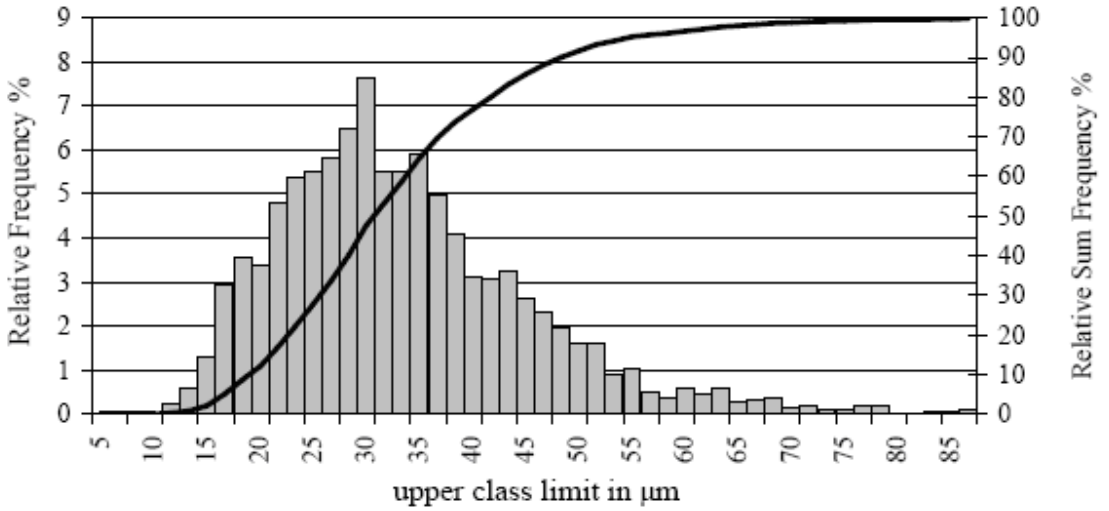

Figure B.4 Fibre thickness distributions profile of sample 4.

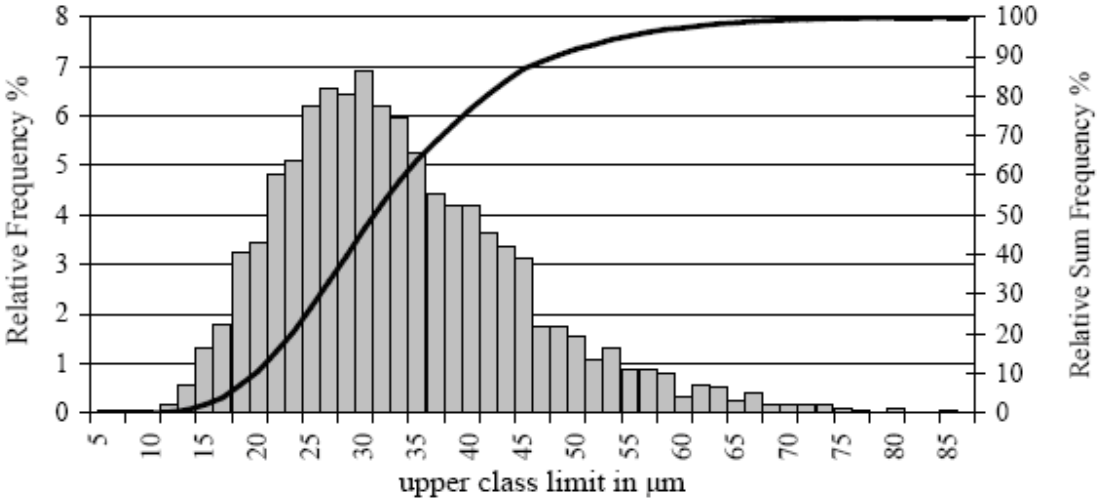

Figure B.5 Fibre thickness distributions profile of sample 5.

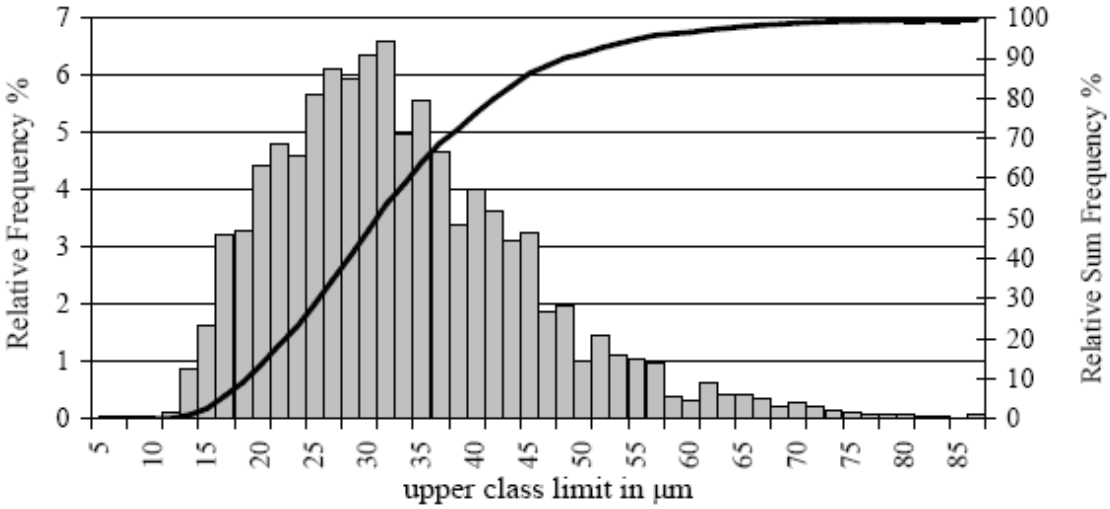

Figure B.6 Fibre thickness distributions profile of sample 6.

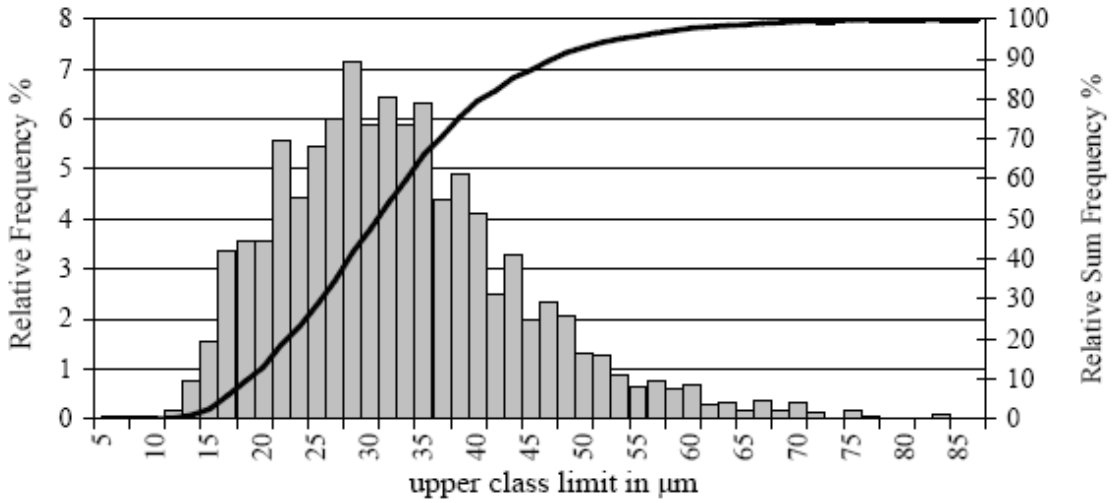

Figure B.7 Fibre thickness distributions profile of sample 7.

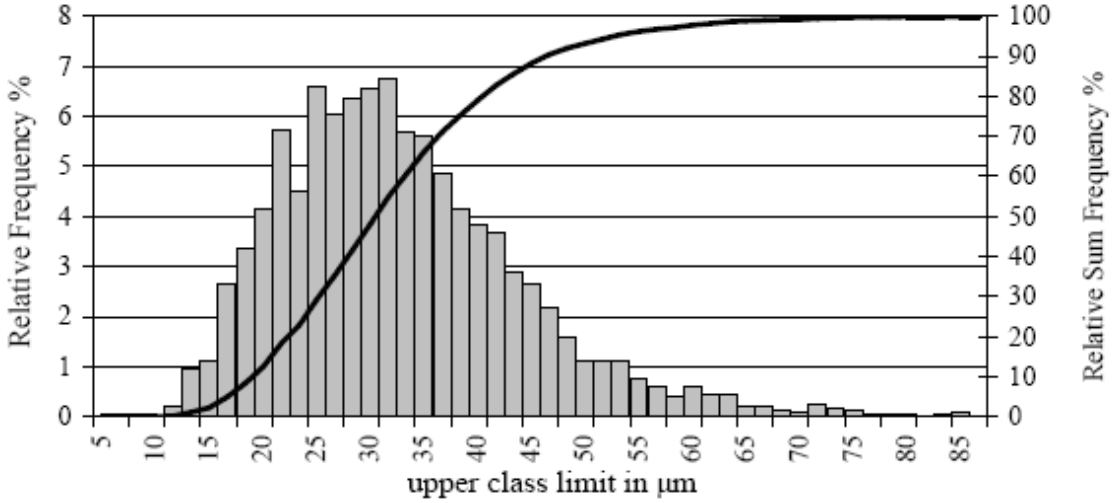

Figure B.8 Fibre thickness distributions profile of sample 8.

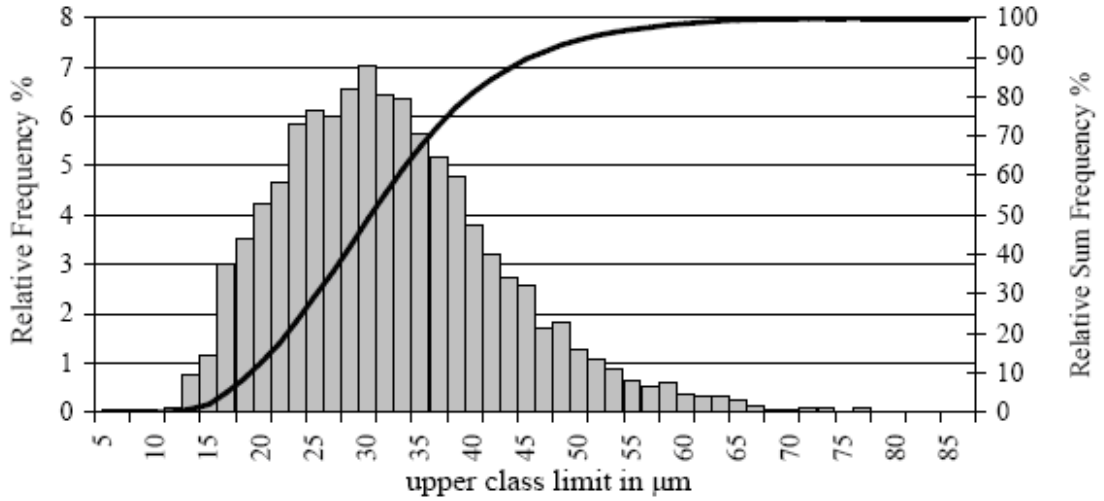

Figure B.9 Fibre thickness distributions profile of sample 9.

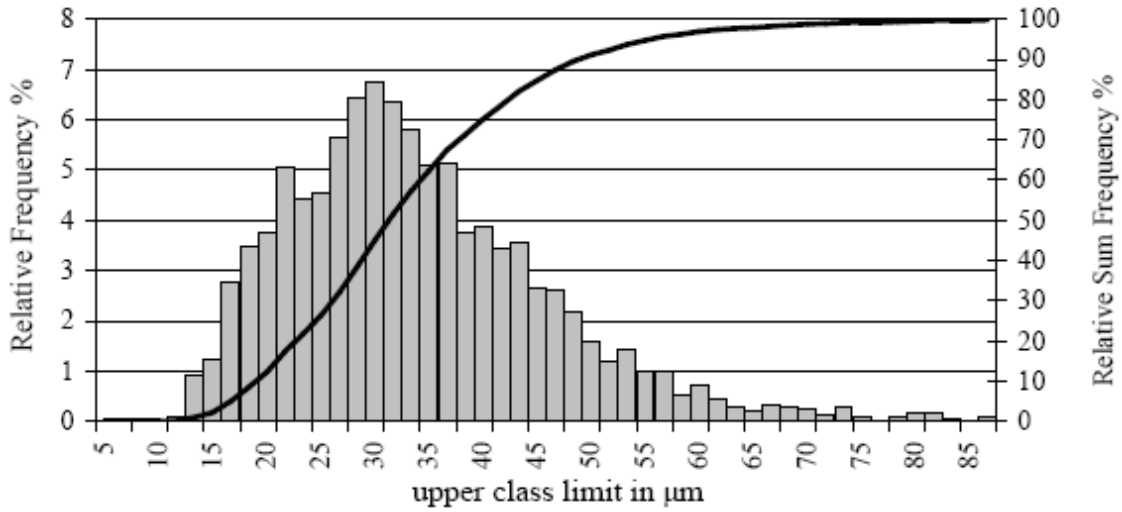

Figure B.10 Fibre thickness distributions profile of sample 10.

APPENDIX C- MECHANICAL PROPERTIES OF UNTREATED/CHEMICALLY TREATED FLAX FIBRE

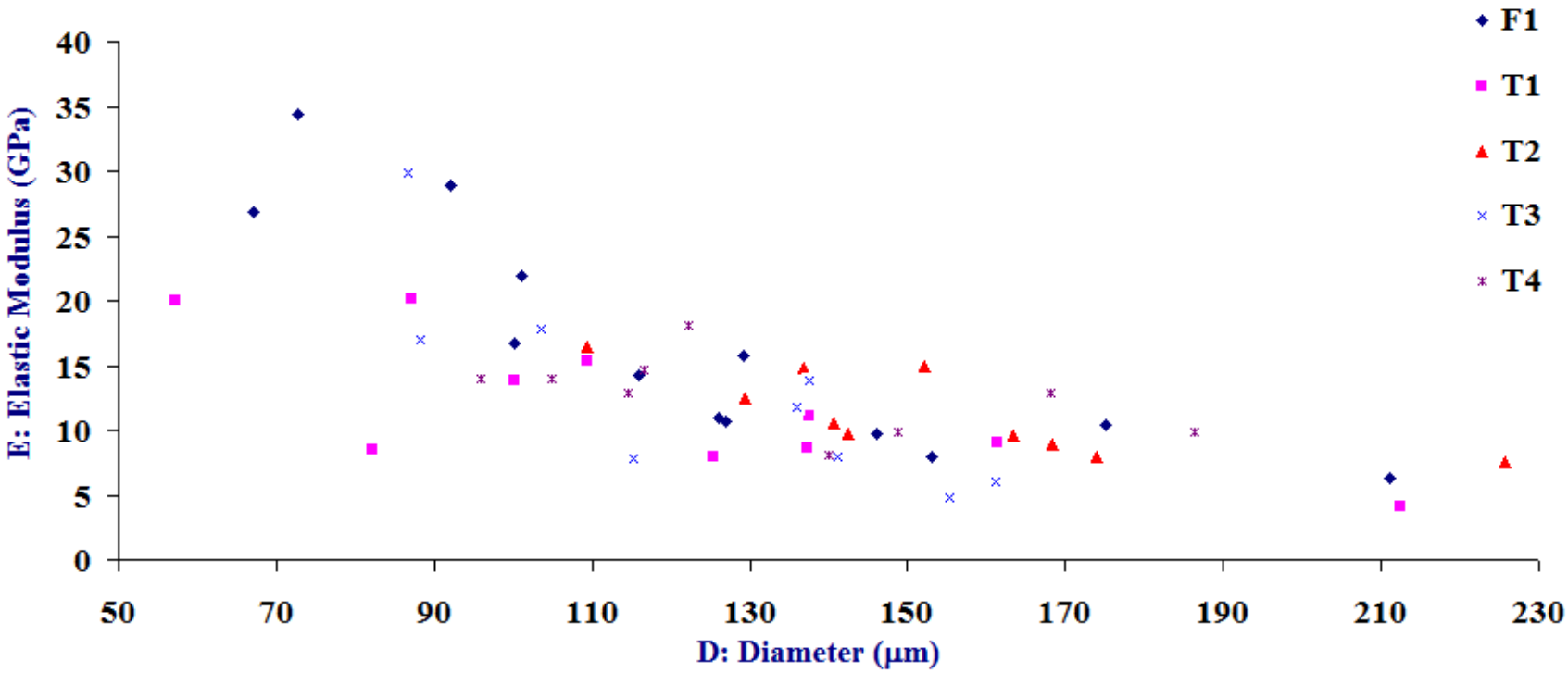

Figure C.1 Elastic modulus versus the diameter for untreated (F1)/chemically treated fibres (T1, T2, T3 and T4).

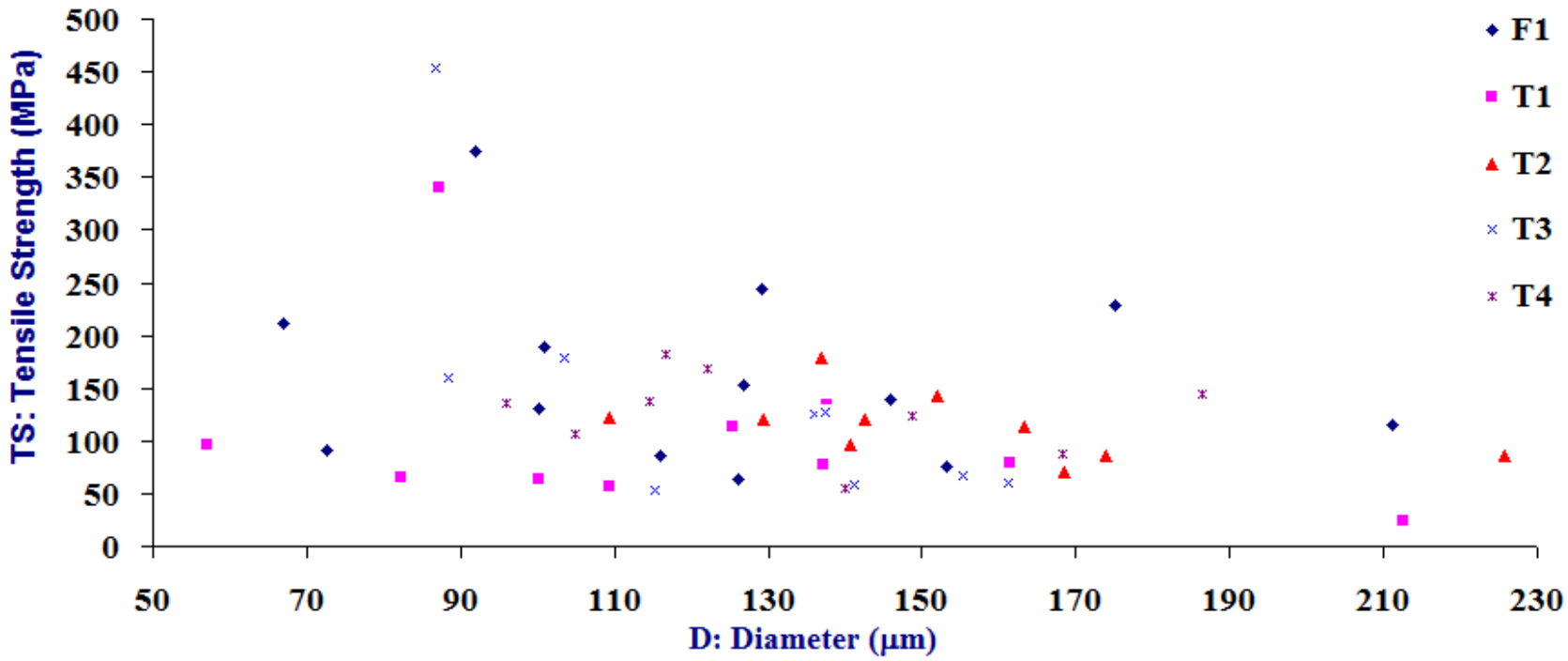

Figure C.2 Tensile strength versus the diameter for untreated (F1)/chemically treated fibres (T1, T2, T3 and T4).

APPENDIX D- PEAK BROADENING

Many factors can cause a peak broadening in X-ray diffraction profiles. In the following figures theses factors are discussed. All figures are reproduced from Lagerlöf (2008).

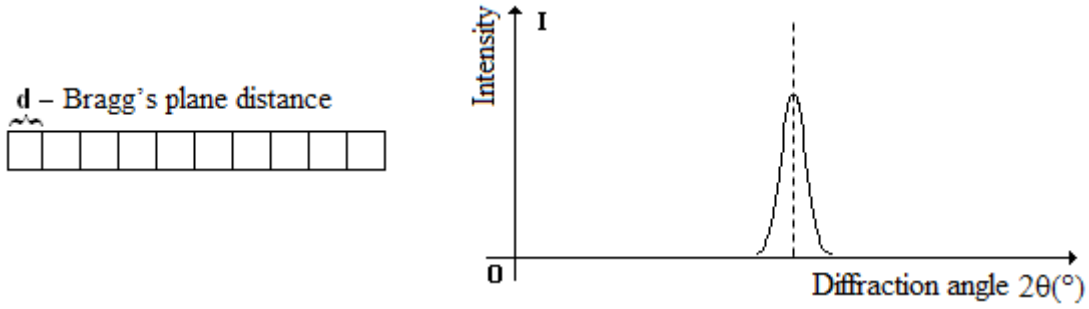

a) b)

Figure D.1 Schematic of peak broadening for a strain free sample: a) one dimensional arrangement of unit cells and b) diffraction peak profile.

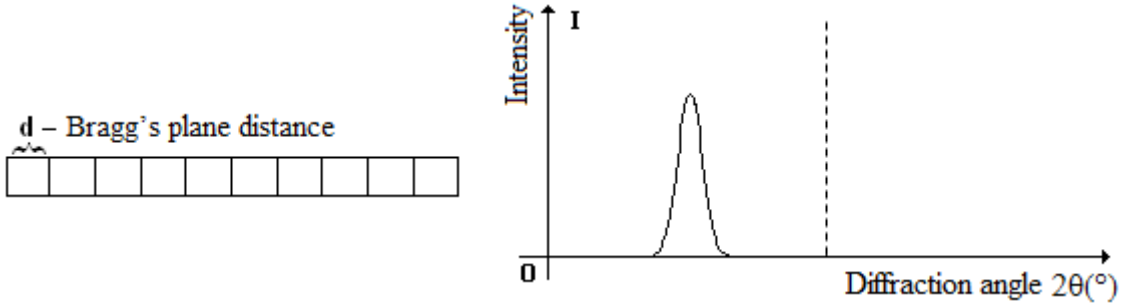

a) b)

Figure D.2 Schematic of peak broadening (left shifting) for a sample subjected to a uniform tension: a) one dimensional arrangement of unit cells and b) diffraction peak profile.

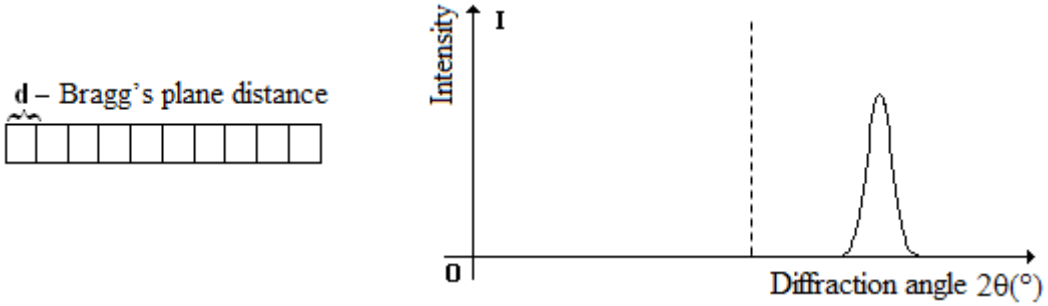

a) b)

Figure D.3 Schematic of peak broadening (right shifting) for a sample subjected to a uniform compression: a) one dimensional arrangement of unit cells and b) diffraction peak profile.

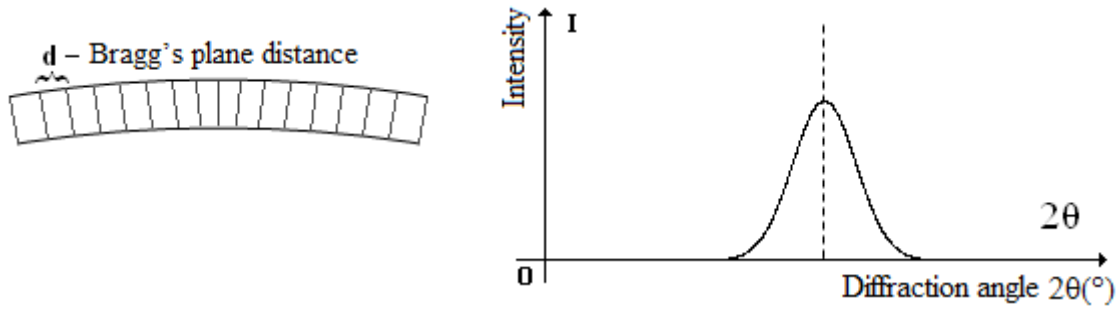

a) b)

Figure D.4 Schematic of peak broadening for a sample subjected to a uniform bending: a) one dimensional arrangement of unit cells and b) diffraction peak profile.

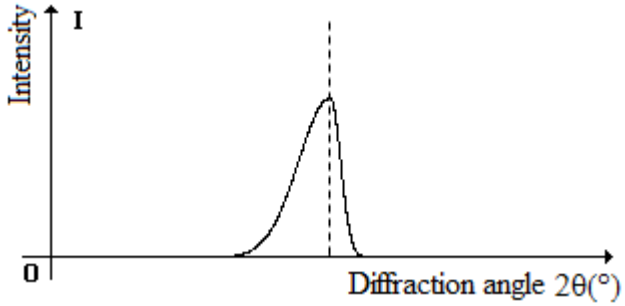

Figure D.5 The presence of point defects (vacancies) in the sample causes local increase in Bragg's plane and also deforms the diffraction peak profile.

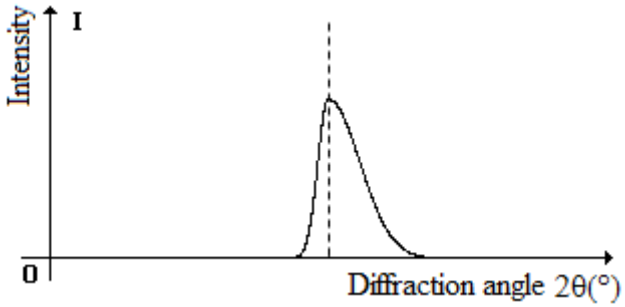

Figure D.6 The presence of point defects (interstitials) in the sample causes local decrease in Bragg's plane and also deforms the diffraction peak profile.

APPENDIX E- DSC THERMOGRAMS

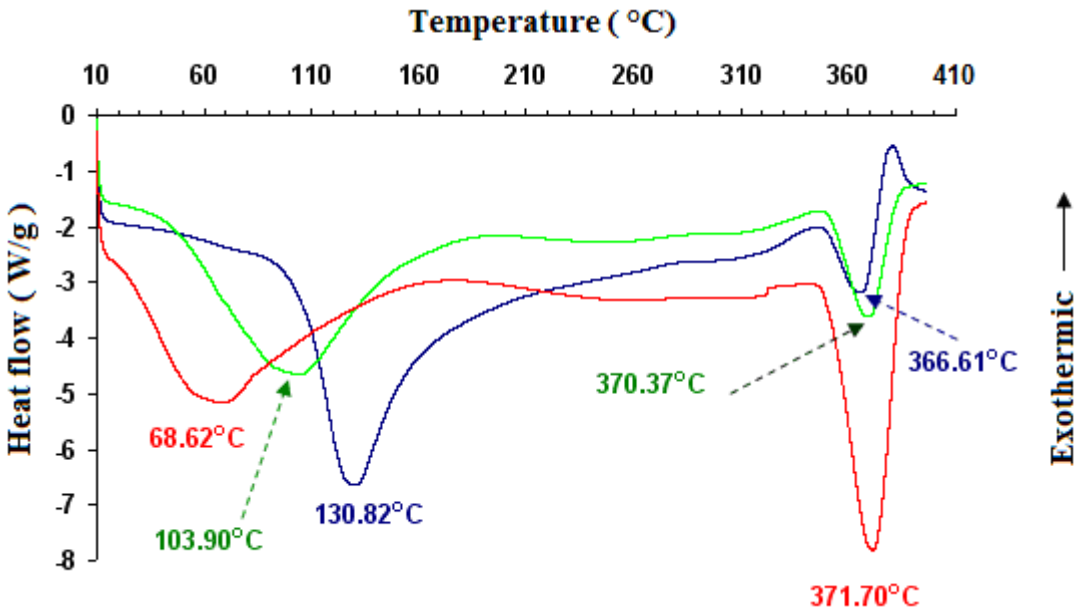

Figure E.1 DSC thermograms obtained from untreated fibre (F1).

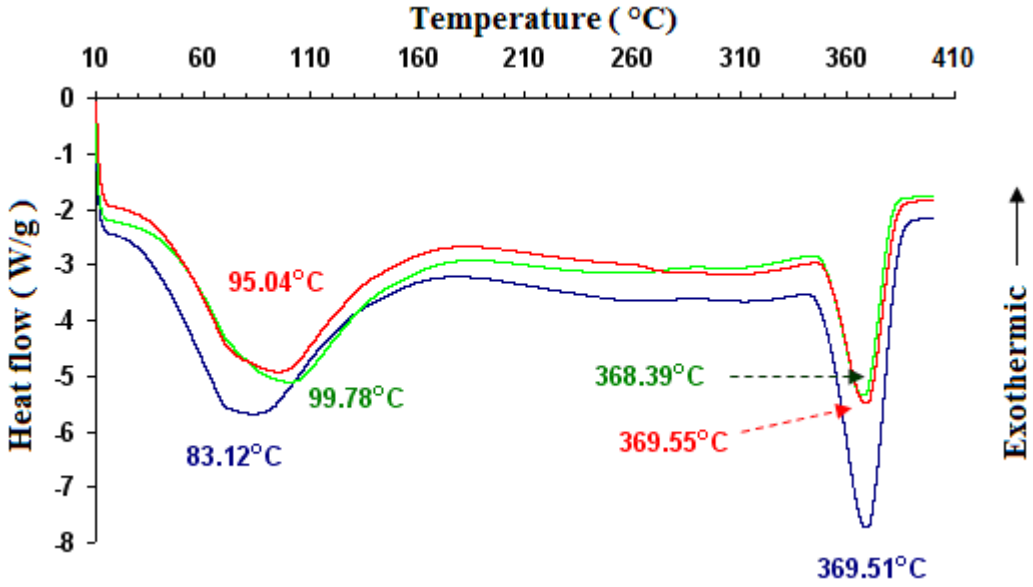

Figure E.2 DSC thermograms obtained from untreated fibre (F2).

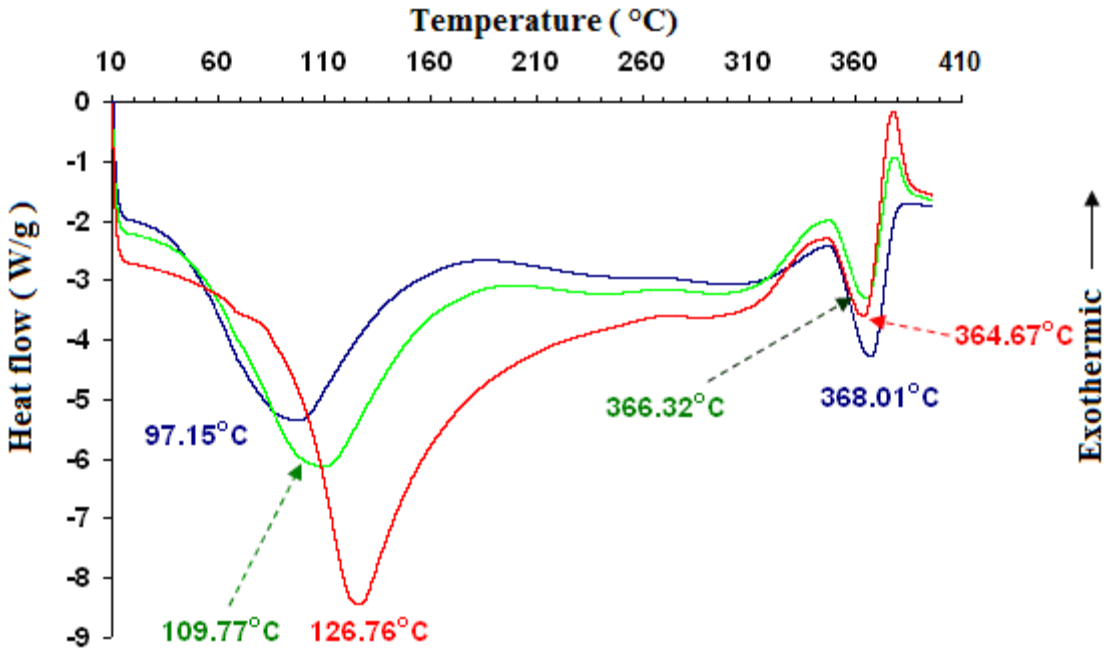

Figure E.3 DSC thermograms obtained from chemically treated fibre (T1).

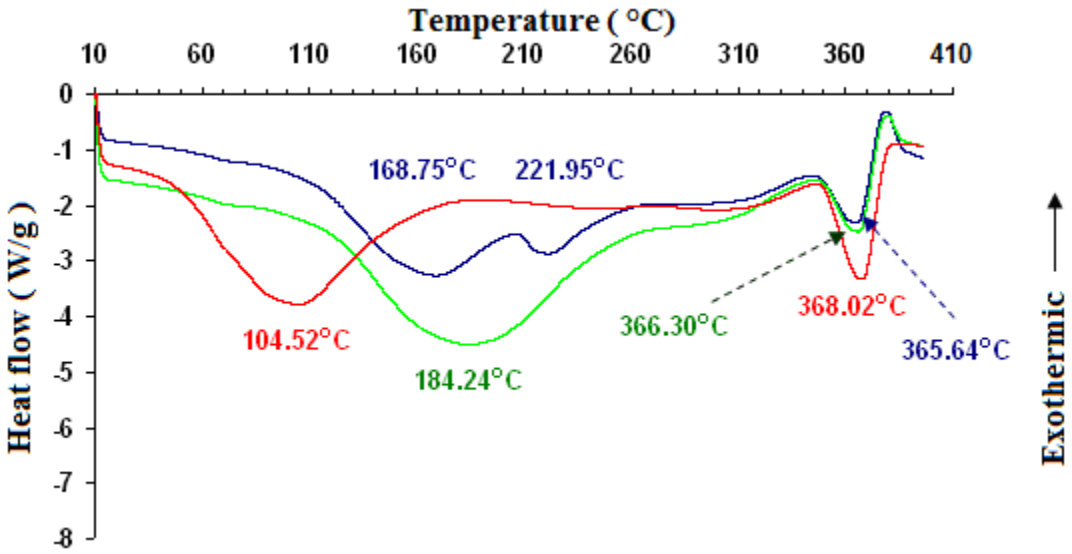

Figure E.4 DSC thermograms obtained from chemically treated fibre (T2).

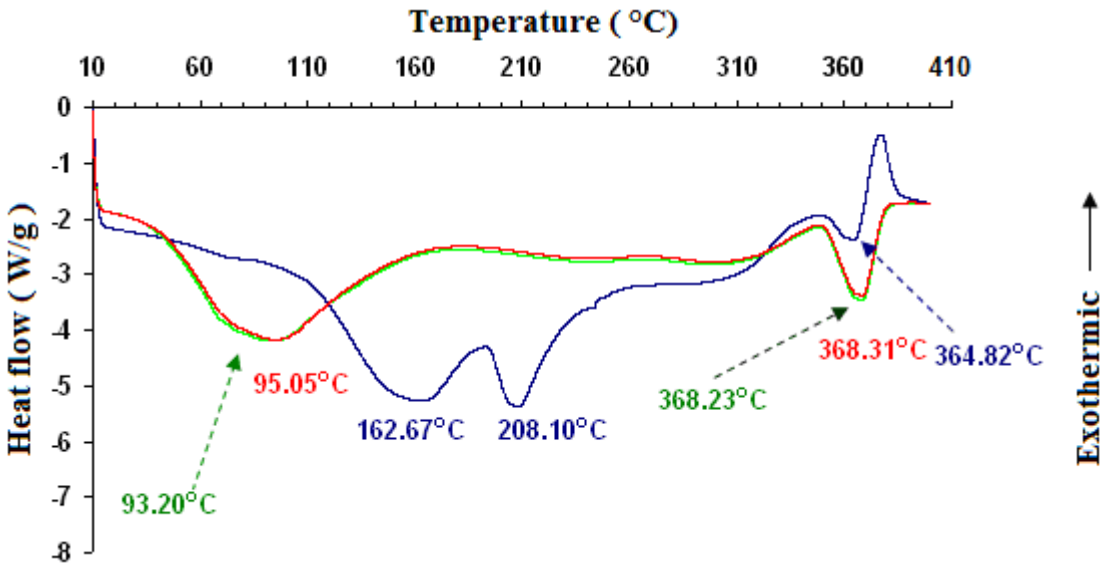

Figure E.5 DSC thermograms obtained from chemically treated fibre (T3).

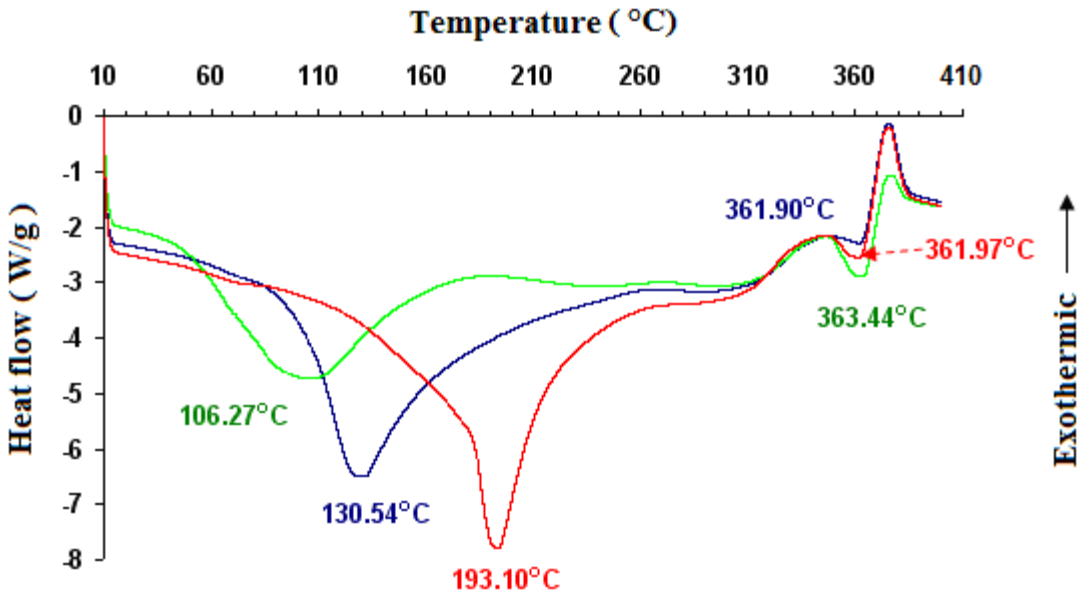

Figure E.6 DSC thermograms obtained from chemically treated fibre (T4).

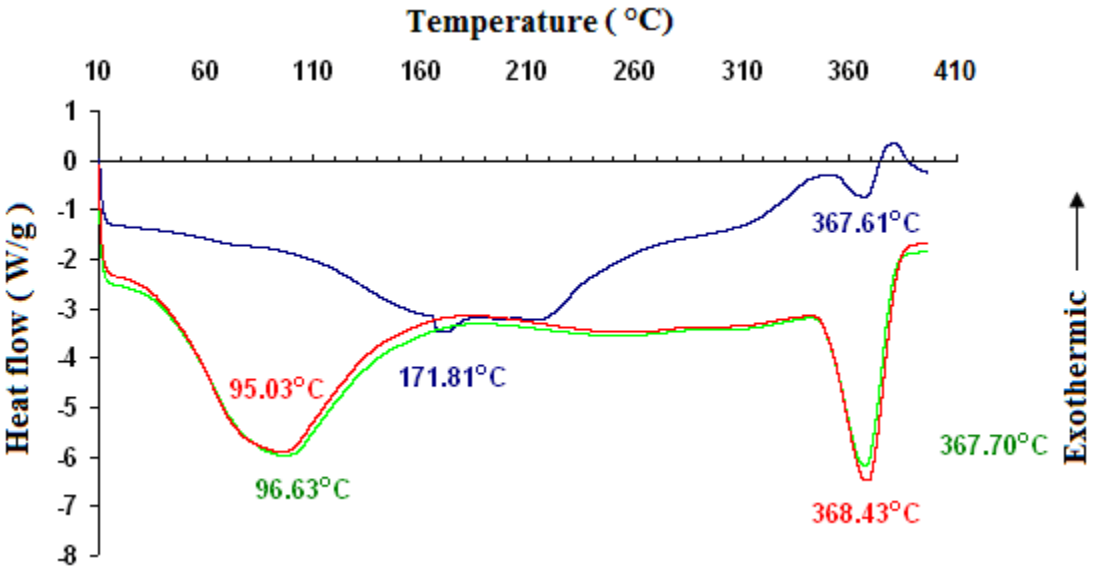

Figure E.7 DSC thermograms obtained from plasma treated fibre (P1).

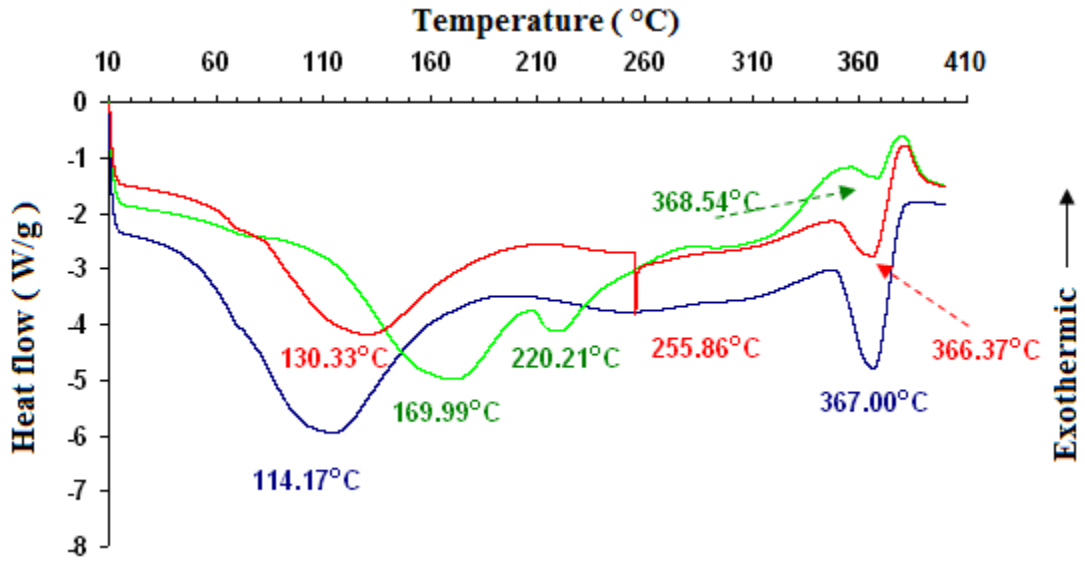

Figure E.8 DSC thermograms obtained from plasma treated fibre (P2).

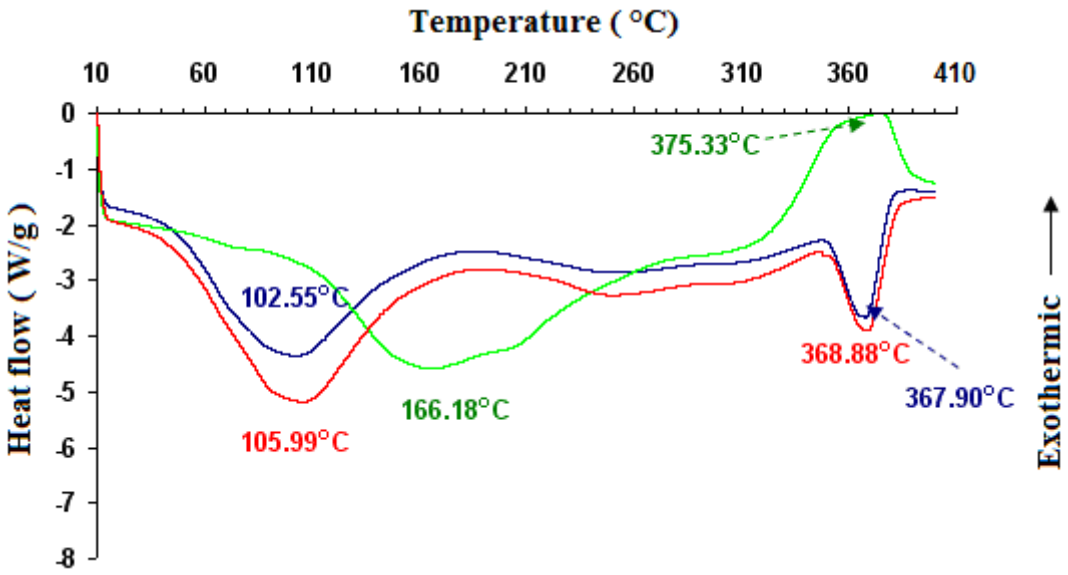

Figure E.9 DSC thermograms obtained from plasma treated fibre (P3).